Advances in antimicrobial biomaterials

HJ Busscher

University Medical Center Groningen and University of Groningen, Department of Biomedical Engineering at the Kolff Institute, Groningen, The Netherlands

Antimicrobial biomaterials are still considered the most ideal solution to control biomaterial-associated infection, despite the difficulties involved in their clinical validation and subsequent regulatory approval. The concept of "the race for the surface" between tissue integration and microbial colonization has long been a guide in developing antimicrobial surfaces, but strangely experimental methods to study the actual race for the surface between tissue cells and microbes have only been recently described [1,2].

With the availability of these so-called co-culture methods [2], it has also become obvious that reduced biofilm formation or improved tissue integration when studied in mono-culture methods are fairly meaningless. This has led to the concept of multiple-function coatings [1], performing antibacterial and tissue integrating functions at the same time. A modular coating platform has been developed, comprising up to three different functionalities along which infection can be counteracted [3].

An overview of developments is presented that led to multi-functional coatings and their advantages, including those of modular coatings, will be highlighted.

ACKNOWLEDGEMENTS: This study was funded by UMCG, Groningen, The Netherlands. HJB is also director of a consulting company SASA BV. The author declares no potential conflicts of interest with respect to authorship and/or publication of this article. Opinions and

assertions contained herein are those of the author and are not construed as necessarily representing views of the funding organization or his respective employer(s).

Anti-microbial PVD coatings

C. Acikgoz, M.H. Lindic, O. Jarry, H. Rudigier

¹ Oerlikon Surface Solutions AG , Headquarters, Iramali 19, LI-9496 Balzers

INTRODUCTION: Coatings are being more and more incorporated into the design of medical devices. The advantages of BALINIT® hard coatings for medical devices are clear from multiple perspectives. They prevent scuffing and ensure trouble-free operation, even when running dry. These low-friction, thin-film coatings are extremely wear-resistant as well as chemically inert. The composition and properties of BALINIT coatings can also be tailored for the intended use. An example to this is our new antimicrobial, highly resistant PVD coatings. These coatings have a high potential for orthopedic and medical devices because they combine the favorable tribological properties of PVD coatings with the promising antimicrobial behavior of silver and the balance between antibacterial efficiency and toxicity can be achieved by fine-tuning the doping concentrations.

METHODS: TiN-Ag coating was developed by a combined arc/sputter process. The coatings were characterised using transmission electron microscopy (TEM), energy-dispersive X-ray spectroscopy (EDX) and X-ray diffractometry (XRD). Anodic stripping voltammetry method was used to determine the silver concentration released from the surface.

RESULTS: The presence of separated Ag and TiN phases in the coating structure could be confirmed by XRD-examination. Characteristic Ag peaks were detected in XRD spectra of the synthesized antimicrobial TiN-Ag coatings. However the observed Ag peaks were wider than typical characteristic ones, particularly for coatings having lower silver concentrations. Wider Ag peaks can be explained by the nanometer grain size of the silver particles, which was confirmed by TEM examinations, having grain sizes of about 8-10 nm x 3-4 nm in TiN-Ag coating (Figure 1). The measured silver ion concentration approximately is $0.1 \, \mu \text{g/cm}^2$ after one day incubation. maximum concentration of Ag released from the coatings in cumulated measurements over 30 days is limited to 0.25 µg/cm² after one day of incubation in NaNO3.

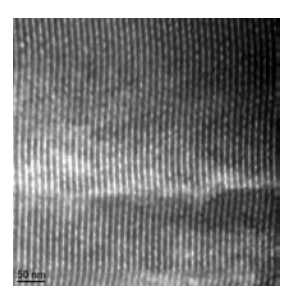


Fig. 1: TEM image of TiN-Ag coating containing 5 at% of silver.

The antibacterial properties of the TiN-Ag surfaces against *S. aureus* were determined by plate count technique. The TiN-Ag surfaces showed a reduction compared with controls of 3 logs in bacterial adhesion. In order to verify the applicability of the coated samples as biomaterials, samples were assayed in terms of their effect on fibroblast cells (cytotoxicity) and the coated surfaces did not affect the cell functionality.

DISCUSSION & **CONCLUSIONS:** The antimicrobial activity of silver is the result of Ag^+ ions binding strongly to electron donor groups of biological molecules. The activity is dependent on the balance between the activity of the Ag^+ ions and the total amount of silver released from the coating, which, if too high, causes cytotoxicity. The measured silver ion concentration is approximately $0.1 \, \mu g/cm^2$ after one day incubation, which is shown to be not toxic and enough to show antimicrobial efficacy.

It was found that TiN-Ag coatings show excellent antimicrobial effect. Secondly, no cytotoxic effect could be measured.

ACKNOWLEDGEMENT: The authors would like to thank Empa (The laboratory for Biomaterials) for the support for bacteria and cell studies.

Mechanoregulation of bacterial phagocytosis and surface colonization

J Moeller¹, V. Vogel¹

¹ Laboratory of Applied Mechanobiology, ETH Zurich, Zurich, CH

INTRODUCTION: Sessile bacteria adhere to engineered surfaces and host tissues and pose a substantial clinical and economical risk when growing into biofilms. Within this work, we describe the kinetic and mechanistic details of a multistep process that macrophages, specialized host immune cells, exploit to pick-up firmly adherent *E.coli* from surfaces. We highlight that the kinetics and mechanical properties of the macrophage filopodia, lamellipodia as well as the E.coli fimbriae have to be tightly tuned to facilitate phagocytosis. We will further show how bacterial filamentation, a common trait of various bacteria including clinically relevant strains of E.coli, P.aeruginosa and S.enterica, critically affect the rate of immune cell uptake as well as bacterial biofilm formation.

METHODS: Phase contrast and DIC live cell microscopy in combination with electron microscopy was used. To allow for the co-adhesion of E.coli expressing the adhesin FimH from the **UPEC** strain J96 and J774A.1 murine macrophages, all experiments were performed on glass model surfaces coated with a mixture of purified human plasma fibronectin and the mannose-presenting glycoprotein RNaseB. Filamentation of E.coli was induced by the betalactam antibiotic cephalexin. For the surface colonization studies, RNase B was patterned on glass substrates using a modified photolithography S1818 photoresist lift-off process with PLL-g-PEG blocking of unspecific protein adsorption.

RESULTS: We show that catch bonds, noncovalent receptor-ligand interactions lifetimes are extended several orders of magnitude if activated by force, play an unrecognized role in the non-opsonized uptake of surface-bound E. coli by macrophages [1]. When encountering a sessile bacterium, a single catch bond forms between the mannosylated membrane receptor CD48 within a macrophage filopodia and the bacterial adhesin FimH located at the tip of E. coli type 1 fimbriae. This long-lived bond enables a multiphase bacterial uptake, which is inhibited by soluble mannose. The tension acting across the filopodium-fimbriae connection triggers local macrophage lamellipodia protrusions towards the adherent bacterium, which facilitates bacterial uptake. We further that bacterial

filamentation significantly slows the phagocytosis rate, as immune cells first have to capture the filament pole to successfully form a phagocytic cup [2]. In addition, we demonstrate that growing into high aspect ratio filaments, triggered by antibiotic treatment, can actually accelerate the rate of surface biofouling as filaments promote the bridging of non-adhesive patches under physiological flow rates [3].

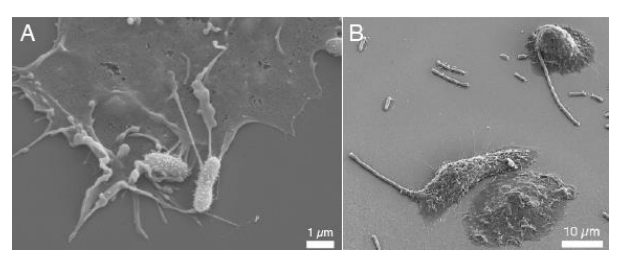


Fig. 1: Scanning electron micrographs of macrophage – E.coli encounters. A) Macrophage lamellipodium localized underneath a surface-bound E.coli [1]. B) Macrophage attack of high-aspect ratio E.coli filaments [2].

DISCUSSION & CONCLUSIONS: Our results highlight the fine-tuned mechanobiological aspects that immune cells use to clear firmly surface-bound bacteria. We further demonstrate that bacterial shape, independent of the receptors involved, coregulates the rate of bacterial phagocytosis and the rate of biofilm formation. In the context of increasing antimicrobial resistance we envision that our findings can lead to new public health recommendations of antibiotic administration and to the development of advanced strategies to fight biofouling of materials.

ACKNOWLEDGEMENTS: The authors acknowledge support from ETH Zurich, Ciba Speciality Chemicals, Basel, CH, BASF, Ludwigshafen, Germany (Nb. 270627-05) and the Commission of the European Communities / ERC Advanced Grant (Nb. EU-231157). The FIRST Centre for Micro- and Nanoscience at ETH Zurich is acknowledged for providing access to the photolithography equipment.

Biomaterials in prophylaxis and treatment of orthopaedic device-related infections

M Morgenstern¹, H Eckardt¹, WJ Metsemarkers²

¹ Dept. of Orthopaedic and Trauma Surgery, University Hospital Basel, Switzerland.
² Dept. of Trauma Surgery, University Hospitals Leuven, Belgium

The most challenging complications in orthopaedic trauma surgery are orthopaedic device-related infections (ODRI) following fracture fixation or joint replacement. The incidence is ranging from approximately 1% after closed fractures or joint replacement, to more than 30% in complex open limb fractures. Despite tremendous efforts with prolonged antibiotic therapy and multiple revision surgeries, these complications are associated with considerable rates of recurrent infections as well as permanent functional loss and show success rates of only 70 to 90%. Furthermore, due to protracted treatment and recovery periods the reported socioeconomic effect of ODRIs is significant.

The primary aim is to prevent infection, because once established, they are difficult to eradicate. The main reason for this is biofilm formation on the implanted device, which allows pathogens to protect themselves from host immune response and antimicrobial therapy. Especially in open fractures with a considerable wound contamination and softtissue damage the efficacy of systemic antibiotics is reduced. Due to local vascular damage, systemic antibiotics may not reach high enough local concentrations to eradicate the bacteria. Locally delivered antibiotics can overcome this problem by providing high local concentrations. Beside prophylaxis, treatment algorithms of ODRIs also encompass next to surgical debridement and systemic antimicrobial therapy, the application of local antibiotics.

Currently, several antibiotic loaded biomaterials for local infection prophylaxis and/or treatment are available. Polymethylmethacrylate (PMMA) bone cement is a well-established biomaterial since decades. Nevertheless it bears various limitations, such as limited antibiotic release, and the need of a revision surgery to remove the non-biodegradable cement.

Biodegradable materials, like calcium-sulphate (CS) pose the advantage over PMMA in that they do not need secondary surgery for removal. CS used as antibiotic-laden bone void filler shows promising results in treatment of osteomyelitis. Other degradable biomaterials for local antibiotic delivery are collagen implants, bioactive glass, calcium phosphates, demineralized bone matrix and allograft bone. Antibiotics can also be administered locally through an implant coating,

e.g. with a layer of poly(D,L-lactide) (PDLLA) loaded with gentamicin. After promising initial results, large scale clinical trials will have to prove its efficacy in prevention and treatment of fracture related infections. Thermo-responsive hydrogels, loaded with antimicrobials are subject of on-going research and would give the surgeon intra-operatively the choice to protect the implants and surfaces with a patient specific "gel-coating". Increasing antibiotic resistance has become a significant global healthcare problem. Addressing this issue, non-antibiotic substances such as antimicrobial peptides (AMP) and silver are also in focus for current and future research.

In the next decades the absolute number of complications after orthopaedic surgery will inevitably rise, since a growing older population with high functional expectations will lead to an increase of surgical interventions. This and the threatening antimicrobial resistance will urgently require joined efforts to improve and launch new prevention and treatment strategies.

Antifouling materials: analysis of the *in vivo* setting for improved, predictive *in vitro* biofilm models

Matthias T. Buhmann¹, Dominik Abt², Oliver Nolte³, Antonia Neels⁴, Beatrice Gutt¹, Qun Ren¹

¹ Department for Biointerfaces, Empa. Swiss Federal Laboratories for Materials Science and Technology, Lerchenfeldstrasse 5, 9014 St. Gallen, CH. ² Department of Urology, Cantonal Hospital St. Gallen, CH. ³ Department of Bacteriology, Center for Laboratory Medicine, St. Gallen, CH. ⁴Center for X-ray Analytics. Empa. Swiss Federal Laboratories for Materials Science and Technology, Überlandstrasse 129, 8600 Dübendorf, CH

INTRODUCTION: Many antimicrobial materials show promising antimicrobial activity in the laboratory but fail in the translation into practice, partially due to the lack of appropriate *in vitro* biofilm models that can be used to predict the long-term antimicrobial and anti-biofilm activity *in vivo*.

The design of predictive *in vitro* biofilm models to mimic the conditions *in vivo* requires a critical analysis of the respective *in vivo* conditions and the consideration of various factors.

We have analyzed the *in vivo* setting for biomaterials used for urinary tract applications for the generation of laboratory *in vitro* biofilm models and to design novel antimicrobial biomaterials.

Here, we will also present examples for *in vitro* models for distinct requirements.

METHODS: Biofilms from clinical ureteral stent samples were extracted using a novel biofilm extraction method and analysed for the biofilm composition and bacterial load by scanning electron microscopy, quantitative *real-time* PCR, X-ray diffraction, as well as microbiology methods.

RESULTS: Several relevant factors for the development of *in vitro* biofilm models have been identified (1, 2). The analysed ureteral stent biofilm samples comprised large amounts of inorganic crystalline components, whereas bacteria were only present in a subset of samples. For the assessment and development of biomaterials for the urinary tract, the precipitation of calcium oxalate and calcium phosphate compounds has to be considered, since the antimicrobial biomaterials may become covered and get de-activated by these compounds. Accordingly, we have developed an artificial urine medium based on an urine metabolomics study that allows growth of relevant pathogenic bacteria which may be found in the

urinary tract, and it comprises components relevant for crystal precipitation (3).

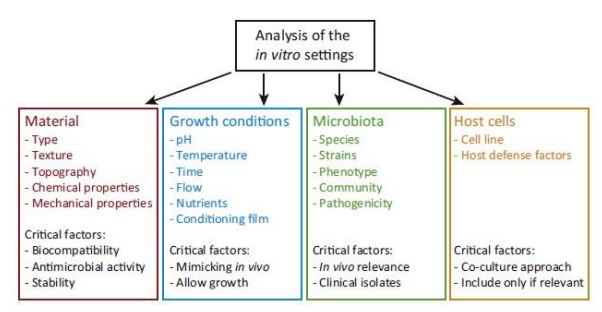


Fig. 1: Factors to be considered for the generation of an in vitro model for the assessment of antimicrobial biomaterials (1).

CONCLUSIONS: The analysis of the *in vivo* setting decides on the required antimicrobial strategy and the appropriate *in vitro* anti-biofilm assessment model.

ACKNOWLEDGEMENTS: We kindly thank Luzia Wiesli and Stefanie Altenried for technical support, and Patrick Betschart and Valentin Zumstein for providing ureteral stent samples.

Ag nanoencapsulation for antimicrobial coatings

SL Abram¹, N Hérault, KM Fromm¹

¹ Department of Chemistry, University of Fribourg, Fribourg, CH

INTRODUCTION: Since long time silver is known for its good antimicrobial properties and biocompatibility. Silver nanoparticle based antimicrobial coatings can make use of these properties to fight medical device related infections by preventing biofilm formation especially if they show activity against multi resistant bacteria strains.

In this context different types of Ag@metaloxide nanoparticles are investigated for their antimicrobial properties in correlation with the particle morphology. The metal oxide shells made of TiO₂ or SiO₂ protect the Ag particles from aggregation and might give control over the release rate of Ag⁺ as antimicrobial active species. Moreover encapsulation offers ways to covalent attachment to implant surfaces as well as to sol gel coatings.

METHODS: Ag nanoparticles synthesized by the polyol process were coated with a silica shell by a modified Stöber method resulting in 100 nm core shell particles (CS, Fig. 1 A). In a second step the inner part of the silica shell was removed by a surface protected etching process¹ which changes the particles' morphology towards a so called nanorattle (NR, Fig. 1 B). In a second synthesis, Ag nanoparticle containing amorphous TiO₂ nanocontainers of about 200 nm were synthesized by removing a polystyrene template (Fig. 1 C). A subsequent calcination step transforms the amorphous shell into crystalline anatase (Fig. 1 D).

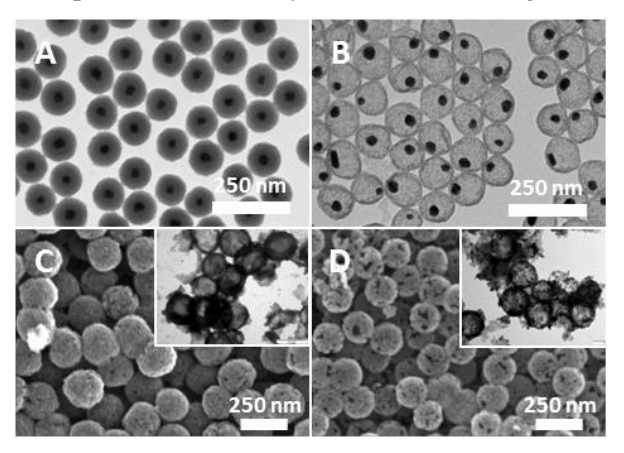


Fig. 1: Electron micrographs of Ag@SiO₂ core shell particles (A) and nanorattles (B) and Ag-TiO₂ nanocontainers (amorphous: C, anatase: D).

RESULTS: Depending the particles' morphology different Ag⁺ release kinetics could be observed by measuring ICP-OES. In the case of silica as shell material the nanorattles show a stronger release than the core shell particles over a long time period, but within the first 24 hours the reverse trend can be observed (Fig. 2, A). This correlates to the core shells better antimicrobial activity. Tests against E.coli show that they are killing at concentrations of about 0.14 mg/ml whereas 0.82 mg/ml of nanorattles are needed to see the same effect. In the case of TiO₂ nanocontainers the anatase particles are able to release more Ag⁺ which is clearly reflected in their better antimicrobial efficiency against both, E.coli and S.aureus (Fig. 2, B). In both cases no Ag related cytotoxicity was found against fibroblasts and macrophage cells. Antimicrobial tests against a multi-resistant S.aureus strain are ongoing.

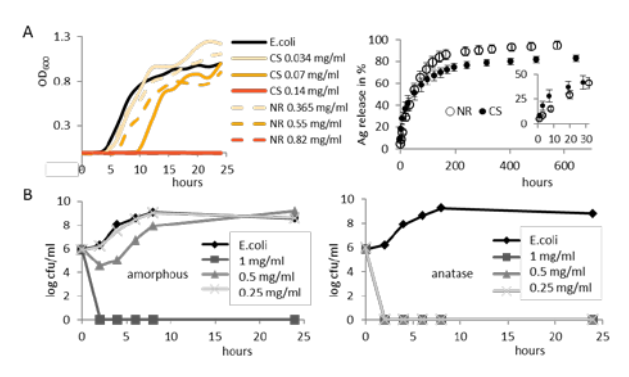


Fig. 2: Growth curves of E.coli in presence of $Ag@SiO_2$ CS and NR and their Ag^+ release (A). Killing curves of E.coli in presence of $Ag-TiO_2$ (B).

DISCUSSION & CONCLUSIONS:

Both types of silver-containing particles thus fulfil the requirements for the development of novel antibacterial nanocoatings on biomaterial surfaces. Currently we are developing strategies to link them to implant model surfaces of titanium or to incorporate them into polymer matrices.

ACKNOWLEDGEMENTS: The authors would like to thank the University of Fribourg and the SNSF for the generous funding of the project which is part of the NCCR "Bio-inspired Materials".

Gentamicin loading of calcium phosphate-coated implants prevents experimental *Staphylococcus aureus* device-associated infection *in vivo*

<u>K Thompson</u>¹, S Petkov^{1,2}, S Zeiter¹, CM Sprecher¹, A Baumann³, RG Richards¹, TF Moriarty¹, H Eijer²

¹ <u>AO Research Institute Davos</u>, Davos, CH. ² Spital Emmental, Burgdorf, CH. ³ DOT GmbH, Rostock, Germany

INTRODUCTION: Osseointegration of orthopaedic implants, such as hip and knee prostheses, is enhanced by coating the implanted devices with materials such as calcium phosphate (CaP). One such coating currently in clinical use is the BONIT® coating (DOT, Germany), a composite of brushite and hydroxyapatite. Despite such advances in implant integration, device associated infection (DAI) is an infrequent but potentially devastating complication associated with all orthopaedic devices. Successful strategies aimed at preventing implant colonization would be a useful tool in orthopedic surgery. Intraoperative loading of CaP coatings by, for example, immersion in antibiotic solution immediately prior to implant placement, could offer a rapid yet simple strategy for antibiotic prophylaxis. The aim of this study was to determine if gentamicin may be effectively loaded into a BONIT® implant coating and to test the efficacy of this strategy for preventing DAI in

METHODS: The optimal loading conditions of gentamicin on to BONIT®-coated titanium allov (titanium, aluminium, niobium: TAN) disks and screws was determined following immersion in a 40 mg/ml gentamicin solution (HEXAL®) for a range of time points (range: 1 sec to 60 min). The kinetics of gentamicin release from the loaded implants was measured by spectrophotometry after derivatization with o-phthaldialdehyde. Antibacterial efficacy of the released gentamicin was assessed in vitro using methicillin-sensitive Staphylococcus aureus NCTC 12973 (MSSA) and the EUCAST Disk Diffusion Method for Antimicrobial Susceptibility Testing. To determine the efficacy of this strategy for preventing DAI in vivo, we implanted BONIT®-coated screws, with or without gentamicin loading, into the tibiae of skeletally mature adult (>12 weeks old) female Wistar rats following inoculation with a clinical strain of S. aureus (1x10⁶ CFU; n=9 per group). Osseointegration of the BONIT®-coated screws in the presence or absence of gentamicin was determined histologically in non-infected animals as previously described.²

RESULTS: The BONIT® coating was rapidly loaded with gentamicin following immersion, with maximal loading observed at <1 min incubation. Increased immersion time did not enhance gentamicin loading into the BONIT® coating. Following loading with gentamicin, the BONIT® coating rapidly released gentamicin in aqueous solution, with >95% gentamicin released within 15 mins as determined by spectrophotometry, and by assessing anti-bacterial efficacy in zone of inhibition assays. Anti-bacterial efficacy was confirmed in vivo, with a gentamicin-loaded BONIT®-coated TAN screw able to completely prevent S. aureus infection in 7/8 inoculated animals (one excluded due to contamination with another bacterial species), whereas all animals not receiving gentamicin remained infected after 7 days. Histomorphometric analysis revealed gentamicin did not inhibit osseointegration of the BONIT®-coated screw after a 28-day period.



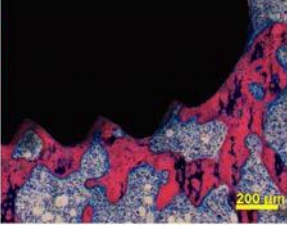


Fig. 1: Histomorphometric analysis demonstrating the osseointegration of BONIT®-coated TAN screws in the absence (left panel) or presence (right panel) of gentamicin after 28 days. Scale bar = 200 µm.

DISCUSSION & **CONCLUSIONS:** In conclusion, gentamicin loading of BONIT®-coated implants is a promising approach for preventing *S. aureus* DAI *in vivo*. However, further studies are required to investigate the efficacy of this strategy in the clinical setting.

Growth condition targeted approach for biofilm prevention

F Rölli¹, S Kötzsch¹, F Hammes²

¹ GuH, Hochschule Luzern, Horw, CH. ² Umik, Eawag, Dübendorf, Zürich, CH

INTRODUCTION: Biofilms on materials are undesirable for many applications. Therefore, considerable efforts are undertaken to prevent biofilm formation, e.g. by surface modifications or antimicrobial coatings. However, in the longterm, complete avoidance of bacterial attachment and eventual proliferation is practically impossible. The greatest potential for success probably is a combined approach of antimicrobial effects and the promotion of adverse growth conditions.

In drinking water microbiology, a key concept is the minimisation of available nutrients. Optimised material formulations and cross-linking properties can lead to a significant lower migration rate of organic carbon compounds from the material and therefore contribute to less favourable growth conditions for bacteria.

During the last few years, the material test "BioMig" was developed, providing a tool to screen and evaluate existing materials on their migration and growth potentials¹. In addition, BioMig provides valuable information during the process of the targeted development of new materials and coatings.

METHODS: The key element of BioMig includes the incubation of a defined surface of a material in water containing a natural mixed bacterial community. In one part of the test package, seven sequential migration steps for 24 h at 60 °C give information about a material's migration potential of organic carbon. By means of subsequent growth assays, conducted for 6 days at 30 °C and 120 rpm, the bioavailability of migrated compounds can be assessed. In a second part, the material is incubated for 14 days at 30 °C and 120 rpm, allowing bacterial growth on the material's surface (sessile) as well as in the water phase (planktonic). The addition of inorganic nutrients during the incubation period allows to determine the material's maximal growth potential together with the concentration of dissolved organic carbon in the water that was not metabolised. Needle sonication and flow cytometry implemented as highly sensitive reproducible techniques to detach and quantify the bacteria within the planktonic phase as well as the biofilm.

RESULTS: Besides repeated tests that were conducted to show the improved sensitivity and

reproducibility compared to conventional methods, a comprehensive set of different materials including polymers, metals and resin coatings were tested (Figure 1).

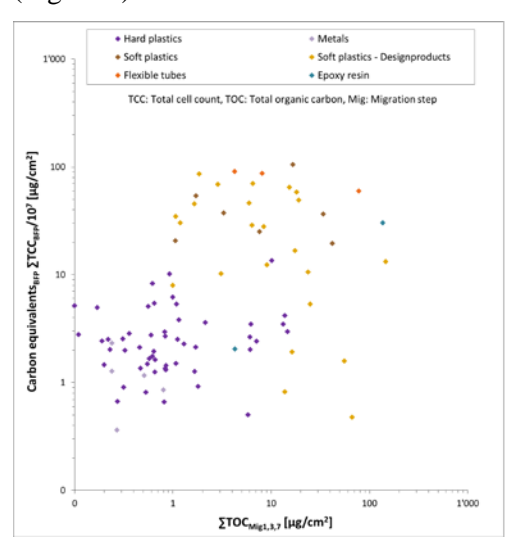


Fig. 1: Extract from BioMig test results.

The results revealed large differences between the materials and that low migration rates (x-axis) were generally associated with low cell growth (y-axis)². In addition, it was found, that the migration rate for some materials was mainly determined by the presence of bacteria instead of higher temperature. This phenomenon hasn't been shown before in this context and was most pronounced in flexible tubes.

DISCUSSION & CONCLUSIONS: The BioMig method allows screening, evaluation and deliberate development of materials with the aim of a nutrient growth limitation. In order to maximise the success in biofilm prevention, such growth-condition-targeted approaches need to be combined with direct antimicrobial material properties.

ACKNOWLEDGEMENTS: This work was financed by a grant from "The Commission for Technology and Innovation CTI" (KTI Nr. 15857.1 PFIW-IW) and by the industrial partners Geberit International AG and Georg Fischer JRG AG.

Influence of early versus delayed antibiotic intervention on treatment of Staphylococcus aureus fracture-related infection in rabbits.

J Puetzler¹, S. Zeiter¹, A Vallejo¹, D Gehweiler¹, RG Richards¹, TF Moriarty¹

AO Research Institute Davos, CH

INTRODUCTION:

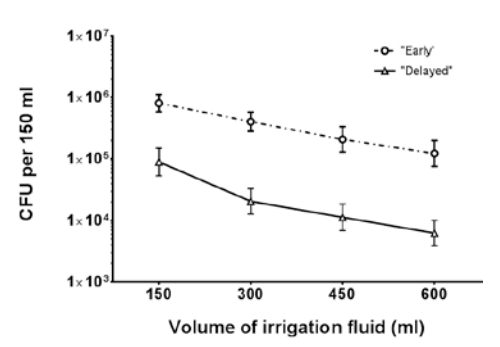
Fracture related Infection (FRI) remains a significant clinical problem. The treatment of FRI over the past decades has been dictated by the classification of Willeneger and Roth¹. This classification stratifies infections based on time of onset of the infectious process: early onset (less than 2 weeks), delayed onset (2-10 weeks) and late onset (>10 weeks) infections. As a general rule, early infections are treated with debridement and antibiotic therapy but do not require implant removal. Delayed and late infections, in contrast, are believed to have a mature biofilm on the implant, and therefore, treatment usually involves implant removal. This distinction between early and delayed infections, and the timing of this transition, has never been established in a controlled clinical or preclinical study ²⁻³. This study tested the hypothesis that early and delayed FRIs respond differently to antibiotic treatment.

METHODS:

A previously described rabbit humeral osteotomy model, with Staphylococcus aureus contamination, was used in this study⁴. In this model, the infection persists for at least 12 weeks without any antibiotic intervention. After bacterial inoculation, the infection was allowed to develop for either 1 or 4 weeks (n= 8 per group). At these time points, treatment commenced and included irrigation and debridement of the wound (no implant removal) and quantitative bacteriological evaluation of the removed materials. Treatment involved two weeks of rifampin plus nafcillin and that was followed by 4 weeks of rifampin and levofloxacin. After a oneweek antibiotic washout period, animals were bacteriological euthanized and quantitative assessment of soft tissue, implant (after sonication) and bone was performed.

RESULTS:

Quantitative measurement of bacterial load at revision revealed that greater numbers of bacteria were recovered by debridement and irrigation in the early group compared with the delayed group (Fig. 1). In both groups, irrigation fluid yielded progressively fewer bacteria (Fig. 1).



1: Amount of bacteria in irrigation fluid removed during revision surgery in the early and delayed groups.

Fig.

At euthanasia, all animals in both the early and delayed groups were infection free. Furthermore, all osteotomies had healed, although radiographic signs of infection were more frequently seen in rabbits of the delayed group (Fig 2).

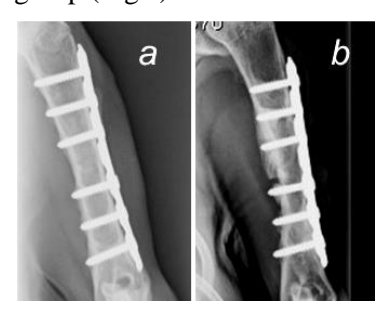


Fig 2. Radiograph illustrating healing of the bone in early (a) and delayed (b) groups at euthanasia. **DISCUSSION & CONCLUSIONS:**

In the delayed group, the total number of bacteria removed was lower, which may indicate retraction of the infection at that stage. However, in both groups, the antibiotic therapy successfully eradicated the infection, suggesting that the biofilm is in fact treatable by antibiotics, and at least in this model, the maturity of the infection does not impact upon treatment success.

Nanocarriers for antimicrobial peptides to fight bacteria and superbugs

M Gontsarik^{1,2}, MT Buhmann¹, A Yaghmur², Q Ren¹, K Maniura-Weber¹, S Salentinig¹*

¹ Laboratory for Biointerfaces, Department Materials meet Life, Empa, Swiss Federal Laboratories for Materials Science and Technology St. Gallen, CH. ² Department of Pharmacy, Faculty of Health and Medical Sciences, University of Copenhagen, Copenhagen Ø, Denmark

INTRODUCTION: Dramatic increase of antimicrobial resistance is of global concern and antimicrobial peptides (AMP's), possessing broad antimicrobial activity, provide a promising alternative to conventional antibiotics¹. However, their solubility in water is generally low and their antimicrobial activity and stability due to chemical degradation in biological systems are poor.² Designing efficient nanocarrier systems for the delivery of membrane active AMP's, with potential to improve their solubility and provide protection degradation, requires against in-depth understanding of their structural characteristics.

METHODS: We examine the effect of integrating the antimicrobial peptide LL-37 at different concentrations into the inverted type cubic phase nanocarriers and evaluate its bactericidal ability against *Escherichia coli*².

Small angle X-ray scattering (SAXS), dynamic light scattering (DLS) and cryogenic transmission electron microscopy (cryo-TEM) were used to characterize and visualize the nanostructres. The antibacterial capabilities were assessed using the broth microdilution assays on *Escherichia coli*.

RESULTS:

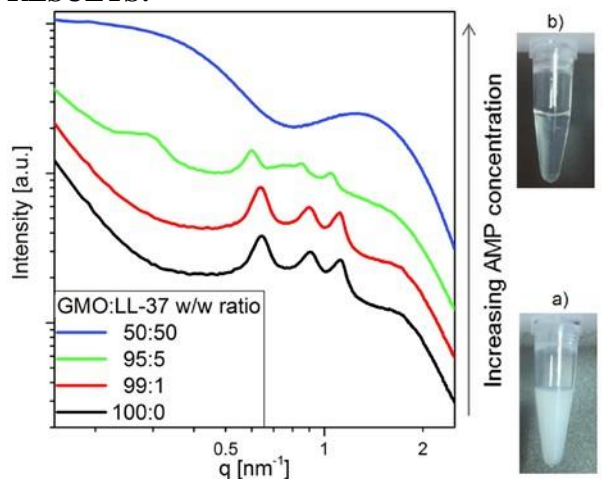


Fig. 1: SAXS curves show Bragg peaks of cubic Im3m phase disappear in response to higher AMP content. The pictures show that the samples are a) turbid at low LL-37 content (cubosomes) and b) transparent at high LL-37 content (vesicles and micelles). Reprinted with permission from Ref. 2. Copyright 2016 American Chemical Society.

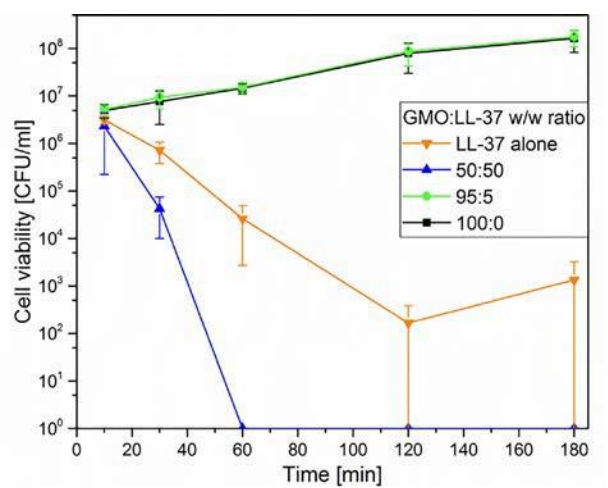


Fig. 2: Bactericidal activity against E. coli of different LL-37 nanoparticlulate formulations. The bacterial culture was treated with LL-37 in form of a free solution (positive control) or as part of selected self-assembled nanostructures: The GMO:LL-37 = 50:50 micelles killed more bacteria after 30 and 60 min compared to free LL-37. Reprinted with permission from Ref. 2. Copyright 2016 American Chemical Society.

DISCUSSION & CONCLUSIONS: SAXS, DLS and cryo-TEM show that LL-37 interacts strongly with the structure forming lipids. It induces nanostructural transformations from inverse cubic to sponge and lamellar phases and micelles in a concentration-dependent manner. These studies, together with in vitro evaluations using *Escherichia coli*, established the composition—nanostructure—activity relationship that can guide the design of new nanocarriers for LL-37 and may provide essential insight into the mechanisms behind the bacterial membrane disruption with peptide-loaded nanostructures.

ACKNOWLEDGEMENTS: Elettra Syncrotrone (Trieste, Italy), CFIM, Department of Biomedical Sciences, (University of Copenhagen, Denmark). *CORRESPONDING AUTHOR: stefan.salentinig@empa.ch

Stem Cells React on Form and Surface – Biological Principles Demand New Platforms for Regenerative Medicine

O. Sterner¹, C. Mathis¹, S. Goehl¹, P. Kugelmeier², S. Zürcher¹, S.G. Tosatti¹

¹ <u>SuSoS AG</u>, Dübendorf, CH. ² <u>Kugelmeiers AG</u>, Zollikerberg, CH

INTRODUCTION:

In modern medical and life science technology, the study of cell clusters is a rapidly expanding field. Availability of scalable cell aggregation and (stem) cell friendly environment is essential. Recently, a unique combination of cell culture vessel form and surface treatment has been developed¹ (Pat. US8911690 B2) and proven to play a critical role in defining the fate of stem cells and simplify the culture and harvesting of a large number of (stem) cell clusters.^{2,3}

Dedicated 3D micro structured cell culture plates consisting of precisely injection-molded microwells provide an optimal environment for cell cluster formation. However, the desired clustering effect can be hindered by cell attachment to the surface of the microwells, which leads to uncontrolled differentiation of stem cells instead of equal cluster formation.

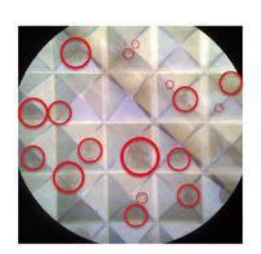
METHODS:

To resolve this cell-adhesion issue, a tailored nonfouling coating is applied via a rapid and simple spray-coating process. Initially an adhesion promoter (AziGrip4TM) is added to the surface followed by functionalization of the structured cellplates with the non-fouling (Polyvynilpyrrolidone, PVP, 1.3 MDa).⁴ The adhesion promoter allows strong covalent bonding between the functional layer and the polymeric substrate material.⁵ This process is so solid that the functional surface remains intact even after x-ray irradiation with 15-20 kGy to meet ISO 11137 for medical use.

RESULTS:

Using the 3D micro-structured cell-culture plates the optimally designed environment enables cell cluster formation. However, structure alone is not sufficient for efficient cluster-formation. A comparison of another product with uncoated microwells with sharp tips versus the non-fouling coated microwells with rounded tips shows cell attachment and dedifferentiation in the first versus

the perfect spherical cell cluster formation in the second product (Sphericalplate 5D).



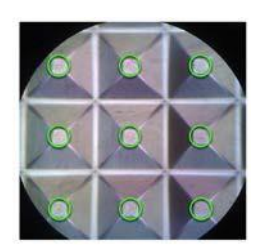


Fig. 1: Stem cell cluster formation comparison between a non-coated surface with sharp tips and a $AziGrip^{TM} EX$ coated cell culture with round tips

DISCUSSION & CONCLUSIONS:

This work describes the successful combination of both geometrical design and surface chemical tuning to arrive at an optimal cell-culture environment to allow cell cluster formation. This methodology reduced uncontrolled also differentiation of cells, resulting from uncontrolled interactions of cells with the substrate material and geometry. The combination of injection molding. spray coating and x-ray sterilisation allows this approach to cover an enormous range of applications with seamless scalability from lab to clinics. Successful laboratory tests for stem cell transplantation applications have been performed and a large scale application for modified human islet transplantation entered preclinical testing.

ACKNOWLEDGEMENTS: The support of Laura Silveira from SuSoS AG is kindly acknowledged.

A standardized rat model for monitoring bone changes in implant-related osteomyelitis with fully automated *in vivo* microCT image processing workflow.

<u>VA Stadelmann</u>^{1,2}, K Camenisch², K Thompson², U Eberli², S Zeiter², TF Moriarty²

¹<u>SCANCO Medical</u>, Bruettisellen, Switzerland, ²<u>AO Research Institute</u> Davos, Switzerland.

INTRODUCTION: Implant-related osteomyelitis is often characterized by bacterial biofilm formation on the implant, followed by osteolysis of adjacent bone and ultimately possible implant failure. However, the temporal patterns of bone morphological changes adjacent to a bacteriacolonized implant are not fully characterized. These patterns, potentially bacteria-, location-, materialand/or patient-specific, could be fundamental in the understanding of implant-related infection, in its diagnostics and its prevention. Here we present a simple rat model with automated and standardized outcome measurements, to study these temporal patterns with various bacterial strains.

METHODS: In this model, the implant is a PEEK miniscrew (Ø1.5×5mm), with 20% BaSO4 for x-ray contrast (RISystem). It is implanted, sterile or preincubated with some bacteria, in a pre-tapped unicortical hole 2mm distal to the growth plate in the medial tibia from a lateral incision. Bone changes are monitored by *in vivo* microCT under

anesthesia at 0, 3, 6, 9, 14, 20 and 28 days post-operatively. The scan region is ø25.6×10mm, centered on the screw, acquired with 25μμm voxels. Scan series are first registered in space then two regions of interest (ROI1 and ROI2) are defined automatically 75 and 700μm from the implant surface respectively (Fig. 1). Bone-implant contact (BIC) is computed from ROI1. In ROI2, periprosthetic bone fraction (BV/TV) is computed directly, then quiescent, resorbed, and newly formed bone are computed from differences

between subsequent scans. Image processing is automatized using IPL (SCANCO); data tidying and processing with R (R Team).

RESULTS: To date, 153 rats have been used with this model, only 3% were excluded for mispositioning of the screw and only 4% of the scans were excluded (mostly due to motion artefacts). In healthy animals, BIC and BV/TV increase rapidly and reach a plateau within 14 days. Screws incubated with *S aureus* show rapid bone loss and are disconnected from bone within 14 days. With *S Epidermidis*, bone loss is observed until day 9 followed by full recovery, and *P Acnes* does not show any significant effect (Fig. 2).

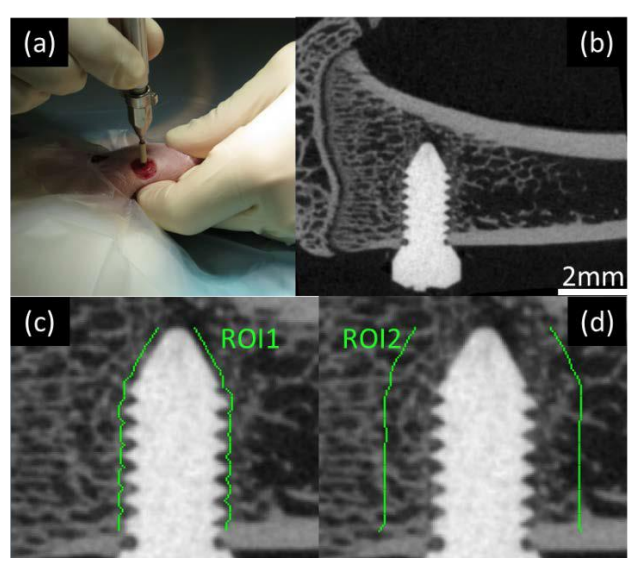


Fig. 1: (a) surgical insertion of a miniscrew in the proximal tibia; (b) post-op microCT; (c) ROI1 for BIC and (d) ROI2 for BV/TV and dynamic histomorphometry.

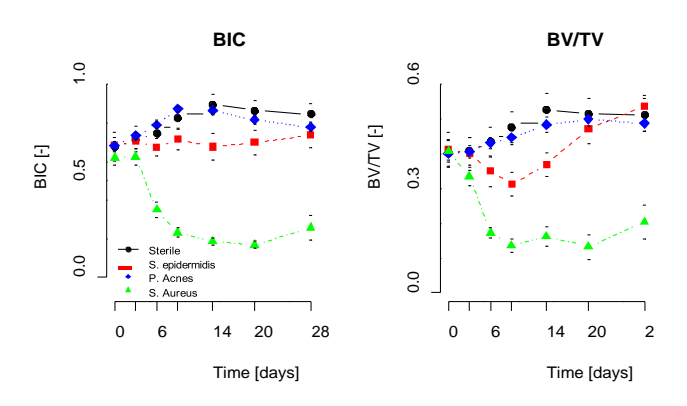


Fig. 2: Evolution of BIC and BV/TV around sterile screws and screws inoculated with S Epidermidis, P Acnes or S Aureus.

DISCUSSION & CONCLUSIONS: The model presented here requires relatively simple surgical and imaging procedures. Image processing has a high CPU cost but is fully automated and user independent, making data comparable between studies or laboratories. The model is sensitive enough to decipher between bacterial strains. Currently, the time course of bone changes under antibiotics treatment is under investigation.

Electrospun scaffolds with organic electronic ion pumps – Novel wound dressings to target skin fibrosis

A G Guex¹, D J Poxson², G Fortunato¹, D T Simon², K Maniura-Weber¹, R M Rossi¹, M Rottmar¹

¹Empa, Swiss Federal Laboratories for Materials Science and Technology, St. Gallen, Switzerland.

²Laboratory of Organic Electronics, Linköping University, Norrköping, Sweden.

INTRODUCTION: The high prevalence of fibrosis in medical conditions, in particular during skin wound healing, has only been addressed marginally, and there is currently no successful and promising therapeutic concept available to specifically hamper fibrosis at an early stage or to prevent scar formation entirely [1]. It has been hypothesised that healing rates can be enhanced by decreasing the pH level of wounds from pH ~8 (chronic stage) to pH ~6 [2]. One potential mechanism has been attributed to an alteration of fibroblast to myofibroblast transition at lower pH. Lowering the pH of wounds by highly specific and controlled H⁺ delivery to the site of interest is thus an attractive concept for the treatment of chronic wounds. Organic electronic ion pump (OEIP) devices have the potential to provide localised proton delivery at high dosage precision [2]. The current project therefore focuses on the design of a novel wound dressing, electrospun scaffolds with technology for controlled proton delivery.

METHODS: Differentiation of human dermal fibroblasts (HDF) into myofibroblasts was induced by TGFβ-supplemented medium. To test our hypothesis of reduced differentiation in an acidic environment, medium pH was adjusted to 6. In follow up studies, proton delivery was controlled by ion pumps. OEIP were designed as previously reported [2]; proton delivery monitored with methyl red pH indicator. Current-controlled H $^+$ delivery to HDF culture was then evaluated with a free-standing OEIP having its delivery outlet aligned with the bottom of the cell culture well. Differentiation of HDFs was assessed by immunofluorescent staining for α-SMA.

RESULTS: Prior to evaluation in cell culture, OEIP function was investigated in modified, buffer-free cell culture medium. At an applied current of 5 μ A, OEIP were shown to provide continuous proton delivery. An immediate local pH change at the OEIP outlet from 7.4 to ~4.4 (based on methyl red pH indicator) was observed (Fig. 1). Our initial hypothesis was then investigated by lowering differentiation medium pH to 6.0. The acidic environment was shown to inhibit fibroblast to myofibroblast differentiation, indicated by reduced

expression of α -SMA compared to fibroblasts cultured in standard differentiation medium (Fig. 2A). We then evaluated OEIP-controlled H⁺ delivery to a HDF monolayer. In close proximity to the OEIP outlet, reduced expression of α -SMA was found, compared to fibroblasts at further distance (several mm) from the outlet (Fig. 2B).

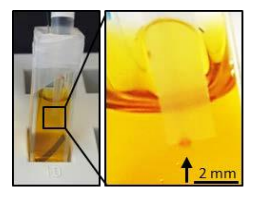


Fig. 1: Photographs of OEIP in modified cell culture medium. A red spot at the orifice indicates locally reduced pH (methyl red).

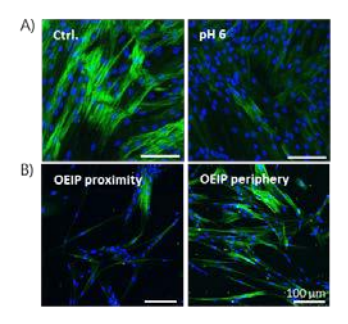


Fig. 2: Confocal microscopy images of fibroblasts / myofibroblasts stained for α -SMA (green) and nuclei (blue). A) Medium pH of 6 induced reduced α -SMA expression. B) In close proximity of the OEIP outlet, α -SMA expression was reduced compared to cells at further distance.

DISCUSSION & CONCLUSIONS: Our results show reduced fibroblast to myofibroblast differentiation in an acidic environment. Furthermore, a local pH change with concomitantly reduced expression of α -SMA in close proximity to the OEIP outlet could be demonstrated. Controlled proton delivery from a wound dressing could thus be a promising therapeutic strategy to reduce or even prevent skin wound scarring.

Tyramine modified hyaluronic acid ink for 3D-printed cellularized construct

D Petta^{1,2}, DW Grijpma^{2,3}, A Armiento¹, D Eglin¹, M D'Este¹

¹ AO Research Institute Davos, Davos, CH. ² Department of Biomaterials Science and Technology, University of Twente, Enschede, NL. ³ Department of Biomedical Engineering, University Medical Center Groningen, University of Groningen, Groningen, NL

INTRODUCTION: Hydrogels are particularly attractive as biomaterial for 3D printing due to their viscoelastic properties and cytocompatibility [1]. In this work, naturally-derived biocompatible hyaluronic acid was modified with tyramine moieties (HA-Tyr) and a double enzymatic and photoinitiated crosslinking mechanism was applied to print stable 3D structures. The constructs were seeded with human Mesenchymal Stromal Cells (hMSCs) and the viability was assessed.

METHODS: HA-Tyr with a degree of substitution 14.5% was synthesized via amidation reaction [2]. A weak hydrogel (G' = 100 Pa) was formed using 0.1 u/ml horseradish peroxidase (HRP) and 0.17 mM hydrogen peroxide (H_2O_2). A 3D Discovery® system from RegenHU Ltd was used for printing; the criss-cross structures were further stabilised with green light (λ =504 nm) in presence of Eosin Y. Resolution of the printed struts was optimized tuning printing speed, pressure and needle inner diameter. Scaffolds were post-functionalized with RGDY adhesive peptide (GenScript USA Inc.). 1.5 10^6 cells/ml hMSCs at P3 were seeded onto the scaffolds both functionalized and not and Live/Dead staining performed at 1 and 10 days.

RESULTS: In the tested conditions HA-Tyr strut size could be varied from 200 µm to 1500 µm (Tab. 1). An increase in the pressure led to a wider strut, whereas an increase in the printing speed led to narrower size. In order to print structures with high shape-fidelity, a 0.35 mm cylindrical needle and a printing speed of 4 mm/s were selected. In these conditions, a pressure of 3 bar resulted in a strut width of 800 µm. Strut diameters wider than 800 µm resulted in the absence of porosity. With the 0.35 mm cylindrical needle pressures below 2 bar were not suitable for printing. No hMSCs attachment was observed seeding the constructs with no RGDY functionalization (Fig. 1a). Cells seeded on top of RGDY-functionalized scaffold showed attachment and spreading throughout the 3D construct at day 10 (Fig.1b).

Table 1. Strut width in μm of 3D printed scaffolds. Colours represent different needle inner diameter (yellow and grey: cylindrical 0.35 mm and 0.4 mm, blue: conical 0.51 mm)

Pressure [bar]	Printing Speed [mm/s]		
	2	4	6
1	797	430	250
1	1369	1095	900
1.5	1689	1100	851
1.5	1500	900	580
2	482	261	200
2	> 1500	1500	1300
3	1000	800	760

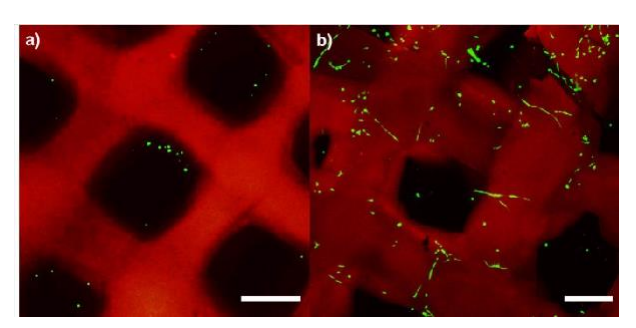


Fig. 1: hMSCs seeded on top of the non-functionalized (a) and RGDY modified (b) scaffold after 10 days of culture (scale bars = $500 \mu m$).

DISCUSSION & CONCLUSIONS: HA-Tyr hydrogel is an effective ink in extrusion-based 3D printing as the dual mechanism of enzymatic and light crosslinking allows for optimal extrusion and shape retention, respectively. A post-printing functionalization of the scaffold is needed in order to promote cell attachment and proliferation onto the 3D construct. Current work is focused on the possibility to fabricate cell-laden HA-Tyr scaffolds.

High hydrostatic pressure for decontamination of soft biomaterials

M D'Este¹, A Plumecoq², M Alini¹, G Demazeau²

¹ AO Research Institute, AO Foundation, Davos, CH. ² HPBioTECH Leognan, FR.

INTRODUCTION: Sterilization of implantable biomaterials for bacteria and spore decontamination is a fundamental step for material preparation. However typical clinical sterilization methods compromise to different extents chemical and mechanical properties of the implants. This issue is particularly sensitive for soft materials such as hydrogels (HGs), intrinsically prone to degradation and even more under the conditions necessary to eliminate microorganisms. Here we tested a novel approach of high hydrostatic pressure (HHP) process for decontamination of bacteria and spores in HGs. A decontamination method was initially developed for vegetative species and extended to a standard panel of microorganisms including bacterial spores and organisms known to be baroresistant. The method was tested against HGs with different gelation mechanisms.

METHODS: Polyvinyl alcohol (PVA) was dissolved at 10% w/v in PBS and freeze-thawed 10 times in cylindrical moulds of 22 mm diameter producing discs of 5 mm height. Carboxymethyl cellulose (CMC) 8% and methylcellulose (MC) 4.5% were dissolved in PBS until homogeneity. For HHP treatment gels were packaged in specific flexible multi-layer films. The HHP process in such a novel approach was defined by 6 parameters: pressure **P**, temperature **T**, pressure application rate VA, and mode MA (with n_A :number of cycles, t_A:duration of each cycle and t_L: latency time (involved in spore decontamination) A parametric study was performed by independent variation of these parameters in order to identify the best HHP treatment conditions in terms of inactivation efficiency. For setting HHP parameters MC and CMC hydrogels were inoculated with Bacillus cereus as spores for quantitative bacteriology before and after HHP treatment; the conditions were then applied to other species. Mechanical spectrum of the hydrogels was measured in triplicate, except for PVA for which an unconfined compression test was performed on 5 replicas.

RESULTS: The following parameters resulted in the best decontamination: P=350Pa; GP= 1MPa/s; LT=5 minutes; MA=3x5 minutes; T=35°C. Under these conditions the following species could be

cleared out of the gels: *E. coli, S. enteritidis, A. brasiliensis, S.cerivisiae, B. subtilis, B cereus, P. aeruginosa, S. aureus.* Steam sterilisation reduces HG rheological properties, while for HHP the changes are barely detectable (fig 1). Likewise HHP treatment did not change significantly PVA gels mechanical properties, whereas thermal treatment brought to their dissolution.

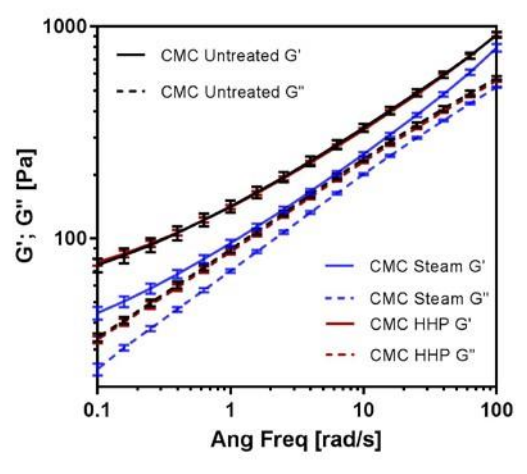


Fig1: Viscoelastic spectrum of CMC hydrogels native, HHP-treated and steam sterilisation-treated.

DISCUSSION & **CONCLUSIONS:** While vegetative organisms are easily eliminated by HHP, bacterial spores are much more challenging. The method here developed was able to eliminate bacterial spore-forming B.cereus and B.subtilis. In HHP the developed energy in the system is a tiny fraction in comparison to steam sterilisation, therefore the change in the rheological and mechanical properties are minor; the variation amount is material-dependent. Further studies are necessary to validate the method by extending micro-organisms range and concentration. Such a novel approach of HHP processes allowing the inactivation of vegetative forms and spores is a promising method for microbial decontamination of soft biomaterials.

ACKNOWLEDGEMENTS: Partial financial support from the Swiss National Science Foundation and Agence Nationale de la Recherche (ANR) though ERANet under EuroNanoMed-II, Project number: 31NM30_152035.

An explant model to study the adhesion and chondrogenic potential of injectable scaffolds for cartilage repair

E Cavalli¹, N Broguiere¹, LA Applegate², M Zenobi-Wong¹

¹Cartilage Engineering + Regeneration, ETH Zürich, Zürich, Switzerland, ²Department of Musculoskeletal Medicine, University Hospital of Lausanne, Switzerland

INTRODUCTION: In this study, we present a cartilage explant model to study the adhesion and chondrogenic potential of injectable scaffolds both *in vitro* and *in vivo* in small animals. The gel used is a novel biomimetic hydrogel based on a modified hyaluronic acid (HA-TG). HA-TG is injectable with a crosslinking time of less than 2 minutes and strongly adheres to cartilage tissue. When seeded with human epiphyseal chondroprogenitor cells (hCCs), this hydrogel is able to promote cell proliferation and cartilaginous matrix deposition. HA-TG is stable and maintain its adhesive properties for up to 6 weeks *in vivo*.

METHODS: HA-TG was synthetized according to a recently developed protocol [1] and mixed with 15 mio/ml hCCs [2]. The gels were investigated both alone and in a bovine ex-vivo explant model (*Figure* 1). The constructs were cultured for 3 weeks in chondrogenic media in either nomoxic (21% O₂) and hypoxic (2% O₂) conditions, then implanted subcutaneously in nude mice. The adhesive properties of the gel were investigated with pushout test before and after implantation. During the time *in vivo* the constructs were also imaged with ultrasound and photoacoustic to non- invasively monitor their size and vascularization.

RESULTS: Adhesive properties of the gels to the cartilage ring investigated by push-out test showed initial bond strength of 1.5kPa, 4 times higher than fibrin glue. The bond strength of the gel to the cartilage was maintained for up to 6 weeks both *in vitro* and *in vivo*.

When the gels were seeded with hCCs and cultured for 3 weeks within bovine cartilage explants, the bond strength increased to 82kPa and 55 kPa for normoxia and hypoxia respectively, likely due to matrix production and remodeling as suggested by collagen production. HA-TG gels were shape-stable for 6 weeks *in vivo*, as confirmed by ultrasound imaging and prevented vascular ingrowth as confirmed by photoacoustic imaging. In addition, the gels supported the construct maturation reaching 300kPa and 153 kPa in bond strength for normoxia and hypoxia respectively.

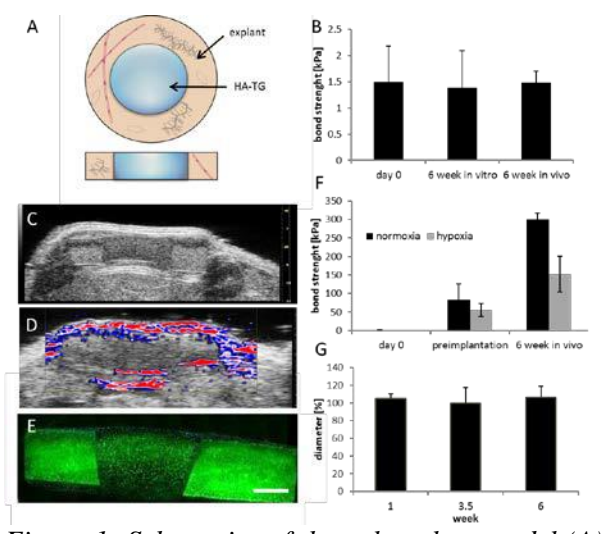


Figure 1: Schematics of the gel-explant model (A). Bond strength of HA-TG gels without cells to cartilage explants after crosslinking, after 3 weeks of in vitro culture and after 6 more weeks in vivo (B). Ultrasound image (C), photoacoustic image (D) and collagen 2 staining (E) of HA-TG in the explant in vivo. Bond strength of HA-TG scaffolds with hCCs on the day of crosslinking (day 0), after 3 weeks of culture in vitro (preimplantation) and after 6 additional weeks in vivo. The data are given both for normoxic and hypoxic culture conditions (F). Diameter of HA-TG during the time of the in vivo culture: 1, 3.5 and 6 weeks after implantation (G). Scale bar: 2mm

DISCUSSION & CONCLUSIONS: The cartilage explant model represents an inexpensive tool to mimic a cartilage defect both *in vitro* and *in vivo* in a subcutaneous mouse model. It allows to rapidly test cartilage-hydrogel interactions and showed that, due to its adhesive properties and injectability, HA-TG represents a promising alternative to the current cartilage repair techniques.

ACKNOWLEDGEMENTS: This project was funded by the ETH Foundation (ETH-50 13-1).

Calcium signaling in tendons: an early response to mechanical loading

FS Passini^{1,2}, KD Ferrari^{3,4}, AS Saab^{3,4}, S Caprara^{1,2}, B Weber^{3,4}, JG Snedeker^{1,2}

¹ Institute for Biomechanics, ETH Zurich, Switzerland. ² Balgrist University Hospital, University of Zurich, Switzerland. ³ Institute of Pharmacology and Toxicology, University of Zurich, Switzerland.

⁴ Neuroscience Center, University and ETH Zurich, Switzerland

INTRODUCTION: Uniquely designed to withstand great forces, tendons play an essential role in the musculoskeletal system to transmit loads from muscle to bone and enable movement. Mechanical loading is the dominant extrinsic factor that controls tendon homeostasis [1]. However, how tendon cells (tenocytes) convert mechanical forces into biological signals is poorly understood. In this study, we investigated the role of calcium, as a ubiquitous intracellular second messenger, in tendon mechanotransduction.

METHODS: Tendon fascicles were gently extracted from the tail of skeletally mature Wistar rats (14-16 weeks old, female). Rat tail tendon fascicles (RTTFs) were stained with 5µM Fluo-4 AM for 2h in a modified Krebs-Henseleit solution at 29°C and 3%O₂. The RTTFs were then mounted on a customdesigned tensile stretching device placed on the stage of a spinning disc confocal microscope. Single RTTFs were stretched at three different strain rates (0.01, 0.1, 1.0%L₀/s) from 0 to 10% strain and images were acquired at the same time. As a control, images of the RTTFs were taken at a preload of 1MPa prior the stretching protocol. The acquired time lapses were analyzed in two steps: first a motion correction was applied, then calcium events were automatically detected and measured using CHIPS (Cellular and Hemo-dynamic Image Processing Suite) [2].

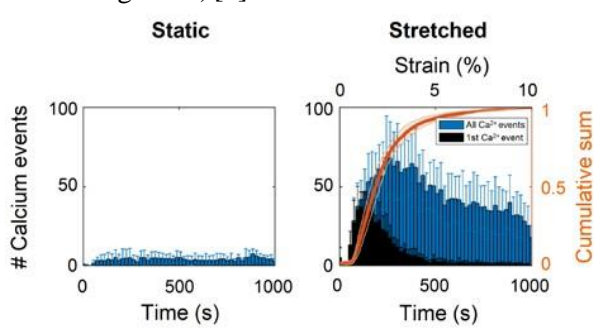


Fig. 1: Left: calcium signaling at the preload (static condition) is nearly absent. Right: once the RTTFs are subjected to stretching (0.01%Lo/s), tenocytes respond with distinct calcium events (stretched condition).

RESULTS: Mechanical loading of the RTTFs caused a marked increase in calcium signal frequency, showing a magnitude-dependent response. The cumulative sum (CS) of the first calcium event of each tenocyte displays a sigmoidal increase, with a $CS_{50} = 1.9 \pm 0.2\%$ strain (Fig. 1). Such mechanical thresholds were observed to be strain rate dependent (Fig. 2). At the tissue level, viscoelastic phenomena were detected, with higher stiffness of the RTTFs at increasing strain rate.

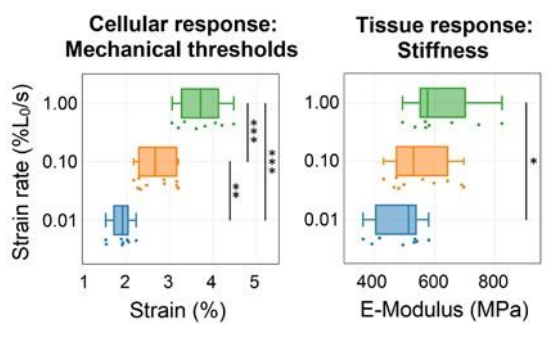


Fig. 2: Left: strain rate dependency of mechanical thresholds (50% threshold of the cumulative sum, i.e. CS_{50}). Right: strain rate dependent stiffness of the RTTFs. Statistical analysis has been done with R using a one-way ANOVA with multiple measures. Statistically significant differences: p<0.05, ** p<0.01, *** p<0.001.

DISCUSSION: To our knowledge, this is the first study to demonstrate calcium signaling in *ex vivo* tendons as an early response to mechanical loading. Tissue specific mechanical thresholds were obtained from magnitude and strain rate dependent calcium signals. Such thresholds provide key information for further basic tendon research as well as for physical rehabilitation purposes. Future studies are needed to better understand the mechanisms and effects of the observed calcium signaling.

Bone marrow mesenchymal stem cells actively participate in the recruitment of murine hematopoietic stem cells in bioengineered minimalistic bone marrows

Q Vallmajo-Martin^{1,2}, A Negro², M Lutolf², M Ehrbar¹

¹ <u>Laboratory for Cell and Tissue Engineering</u>, Division of Obstetrics, University Hospital Zürich, CH. ² <u>Laboratory of Stem Cell Bioengineering</u>, Institute of Bioengineering, EPFL, Lausanne, CH

INTRODUCTION: Bone marrow transplants are the only available therapy for many cancers involving blood cells, such as leukemia or lymphoma. A major limitation of this treatment is the availability of hematopoietic stem cells (HSCs). Their expansion ex vivo remains a major challenge in medicine today. HSCs grown in vitro rapidly lose their regenerative capacity likely due to the lack of niche-derived signals comprising molecular and cellular components [1]. Identification of critical hematopoietic niche components necessitates the generation of more tractable in vivo models. An attractive solution is to combine a blank biomaterial with different growth factors and cell types known to be present in the niche in vivo. To date, novel approaches for heightened throughput of screening such systems in vivo are lacking. Here, we present a minimalist human bone marrow model based on a synthetic material, and have applied it for use in discovery of critical HSC niche factors.

METHODS: Human mesenchymal stem cells (hMSCs) were encapsulated in functionalized biomimetic polyethylene glycol (PEG) hydrogels [2] with or without bone morphogenetic protein-2 (BMP-2). These PEG gels were polymerized directly in eight individual wells of a novel multiplexing polydimethylsiloxane (PDMS) device. Then, the screening devices containing PEG hydrogels were subcutaneously implanted in immunocompromised mice (4x per animal), resulting in 32 unique conditions per mouse (Fig 1). At 8 weeks the devices were harvested and analyzed for bone and bone marrow formation by microCT, histology, and FACS.

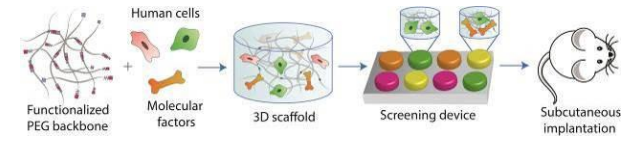


Fig.1: In vivo niche screening device. Modular PEG hydrogels, growth factors and cells are employed to create microenvironments of variable composition in the 4x 8-well screening devices that are subcutaneously implanted per mouse.

RESULTS: MicroCT analysis revealed mineralization in all wells containing gels with

hMSCs, with or without BMP-2. Histological analysis corroborated these findings. Hydrogels containing hMSCs and BMP-2 developed into bone marrow-like constructs including a typical bone shell filled with marrow and trabecular bone structures (Fig 2A). Ultimately, long-term HSC enrichment in the constructs containing cells and BMP-2 compared to only BMP-2 gels was confirmed by FACS analysis on the recruited murine cell population (Fig 2B). Intriguingly, qPCR of retrieved hMSCs revealed heightened expression of osteogenic markers in all samples irrespective of BMP-2 addition. These results indicate the formation of a functional ectopic niche in cell-laden and fully synthetic hydrogels.

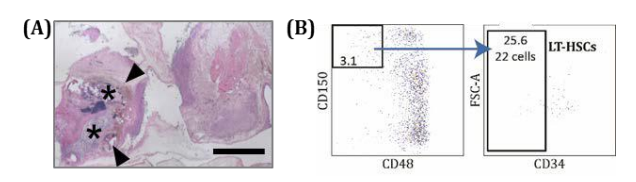


Fig. 2: Evaluation of HSC niche. (A) H&E staining show ectopic ossicle formation (arrows) and bone marrow-like cavities (*) in cell-laden gels loaded with BMP-2, scale bar 2mm. (B) FACS analysis of ossicles shows presence of long term HSCs.

DISCUSSION & CONCLUSIONS: Hydrogel conditions, cell type, and soluble factors were screened to optimize conditions for bone marrow niche formation *in vivo*. Results indicated a direct participation of hMSCs in both bone formation and murine HSCs recruitment. This device represents a powerful new tool for heightened *in vivo* screening of tissue engineering constructs with a broad range of applications.

ACKNOWLEDGEMENTS: This work was funded by the Swiss National Science Foundation grant 153316.

Functionalization of poly lactic acid surfaces with Ca-complexing groups for bone cement applications

E. Mulky¹, D. Hegemann², G. Fortunato², J. Sague¹, K. Maniura², M. Frenz³, R. Luginbuehl¹ *RMS Foundation, Bettlach, CH.* ²*Empa, St. Gallen, CH.* ³ *University of Bern, Bern, CH.*

INTRODUCTION: Polymer reinforced calcium phosphate (CaP) based bone composites mismatch in their interfacial energy between the hydrophobic poly lactic acid polymer (PLA) and the hydrophilic calcium phosphate matrix. This mismatch results in weak interfaces and poor mechanical composite properties [1]. Chelating molecules such as the aspartic acid have a high affinity towards calcium ions. It is hypothesized that the presence of such molecules attached at the surface of the PLA results in enhanced ion adsorption and therefore an increased interfacial adhesion between the CaP matrix and the PLA manifested in improved mechanical properties CaP.

In this work, the surface of PLA monofilaments was modified using water vapor based RF plasma [2], and subsequently chemically reacted with aspartic acid, a natural amino acid as chelating molecule. The adhesion strength of the modified surfaces versus CaP was analysed by pull out tests of embedded filaments in CaP cylinders. Finally, the PLA filament surface was analysed for calcium content.

METHODS: The surface of poly lactic acid based monofilaments was coated using a water vapor based radio frequency plasma of 13.56 MHz (WV) with a gas mixture consisting of Ar, H₂O and C₂H₄. A subset of the treated filaments was immersed in a 2-(N-morpholino)ethanesulfonic acidic buffer at pH 6 and reacted with aspartic acid (ASP) using ethyl(dimethylaminopropyl) carbodiimide and N-Hydroxysuccinimide. PLA monofilaments of 80 mm length and 0.8 mm diameter were embedded at a depth of 10 mm into brushite cement cylinders of 30 mm height and 20 mm diameter, which were left to set for 3 days, and subjected to pull-out tests. Calcium residues and surface roughness of the filaments were subsequently analysed using scanning electron microscopy (SEM) and their calcium content quantified using energy dispersive X--ray spectroscopy (EDX).

RESULTS: Samples containing either aspartic acid or the WV only exhibited the highest concentrations of adsorbed calcium (5±4%, 4±3% w/w) when compared to untreated control group (2±2% w/w). Pull-out strength was 18±5 MPa for the ASP filaments, 13±6 MPa for the WV

filaments and 15 ± 2 for the control filaments. Filament roughness was highest in the WV group, followed by the ASP with the control samples having the lowest roughness.

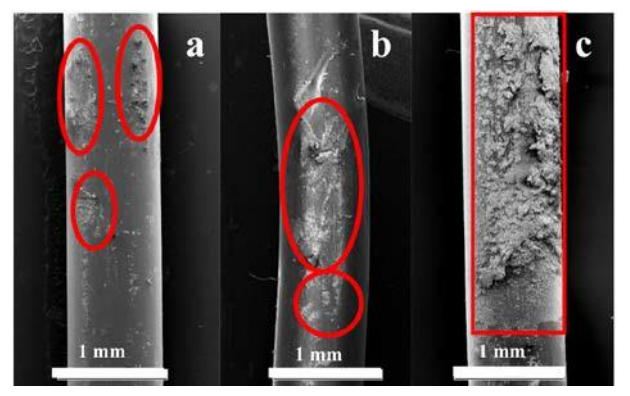


Fig. 1: SEM micrographs of PLA filaments pulled out from CaP samples. The different surface treatments are: a) control, b) WV, c) ASP. CaP residues are indicated with red borders

DISCUSSION & CONCLUSIONS: The EDX

results show that both WV and ASP resulted in an increase in the adsorption of calcium on the surface of PLA compared to the untreated controls. While the pull-out test results were inconclusive, the increased presence of calcium (Fig. 1) coupled with a lower roughness of the ASP samples as compared to the WV and control samples indicate a beneficial effect of ASP. These results show that the surface treatment of PLA with ASP increases surface calcium adsorption which could possibly be beneficial for cell adhesion on polymeric substrates.

ACKNOWLEDGEMENTS: This work was partially supported by the Swiss National Research Fund, grant no. 406440_131273. The authors would like to acknowledge Thomas Niessen and Stefan Röthlisberger for their help with plasma processing and pull-out testing.

Hybrid polymeric structure for drug delivery purpose adaptable to photo-crosslinkable resin <u>O. Guillaume</u> ¹, X. Zhang ², R.G. Richards ¹, T. Peijs², D. Eglin ¹ and J. Gautrot ²

1 AO Research Institute Davos, CH.

2 School of Engineering and Materials Science, Queen Mary, University of London, UK.

INTRODUCTION:

Poly(trimethylene carbonate) (PTMC) is a biocompatible and degradable polymer material with great potential in the field of drug delivery system and tissue engineering. Nevertheless, the first limitation is due to its poor mechanical property. Secondly, PTMC-based biomaterials are commonly fabricated using photo-reaction, which restricts the possibility to incorporate therapeutics within the photo-polymerizable matrix due to incompatibility and loss of biological activity.

To alleviate such limitations, we developed a polymer-polymer hybrid film loaded with drug model (*i.e.* dexamethasone), which improves mechanical stability [1] and maintains its therapeutic activity after photo-fabrication.

METHODS:

<u>Dexa-loaded PLA fibers</u>: PLA solution at 9 wt% in chloroform/DMF (3/1) was loaded with Dexa (0.68 weight % in respect to PLA). Electro-spinning was carried out at voltage of 18-20 kV and at a distance of 15 cm. PLA nanofibers without or with Dexa were produced (PLA- and PLA+).

Hybrid photo-crosslinked PMTC/PLA films: Solution of three-armed PTMC methacrylate-ended was prepared with photo-initiator (I2959) with PLA nanofibers, and composite films were pre-formed in a hot press (60 °C for 5 min under 25 bar). Finally, UV-curing was performed at 15 mW/cm² for 100 sec.

In vitro osteogenic experiments:

Human bone marrow mesenchymal stem cells (hBMSCs) were seeded at 20 000 cells/cm² on Dexafree (PTMC/PLA-) and compared to PTMC/PLA + loaded with Dexa. During 28 days, films were maintained in osteogenic media but depleted of any Dexa. Osteogenic differentiation of hBMSCs were analysed by Alkaline Phosphatase and Alizarin Red (calcium deposition) staining.

RESULTS:

PLA-loaded Dexa nanofibers were electrospun and incorporated into PTMC photo-crosslinkable matrix (Fig. 1A and B). The *in vitro* experiments revealed that Dexa released from PTMC/PLA+

was able to significantly increase ALP activity and mineralization (ARS). In comparison, low degree of staining for ALP and ARS was observed for Dexafree PTMC/PLA- groups.

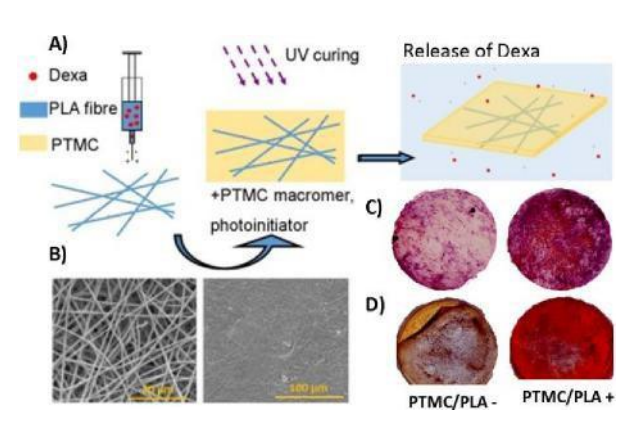


Fig. 1: Release of Dexa from polymer-polymer composite drives osteogenic hBMSCs differentiation. A) Fabrication and SEM observation of PLA nanofibers incorporated into photocrosslinkable PTMC matrix. Osteogenic differentation of stem cells cultivated on PTMC/PLA+, analysed by ALP (C) and ARS (D) staining after 21 days (PTMC/PLA – corresponds to the Dexa-free negative).

DISCUSSION & CONCLUSIONS:

We have already shown that incorporation of PLA nanofibers within the photo-crosslinked PTMC matrix reinforced the polymeric structure [1]. In this second study, we demonstrated that this hybrid polymer-polymer structure can be loaded with drug, such as Dexa, which maintains its biological activity on stem cells even after matrix photo-crosslinking. This work opens the field of drug-loaded polymer matrices fabricated using photo-reaction, such as stereolithography.

ACKNOWLEDGEMENTS:

Funding provided by NSFC-DG-RTD Joint Scheme (Project No. 51361130034) and the RAPIDOS project under the European Union's 7th Framework Programme (Project No. 604517).

Enhancing endothelialisation of electrospun membranes *via* biofunctionalization for a bioinspired blood material interface

A Mertgen^{1,2,3}, AG Guex^{1,2}, G Faccio¹, G Fortunato², RM Rossi², M Rottmar¹, K Maniura-Weber¹

¹Biointerfaces and ²Laboratory for Biomimetic Membranes and Textiles, Empa, Swiss Federal

Laboratories for Materials Science and Technology, St. Gallen, Switzerland.

³Lab for Applied Mechanobiology, D-HEST, ETH Zürich, Switzerland.

INTRODUCTION: Although ventricular assist devices are, due to donor organ shortages, increasingly used for long-term treatment of heart failure patients, the materials in these pumps eventually induce blood coagulation, often with fatal outcome. The aim of this study is to prevent coagulation by mimicking the perfect blood tissue interface found in nature: the inner blood vessel wall. On the luminal side is a monolayer of endothelial cells (EC) in direct blood contact, with layers of extracellular matrix and smooth muscle cells (SMC) as support structure underneath. Here, electrospun polymer membranes will be decorated with cell type specific adhesion peptides for EC or SMC to locally steer cell attachment. Ultimately, this will allow controlled and targeted cell attachment, intercellular communication, cellular functionality similar to their natural environment [1,2].

METHODS: Nanofibrous scaffolds were produced by electrospinning of poly-ε- caprolactone (PCL). For the subsequent peptide immobilization, dopamine was polymerized on the mesh surface (PCL-Pdop) followed by binding of RGD peptides via Michaels addition on the polydopamine layer (PCL-Pdop-RGD) [3]. Surfaces were assessed by X-ray Photoelectron Spectroscopy (XPS). Human Umbilical Vein Endothelial Cells (HUVECs) were seeded on PCL- Pdop and PCL-Pdop-RGD scaffolds and cultivated for 4 hours in serum free medium; their adhesion was evaluated by immunofluorescent microscopy

RESULTS: Polydopamine coating and peptide immobilization increased the nitrogen surface concentration as shown in Fig. 1a. Variations in O/C and increase in N/C ratios show the effective immobilization of RGD peptides (Fig. 1b). When cultured on the functionalized membranes for 4 hours, HUVECs were more spread on the PCL-Pdop-RGD membranes than on PCL-Pdop samples, also indicating the successful immobilization and bioavailability of the peptides.

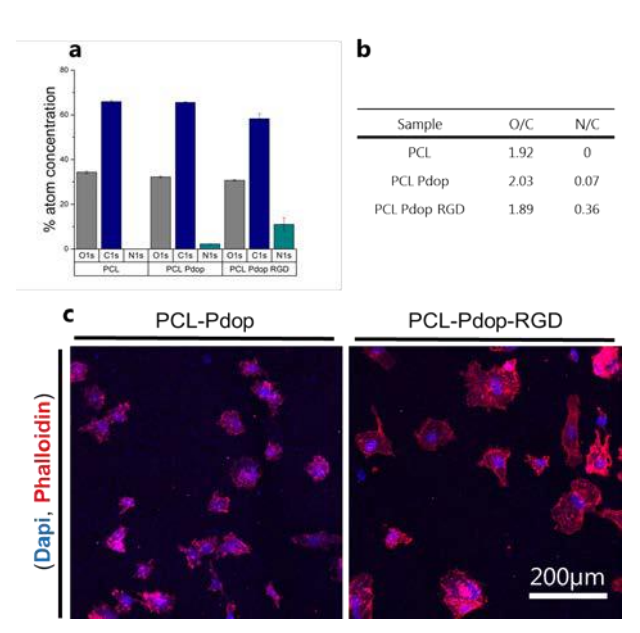


Fig. 1: (a) atomic concentration on PCL, PCL-Pdop, and PCL-Pdop-RGD surfaces measured by XPS. (n=2) (b) O/C and N/C ratios derived from XPS measurements (c) HUVECs on PCL-Pdop or PCL-Pdop-RGD fibres after 4 hours and stained for actin (red) and nuclei (blue).

DISCUSSION & **CONCLUSIONS:** The proposed biofunctionalization allows steering the initial attachment of HUVEC on PCL substrates. The long-term stability of these surfaces is currently assessed. In the next step, cell-specific adhesion peptides and combinations thereof will be immobilized to identify optimal conditions for targeted and locally encoded EC and SMC adhesion.

ACKNOWLEDGEMENTS: This project is part of the Zurich Heart Project (Hochschulmedizin Zürich).

Tyramine-modified hyaluronan hydrogel for human chondrocyte encapsulation: cell viability, rheological and bioadhesive properties

P Behrendt^{1,2}, S Lippross², RG Richards¹, M. Alini¹, D Eglin¹, AR Armiento¹

¹ <u>AO Research Institute</u> Davos, AO Foundation, Davos, CH. ² <u>Department of Orthopaedics and Trauma Surgery</u>, University Medical Center, Kiel, Germany

INTRODUCTION: Regeneration of cartilage defects using cell-laden injectable hydrogels provides a desirable approach for autologous chondrocyte implantation. For this purpose, a tyramine-modified hyaluronic acid-based (HA-Tyr) hydrogel has been developed that covalently crosslinks in a horseradish peroxidase (HRP)-catalysed reaction in presence of hydrogen peroxide (H₂O₂) [1]. In this study, the influence of the crosslinking conditions on the cytocompatibility of human chondrocytes in 2D and HA-Tyr hydrogel as well as the rheological properties and the bonding strength of HA-Tyr to native cartilage are reported.

METHODS: Monolayer expanded human articular chondrocytes (hCh) were exposed to various concentrations of HRP (0.1-1.0U/ml) and H₂O₂ (50–1200μM) and cell viability was assessed using CellTiter-Blue® after 24h and 96h of treatment. A reduced range of HRP (0.5-1.0 U/ml) and H₂O₂ (150-1200µM) concentrations was used to determine the viability of hChs embedded within HA-Tyr hydrogel. Live/dead staining was analysed by confocal microscopy. The visco- elastic properties of HA-Tyr with and without cells were determined by rheological measurement. To measure the adhesive strength of cell-free HA-Tyr (degree of tyramine substitution: 14 w/v%) to native cartilage, push-out tests were performed using articular cartilage isolated from bovine stifle joints. Samples were processed for histological analysis before and after the push-out test. All experiments performed in triplicate, statistical significance p > 0.05.

RESULTS: In monolayer culture, all concentrations of HRP tested alone caused a moderate decrease in cell viability at both 24h and 96h, whereas $\rm H_2O_2$ alone caused a dose-dependent decrease in cell viability with no recovery at 96h after exposure at $1200\mu M$. Simultaneous treatment with HRP and $\rm H_2O_2$ resulted in a dose-dependent decrease in cell viability with increasing concentration of HRP positively influencing cell viability (ED50 at 96h [μM $\rm H_2O_2$]: HRP $\rm 1.0 = 1386.43$, HRP $\rm 0.5 = 897.19$, HRP $\rm 0.1 = 676.69$).

In 3D culture, live/dead staining imaging showed a homogenous cell distribution. hChs appeared viable and round-shaped at 24h and after 14. Live/dead and CellTiter-Blue® data correlated and a trend for decreasing cell viability with higher dosages of H₂O₂ was found. Within a biocompatible dosage range of HRP (1–0.5U/ml) and H₂O₂ (150–600 μ M) the rheological properties of HA-Tyr can be precisely tailored (G' 60–2550 Pa). HA-Tyr (HRP 0.5U/ml+ 600 μ M H₂O₂) revealed a bonding strength of 16.8 ±11.9kPa to

revealed a bonding strength of 16.8 ± 11.9 kPa to cartilage. This was improved by chondroitinase ABC pre-treatment of articular cartilage prior to in situ crosslink (35.2 ± 5.7 kPa).

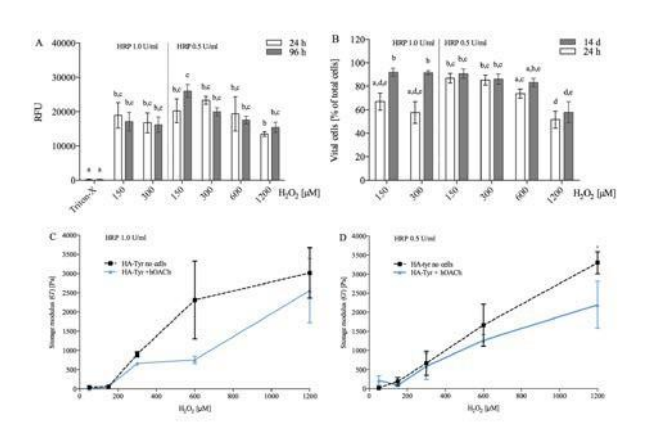


Fig. 1: Cell viability (**A-B**) and rheological properties (**C-D**) of encapsulated hCh in HA-Tyr after 24h and 96h and combined treatment with increasing dosages of HRP and H₂O₂(A CellTiter-Blue®; B Live/Dead quantification).

DISCUSSION & CONCLUSIONS: Except from the highest dosage of H₂O₂, viable hChs can be embedded and maintained in a 3D. HA-Tyr viscoelastic properties can be tailored in presence of hChs and simultaneously bind to native cartilage. Therefore, we propose HA-Tyr to be a promising candidate as cell carrier and bio-adhesive for cartilage defect repair.

Fungicidal PMMA-undecylenic acid composites

M Petrović^{1,2}, D Bonvin¹, H Hofmann¹, M Mionić Ebersold^{1,3,4}

¹ <u>Powder Technology Laboratory</u>, Institute of Materials, Ecole Polytechnique Fédérale de Lausanne, Switzerland. ² Department of Stomatology, Faculty of Medicine, University of Niš, Serbia. ³ <u>Department of Radiology</u>, University Hospital (CHUV) and University of Lausanne (UNIL), Lausanne, Switzerland. ⁴ <u>Center of Biomedical Imaging (CIBM)</u>, Lausanne, Switzerland.

INTRODUCTION: Dentures, typically made of PMMA polymer, are known to be susceptible to the attachment of various funguses, especially *Candida albicans* (*C.a.*). Thus, prevention of biofilm formation and even more, fungicidal effect in denture material, *i.e.* PMMA would be needed. The aim of this study was to make PMMA-UDA composites with UDA, which is known as antifungal agent, to characterise the obtained composites and to study their antifungal properties *in vitro* on the example of *C.a.*

METHODS: In cold polymerized acrylic resin **PMMA** and **MMA** (Ivoclar Vivadent. Liechtenstein), we physically incorporated UDA to obtained composites with 0, 3, 6, 9 and 12wt% of UDA. Then, solid composite samples (Ø 20mm) were prepared in Teflon molds. ATR-FTIR was used for chemical analysis of the surface of composites and native materials, while ImageJ was used for water contact angles measurement on these surfaces by sessile drop method. In disk diffusion test (DDT), disks of composites were placed on Sabouraud agar plates inoculated with

C.a. and the zone of inhibition was measured after 48h incubation at 37°C. In XTT reduction assay, PMMA-UDA composites were incubated at 37°C for 24h with C.a. suspension (density 10⁶ cell/ml). Both XTT and DDT were done in two time points: upon preparation of composites (T₀) and six days after that (T₆). In embedded filamentation test (EFT) 50 µl of C.a. (10⁶ cells/ml) were incubated in 5ml of YPD agar with 0.0125wt% and 0.4wt% of UDA at 37°C and imaged by optical microscope after 24h and 48h. Upon 1 and 6 days incubations of cell culture medium with composites at 37°C, we obtained equivalent medium which was used for MTS toxicity test on A459 cell line.

RESULTS: Native materials and composites showed characteristic peaks in ATR-FTIR spectra with peak intensity analogous to the amount of UDA in composites (from 0 to 12wt%). Contact angle was 76.7±2.4, 72.5±0.6, 73.9±0.9, 64.7±4.7, 62.1±1.4, on composites with 0, 3, 6, 9 and 12wt% of UDA, respectively. DDT showed in both time points that an inhibition zone around composite

discs in minimum 4.4 ± 0.5 mm for composites with \geq 6wt% of UDA. Viability of *C.a.* cells both *on* the surface of composites and *in* the medium above composites obtained by XTT test (see Table 1 for the results *on* the surface), gave similar values in 2 different time points (T_0 and T_6). MTS toxicity test showed cell viability for composites with 9 and 12wt% of UDA in T_0 below 55% and in T_6 below 35%, while for 3 and 6wt% UDA results were \sim 100% and \sim 60%, respectively.

Tabela 1. Viability of C.a. cells on the surface of composites in 2 time points: T_0 and T_6 .

Sample name	T_0	$\underline{T_6}$
0wt% UDA	$100.0\pm23.3\%$	100.0±32.7%
3wt% UDA	$65.7 \pm 8.6\%$	68.6±5.6%
6wt% UDA	$3.9\pm0.8\%$	28.5±9.2%
9wt% UDA	$3.2\pm1.0\%$	$4.2\pm1.0\%$
12wt% UDA	5.6±1.9%	5.3±2.9%

DISCUSSION & CONCLUSIONS: Presence of UDA in composites, confirmed by FTIR, decreases hydrophobicity of the PMMA native surface for minimum 15% at ≥9wt% of UDA. Expected fungicidal effect was observed by DDT which showed an increase of inhibition zone along with concentration of UDA, especially in composites with >6wt% of UDA. Moreover, presence of UDA in composites reduces C.a. cell viability both in medium above and directly on the surface of composites in both time points. But, the efficient reduction is obtained for 6 or more wt% of UDA. EFT test showed hyphal formation at 0.0125wt% after incubation of 48h, while C.a. cells could not be observed in any form at UDA concentration of 0.4wt% after both incubation periods. confirms strong fungicidal effect of UDA on C.a. However, not only *C.a.* cells, but also tested A459 cell line showed quite low cell viability in the presence of UDA. Thus, possible compromise could be found between 3 and 6wt% of UDA, the conditions at which C.a. starts to be affected, but presumably not the cells of the host. In summary, we report new PMMA-UDA composites which have fungicidal effect based on this study on *C.a.*

Matrix topography regulates tendon-derived cell response to paracrine macrophage signalling

AD Schoenenberger^{1,2}, U Silvan^{1,2}, J Foolen^{1,2}, JG Snedeker^{1,2}

¹ ETH Zurich, Zurich, Switzerland. ² University of Zurich, Zurich, Switzerland.

INTRODUCTION: The recently reported presence of immune cells in human tendinopathies points to inflammation as a central player in the regeneration of diseased tendon with potential crosstalk between immune-cells and tendon-derived cells (TDCs). In the present study we hypothesized that pro-inflammatory M1-like macrophages would stimulate markers of catabolic matrix activity in TDCs, and that this regulation would be more pronounced in a novel model system of tendinopathy.

METHODS: Primary human TDCs were cultured on nanofiber polymer mats that structurally mimic either a healthy tendon environment (aligned nanofibers) or a diseased one (randomly organized nanofibers). A TDC/macrophage Transwell system was used to study the effect of macrophage-produced soluble factors on cells on both substrates (Fig. 1). THP-1 monocytes, differentiated to macrophages (M0), were chemically polarized to the pro-inflammatory M1- like phenotype or the anti-inflammatory M2-like phenotype. After 24h, TDC response was assessed using quantitative PCR against lineage-specific markers.

RESULTS: Aligned nanofibers induced highly elongated tendon cell morphology, whereas randomly aligned nanofibers yielded more polygonal tendon cells spread over multiple fibers (Fig. 1). No notable changes in tenogenic gene expression (TNMD) was detected between substrate types or from macrophage involvement (not shown), however, significant differences in matrix turnover was observed for cells on aligned scaffolds (Fig.2). Interestingly, paracrine signaling by M1 macrophages induced a significant up-regulation of matrix degrading enzymes by tendon cells (MMP1, 3 and 13), whereas M2 macrophages only had a modest effect (Fig. 2A). In addition, a trend was observed for increased MMP expression when tendon cells were cultured on the tendinopathy substrate models, compared to those on healthy matrix models. On the other hand, a significant down-regulation of matrix production genes (Col I/III, Bgn) was found when co-culturing TDCs with differently polarized macrophages (Fig. 2B). Furthermore, this down-regulation was more pronounced on the aligned substrates.

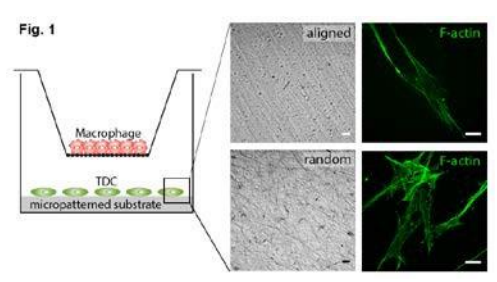


Fig. 1: Coculture model system. TDCs (green) were

cultured on microstructured substrates mimicking healthy or diseased substrates in indirect contact with immune cells (red).

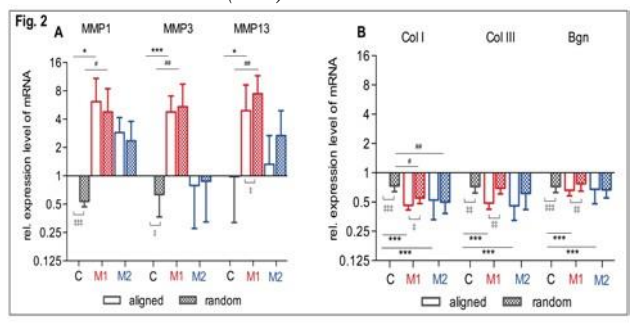


Fig. 2: Coculture with M1 macrophages results in a significant up-regulation of MMP1, 3 and 13 (A), and in a significant downregulation of the matrix production genes Col I/III and Bgn (B). Gene expression is normalized to control (C: medium only, aligned substrates). Statistical analysis was performed using one-way ANOVA comparing every treatment with its corresponding control. ($n = 6, *P \le 0.05, **P \le 0.01, ***P \le 0.001$.)

DISCUSSION: A novel in vitro co-culture system was used to study the effect of paracrine macrophage signaling on TDCs exposed to a cell environment that mimics either healthy pathological topographies. Paracrine signaling by pro-inflammatory M1 macrophages up-regulated the matrix degrading potential of tendon cells. The M2-like phenotype did not provoke a similarly significant response; in support of the paradigm that optimal tendon healing may involve regulation by macrophages driven to this phenotype. Furthermore co-culturing with macrophages lead to a downregulation of the matrix production of tendon cells. Our results further expose the importance of morphological changes, similar to those observed in tendinopathic tissues, in the regulation of the crosstalk between immune and tendon cells.

Development of conductive collagen via magnetically oriented nanoparticles

T Serra¹, V Bonfante², D Manno³, A Serra³, L Salvatore², A Buccolieri⁴, G. Giancane⁵

¹AO Research Institute, AO Foundation, Davos, CH. ²Department of Engineering for Innovation, University of Salento, Italy. ³Department of Mathematics and Physics "E. De Giorgi", University of Salento, Italy. ⁴Department of Biological and Environmental Sciences and Technologies DiSTeBA, University of Salento, Italy. ⁵Department of Cultural Heritage, University of Salento, Italy

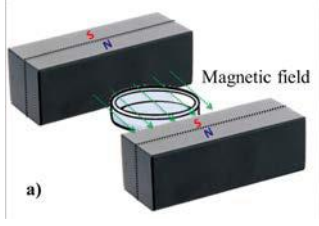
INTRODUCTION: Developing electroconductive biomaterials with the aim of tuning on demand cell fate represents an emerging approach in the field of tissue engineering ¹. Thanks to its high biocompatibility, low immunogenicity and tuneable biodegradability, collagen is one the most conventional biomaterial used to develop 2D and 3D matrices for tissue regeneration ². In this work, we have developed a smart and quick method to obtain conductive collagen films in presence of very stable paramagnetic iron oxide nanoparticles (IOPs).

METHODS: Firstly, paramagnetic IOPs capped by biocompatible polyethylene glycol (PEG) were synthetized and sprayed on a Type I collagen slurry. Secondly, the system was subjected to a static external magnetic field, being at the same time free to dry in air. X-ray diffraction (XRD) profile and infrared spectroscopy analysis (FTIR) of the paramagnetic nanostructures were Transmission electron microscopy (TEM) analysis onto IOPs and atomic force microscopy (AFM) measurements on the collagen/PEG@IOPs films were carried out. Scanning electron microscopy (SEM) was used to evaluate the morphology of collagen films. Electrical conductivity was measured by the standard Van Der Pauw DC fourprobe method at 300 K. IOPs content of the conductive collagen film was determined by means of thermogravimetric analysis (TGA) and atomic absorption spectroscopy. Finally, cytotoxicity evaluation by seeding mouse fibroblast cells (NIH3T3) on collagen/nanoparticles films was performed through MTT assay.

RESULTS: Chemical composition investigation by XRD showed typical profile of γ -Fe₂O₃ according with the paramagnetic behaviour of nanostructures. FTIR successfully confirmed the presence of PEG surrounding the nanoparticles. TEM analysis showed spherical nanostructures of about 80 nm. At higher magnification, a typical "mosaic structure" with small particles of about 2 nm aggregated was observed. Morphological analysis (Figure 1) confirmed that the application of static external magnetic fields allowed the

orientation of IOPs nanoparticles along the magnetic field lines, inducing the formation of long range aligned channels in the collagen matrix. TGA thermograms highlighted the typical behaviour of collagenous materials. The PEG@IOPs content of conductive collagen sample, by evaluating the residual weight at 1000

°C, was estimated about 3%. The iron release kinetic analysis showed that iron concentration increased in time until the eighth day, when it reached a plateau. This suggested that the collagen/PEG@IOPs films are highly stable in physiological condition. Moreover, iron amount detected after 15 days was about 0.2 μg/mL, noncytotoxic for cells ³.



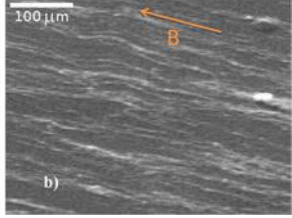


Fig. 1: a) Magnetic field lines created by two magnets with the two opposite magnetic poles placed opposite to each other. b) SEM topographies of the collagen film decorated with oriented PEG@IOPs evidence the aligned structures some hundreds of micron length.

DISCUSSION & CONCLUSIONS: An enhancement of 5 orders of magnitudes in electrical conductivity was recorded in the collagen matrix containing aligned nanoparticle. MTT analysis showed NIH3T3 cell viability around 97% and 99% after 48 h of incubation in presence of nanoparticles and collagen/ nanoparticles, respectively. It proved the biocompatibility of the conductive collagen.

Antibacterial and cell-adhesive effects of bio-inspired nanostructured materials

K Mukaddam¹, J Spicher¹, M Astasov-Frauenhoffer², I Hauser-Gerspach², J Köser³, T Glatzel⁴, M Kisiel⁴, D Mathys⁵, R Steiner⁴, E Meyer⁴, L Marot⁴, S Kühl¹

¹ Department of Oral Surgery, Oral Radiology and Oral Medicine, University Center for Dental Medicine, University of Basel, Hebelstrasse 3, 4056 Basel, Switzerland. ² Department of Preventive Dentistry and Oral Microbiology, University Center for Dental Medicine, University of Basel, Hebelstrasse 3, 4056 Basel, Switzerland. ³ Institut für Chemie und Bioanalytik, Hochschule für Life Sciences, Gründenstrasse 40, 4132 Muttenz, Switzerland. ⁴ Department of Physics, University of Basel, Klingelbergstrasse 82, 4056 Basel, Switzerland. ⁵ University of Basel, Bio-Pharmacenter, Swiss Nanoscience Institute (SNI), Nano Imaging Lab, Klingelbergstrasse 50/70, CH - 4056 Basel, Switzerland

INTRODUCTION:

Nanostructuration of titanium (Ti) enhances soft while reducing integration bacterial colonization. Surface roughness is an important parameter in implant dentistry and influences primary stability and osseointegration. While the interaction of osteoblast with (nano-)structured surfaces is well-investigated, little is known on soft tissue integration of the transgingival implant surface and the interaction with relevant cell types. The aim of this study is to test the in vitro performance of a novel nanostructured Ti surface with regard to its influence on viability, proliferation, morphology and adhesion of oral mucosa cells as well as to study bacterial adhesion.

METHODS: Heated Ti samples were exposed to helium (He) plasma using an unbalanced magnetron sputtering source. By controlling the temperature (350°C), the negative voltage on the sample (-85V) and the time of exposure, the surface developed a nanostructured pattern. Ti samples were incubated with *Porphyromonas gingivalis* (ATCC 33277) for 6 h at 37°C in anaerobic conditions to investigate antimicrobial effect of the nanostructure. Human gingival fibroblasts (HGF-1 cells; ATCC; CRL-2014) were cultured on the modified nanosurfaces under standardized conditions. Cell morphology was qualitatively assessed by scanning electron microscopy (SEM).

RESULTS: By controlling the time of plasma exposure, the nanostructure i.e. the cones height on the Ti surface was reaching micrometers (Fig. 1A). The *P. gingivalis* cells showed deformation in their structures when coming in contact with the surface (Fig. 1B). HGF-1 cells were flattened and elongated on the nanostructured surface (Fig. 2)

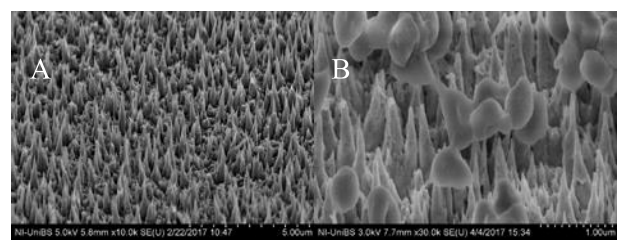


Fig. 1: SEM images of the nanostructured Ti surface and of the damaged P. gingivalis cells adhered to the surface (B).

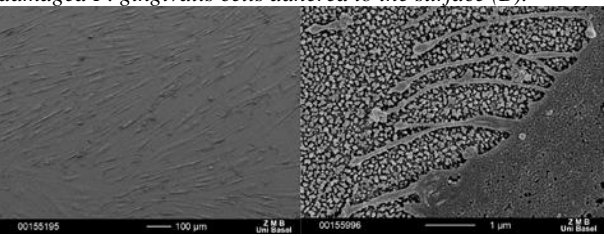


Fig. 2. SEM images of the nanostructured Ti surface and of the flattened and elongated HGF-1 cells adhered to the surface.

DISCUSSION & CONCLUSIONS: An antimicrobial effect against *P. gingivalis* and a cell-adhesive effect on HGF-1 is revealed by nanostructured Ti. Fibroblasts are able to respond to the micro- & nanotopography of the substratum surface. This phenomenon has first been described in 1911 as "contact guidance", revealing that the orientation, alterations in cell shape, polarity and alignment of the cell are dependent to the micro- or nanostructure of different surfaces. *In vitro* experiments have also shown that fibroblasts also conform to the topography of the material's surface leading to mechanical interlocking.¹

ACKNOWLEDGEMENTS: This template was modified with kind permission from eCM Journal.

Protein adsorption, blood interaction, and cell studies on nanoparticle gradients

Rebecca Huber^{1,2}, Markus Rottmar², Eike Müller², Katharina Maniura-Weber², Nicholas D. Spencer ¹

¹ Laboratory for Surface Science and Technology, Department of Materials, ETH Zurich, CH ² Laboratory for Biointerfaces, Empa, St. Gallen, CH

INTRODUCTION: The success of a surgical implant is dependent on an appropriate biological response to the implant surface¹. Wound healing around implants is a complex process in which blood proteins adsorb to the surface and a fibrin network is formed, before osteoblastic cells respond to the protein-covered surface². Blood-protein adsorption and blood coagulation are greatly influenced by the topography of titanium surfaces^{3,4}, which may further impact the eventual adhesion, migration and differentiation of primary human osteoblastic cells on a titanium implant.

The aim of this study is to understand the early interaction between blood and the implant and how this further steers osseointegration. Ultimately, this understanding can facilitate the design of new implant surfaces.

METHODS: To study the effect of nano-rough surfaces on protein adsorption, blood coagulation as well as cell behavior, nanoparticle density gradients were fabricated. The TiO₂-coated gradients were exposed to protein mixtures or single protein solutions incorporating fluorescently labelled albumin and fibrinogen.

In the second step, the gradients were incubated for 2 to 10 min with partially heparinized (0.5 IU/ml) whole human blood from healthy volunteers before investigating the blood-material interaction by scanning electron microscopy.

Gradient samples with pre-adsorbed blood components were also seeded with human bone cells (HBC) prior to analysis by ALP/Actin/DAPI staining and fluorescence microscopy on days 7 and 10.

RESULTS: Gradients with particles of three different diameters (12, 39 and 72 nm) were evaluated. The protein-adsorption experiments showed no significant influence of nano-features on protein adsorption for gradients with 39 and 72 nm nanoparticles. However, fibrinogen in competition with serum showed an enhanced adsorption in the high-particle-density region of 12 nm gradients.

Interestingly, blood incubation experiments showed that the appearance of the blood-surface interaction changes with the particle density on the 39 nm gradients, (see *Fig. 1 middle*).

While platelet adhesion was observed everywhere on the sample, the fibrin network was more pronounced towards the high-density end of the gradient when compared to the low-density end. Gradients with smaller (12 nm) and bigger nanoparticles (72 nm) showed no effect on fibrin network formation.

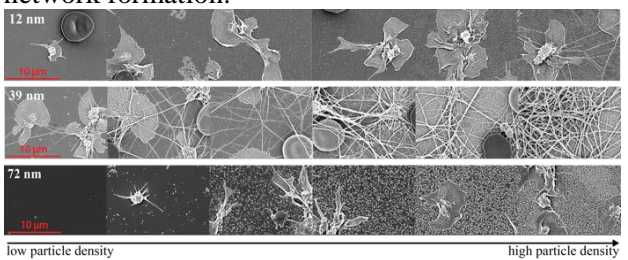


Fig. 1: SEM images taken every 2 mm along nanoparticle density gradients after incubation for 5 min in whole human blood.

Fluorescence microscopy images of HBC on day 7 show a clear influence of the nanostructure on HBC number and morphology (Fig. 2).

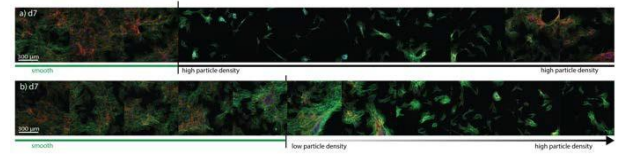


Fig. 2: Day 7 of HBC culture. ALP/Actin/DAPI staining on 39 nm particle samples: a) homogenous density and b) density gradient

DISCUSSION & **CONCLUSIONS:** Nanostructures with a defined size (39 nm) were found to influence blood coagulation, but appear to have only little influence on protein adsorption from solutions. Nanoparticle density seems to also have

an effect on HBC number and morphology.

ACKNOWLEDGEMENTS: We would like to thank the ScopeM of ETH Zurich for their skillful SEM support. The Swiss National Science Foundation (SNF, Grant no: CR31I3_146468) is gratefully acknowledged for funding.

Antimicrobial efficacy evaluation of copper coated glass items for use at ambient conditions – lessons learned

J Koeser¹, P Meier², A Romanyuk², J Bercher¹, U Pieles¹

¹ School of Life Sciences, University of Applied Sciences and Arts Northwestern Switzerland, Muttenz, CH. ² Glas Troesch AG, Buetzberg, CH

INTRODUCTION: The analysis of bactericidal applications in dry surfaces intended for environments presents a challenge since typical antimicrobial efficacy testing procedures largely rely on wet procedures. For biocide releasing surfaces the liquid volume and incubation time employed for antimicrobial testing largely influence the assay outcome. The often used ISO 22196/JIS Z 2801 international standards are designed to evaluate the activity of antibacterial- treated plastics and other hard, non-porous surfaces and assess the antimicrobial activity of surfaces under liquid conditions for 24 hrs, which is not reflecting the conditions and timeframes desired for many antimicrobial active products at ambient conditions. The real world performance of antimicrobially equipped high touch surfaces under ambient conditions is much better represented by typical sanitizer tests, e.g. the ASTM disinfectant validation procedure E 2197 or EPA's "Test Method for Efficacy of Copper Alloy Surfaces as a Sanitizer" where a small bacterial inoculum is dried on the surface of a test carrier. Here we present the results from antimicrobial efficacy assays of copper modified glass surfaces under conditions simulating typical usage conditions of touch-contaminated surfaces like interior items or touchscreens.

METHODS: Glass samples were coated with various copper-containing layers by magnetron sputter deposition. *S.aureus* ATCC 6538 were cultured in nutrient broth until OD₆₀₀=0.4-1 and diluted to 0.5 x 10^5 cfu/ml in 5% fetal calf serum (FCS). 20 μ l of this dilution was spread on a 2 cm x 2 cm sample surface, dried and kept at ambient air for 60 minutes after which the bacteria were replica plated and the surviving bacteria quantified by colony counting 24 hrs later.

RESULTS: When analysing the antimicrobial activity of different copper coated glass samples on dried bacterial inocula, killing rates in the typical range of 50 to 90% were observed. These killing rates were considerably lower than the ones determined according to ISO 22196, which for most samples were close to 100%. Interestingly we observed a certain dependence of the antimicrobial

activity on the humidity level in the laboratory. This effect might be due to influences on the drying time or the humidity dependent adsorbed water layer on the surface of the samples, which is also expected to influence the copper release [1]. During these experiments, the drying time was in the range of 10-20 minutes, which is still not completely representative for applications in dry conditions. Thus the volume of the bacterial inoculum in 5% FCS was reduced to 2 µl which decreased the drying time to a few seconds. The reduced drying time was decreasing the copper release from the sample surface, but no drastic change in killing rates was observed (Fig. 1a). This might be due to the reduced amount of FCS in the smaller inoculum, since FCS strongly quenches the antimicrobial activity of copper ions (Fig. 1b). We also observed an increased release of copper from different samples in the presence of 5% FCS as compared to pure water. Future experiments will investigate the quenching of copper antimicrobial efficacy by different soils in more detail.

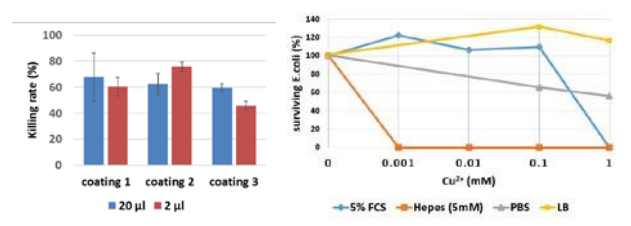


Fig. 1: Killing rates of copper coated glass samples after inoculation with 20 μ l or 2 μ l S. aureus suspension (left). Antimicrobial activity (60') of Cu^{2+} against E.coli in different solutions (right).

DISCUSSION & CONCLUSIONS: Here we present a new method to assess the antimicrobial activity of biocide releasing surfaces. This method is a valuable tool for the evaluation and optimization of new antimicrobial surfaces for the intended use in ambient air.

ACKNOWLEDGEMENTS: The authors acknowledge the financial support by the Swiss Commission for Technology and Innovation.

Antibacterial effect of copper functionalized titanium implants on oral bacteria

M. Astasov-Frauenhoffer¹; A. Zimmermann²; T. Waltimo¹; I. Hauser-Gerspach¹; C. Jung²

¹UZB-Universitätszahnkliniken, Klinik für Präventivzahnmedizin und Orale Mikrobiologie, Basel, CH; ²KKS Ultraschall AG, Medical Surface Center, Steinen, CH

INTRODUCTION: Implant associated infections are often observed. Thus, infection preventing measures would be welcomed in trauma, orthopaedics as well as dental field. We have recently developed an electrochemical method to deposit antibacterial copper (Cu) on titanium implants [1,2]. In this in vitro study, the antibacterial effect of Cufunctionalized surfaces on two oral bacteria Streptococcus sanguinis (DSM 20068) Porphyromonas gingivalis (DSM 20709) was tested.

METHODS: CpTi grade 4 (Ø12 mm, 2 mm) discs were Cu-deposited using the spark-assisted anodizing method in a combined deposition- anodization process using proprietary electrolyte and proprietary process parameters (KKS TioCelTM) [1]. The amount of deposited Cu was determined by incubation the discs in 65% HNO₃ at 50°C for 24 h and ICP/MS analysis of the dissolved Cu (15±4

μg/disc). Cu deposits were demonstrated using electron backscattered SEM (Hitachi TM3000). *S. sanguinis* and *P. gingivalis* were harvested in stationary growth phase, suspended in simulated body fluid (SBF) supplemented with 0.2% glucose, and thereafter seeded onto Cu-doped anodized titanium discs at 37°C for static incubation. Cu-free anodized titanium served as reference. Colony forming unit (CFU) were determined after 2, 4, and

6 h. Additionally, bacteria on the surfaces were coated with 20nm gold layer and seen in secondary electron mode SEM (Fei Nova NanoSEM 230).

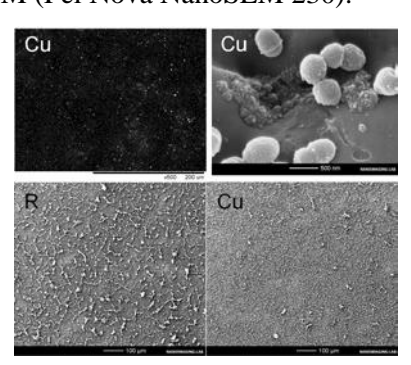


Fig. 1: SEM images for the disc surface with Cu deposits (white spots, top left) and for S. sanguinis adhered on reference (R) and on Cu-deposited discs (top right and bottom left and right).

RESULTS: SEM images revealed less *S. sanguinis* cells and a large number of cell debris on the Cudeposited surface compared to the reference after 6 h (Fig. 1). CFU were significantly lower on the Cudeposited discs and in the medium compared to the

reference (Fig. 2). *P. gingivalis* showed after 6 h a significant stronger decrease of CFU on Cudeposited discs and in medium compared to *S. sanguinis* (Fig. 3).

DISCUSSION & CONCLUSIONS: The antibacterial effect of Cu on two oral bacteria strains is clearly demonstrated. However, the effect on the gram-negative *P. gingivalis* is more pronounced than on the gram-positive *S. sanguinis*. For a Cu concentration of ca. 15μg/disc which corresponds to a survival rate of human gingival cells (osteoblasts, fibroblasts, keratinocytes) of 50% [3] all *P. gingivalis* cells are killed after 6 h. This encourages that Cufunctionalized implants or other medical devices for dental applications might be feasible.

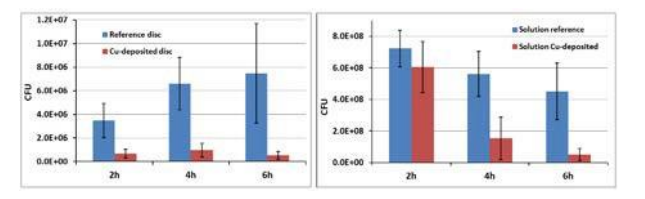


Fig. 2: CFU for S. sanguinis at different incubation times determined on discs and in the medium for the reference (R) and for Cu-deposited discs.

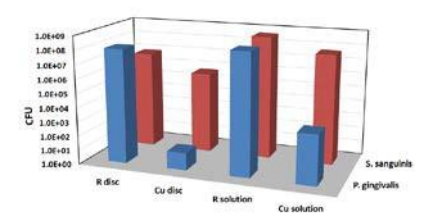


Fig. 3: CFU for S. sanguinis and P. gingivalis after 6 h incubation determined on discs and in the medium for reference (R) and Cu-deposited discs.

ACKNOWLEDGEMENTS: We acknowledge the support by the Nano Imaging Lab of the Swiss Nanoscience Institute, University of Basel for making the SEM images of the cell adhered discs.

Poly(ε-caprolactone) particulate carrier systems for antibiotic drug delivery applications

S G Rotman¹, D W Grijpma², T F Moriarty¹, R G Richards¹, D Eglin¹ and O Guillaume¹

¹ <u>AO Research Institute</u>, AO Foundation, Davos, CH. ² <u>Department of Biomaterials Science</u> and Technology, University of Twente, The Netherlands.

INTRODUCTION: Infections are classically treated by systemic antibiotics, but with limited effectiveness due to the short biological half-life of antibiotics [1]. Alternatively, local drug delivery system based on poly(ε-caprolactone) (PCL) particles has been reported, and could provide sustained release of antibiotics [2]. Hence, the aims of this study are to compare PCL microparticles fabrication processes, release kinetic and preserved antimicrobial activity of loaded hydrophobic antibiotics, *i.e.* rifampicin (RIF) and gentamicindioctyl sodium sulfosuccinate (Gen-AOT).

METHODS: 10 w/v% PCL (M_w = 80.000 g·mol⁻¹, PDI = <2, Sigma Aldrich, Steinheim Germany) dichloromethane solutions were sprayed in Taylorcone mode using the <u>electrospray</u> (ES) technique. Emulsion based techniques required a 1 w/v% poly(vinyl alcohol) (M_w = 31.000 g·mol⁻¹ Carl Roth, Switzerland) solution in water as aqueous phase. The aqueous phase was stirred (10.000 rpm) using a high speed homogenizer (HSH) and the

polymer solution was added dropwise. Other emulsions were prepared by <u>sonication</u> (SON). Both emulsions were dried *in vacuo*. The PCL particles were collected after washing to remove surfactant. For drug loaded particles, the methods remained identical, adding 25 wt% RIF or Gen- AOT relative to the polymer mass. Release profiles were measured in phosphatase saline buffer (PBS) using high performance liquid chromatography (HPLC). Scanning electron microscopy (SEM) images were conducted for size and surface analysis. Antimicrobial activity was quantified by zone of inhibition (ZOI) tests on *S. aureus*.

RESULTS: SON based emulsification particles had an average diameter in the low μm range. Particles fabricated with HSH were significantly larger in size. ES particles were highly uniform in size and produced the largest particles. Fabrication yield of emulsion based techniques was above 45%, the yield of electrosprayed particles was low (<1%). Drug loading did not alter observed diameter and size distribution trends. Size, encapsulation efficiency (EE) and drug loading (DL) are presented in table 1. Release profiles of RIF and Gen-AOT from PCL particles showed a burst release of 26% and 9% of the loaded drug,

respectively. Gen-AOT loaded particles showed a prolonged drug release over 8 days while no released RIF could be quantified after 48 hours. ZOI experiments showed inhibition against *S. aureus* comparable to RIF and Gen solution. Gen- AOT loaded particles showed a prolonged antimicrobial activity (fig. 1B) compared to Gen solution.

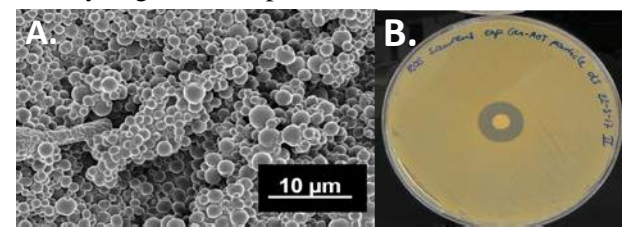


Fig. 1: A) PCL loaded with RIF prepared by sonicated emulsification. B) Antimicrobial activity against S. aureus of Gen-AOT loaded PCL spheres after 72h.

Table 1. Size, encapsulation efficiency (EE) and drug loading (DL) of RIF- and Gen-AOT-PCL.

Drug/r	nethod	Size (µm)	EE (%)	DL (%)
RIF	SON	3.4 ± 1.5	1.0 ± 0.1	0.2 ± 0.0
	HSH	9.1 ± 5.2	0.8 ± 0.0	0.2 ± 0.0
Gen-	SON	2.5 ± 1.2	76.7 ± 4.9	19.0 ± 1.1
AOT	HSH	7.8 ± 4.8	60.0 ± 0.8	12.5 ± 0.3
	ES	15.0±3.2	<u>-</u>	

permitted the preparation of micron size particles without PVA. Due to hydrophilicity of RIF in water (solwater = 1.31 g/L), its EE% and DL% were low compared to the extremely hydrophobic Gen- AOT. Release profiles of both drugs show gradual elution from the polymer particles. Released drugs maintained their antimicrobial activity by inhibiting S. aureus growth. Gen-AOT, being more hydrophobic, diffused slower resulting in longer antimicrobial properties. While optimization is still required, the drug delivery system shows potential for prolonged infection treatment.

The interplay of surface chemistry and (nano-)topography defines the osseointegrative potential of Roxolid® dental implant surfaces

Eike Müller¹, Markus Rottmar¹, Stefanie Guimond¹, Ursina Tobler¹, Marc Stephan², Simon Berner², Katharina Maniura¹

¹Biointerfaces, Empa, Swiss Federal Laboratories for Material Science and Technology, St. Gallen, CH, ²Institut Straumann AG, Basel, CH

INTRODUCTION:

Titanium and titanium alloys have been the gold-standard for dental implant systems since several decades. Material surface characteristics such as roughness and chemistry are known to be decisive parameters for effective osseointegration of dental implants. However, even though hydrophilic and nanostructured titanium surfaces, i.e. SLActive[®], significantly improve the implant's osseointegration potential¹, it remains unclear how the interplay of nanostructures (NS) and hydrophilicity influences protein adsorption and human primary bone and progenitor cell (HBC) fate decisions.

This study aims to investigate the interplay and influence of surface hydrophilicity and topography on protein adsorption, blood coagulation, and HBC fate decision using hydrophilic and hydrophobic micro- and nanostructured Roxolid[®] (RXD) surfaces. For this, thorough protein adsorption studies were performed. Furthermore an advanced *in vitro* model² was employed to study the early interaction of the surfaces with human whole blood and the osteogenic fate decisions of HBCs.

METHODS:

Protein adsorption as a function of the surface was quantified using fluorophore conjugated fibrinogen (FG) or fibronectin (FN). The concept of the *in vitro* model is described by Kopf et al.². In brief, human whole blood from healthy volunteers (ethical approval BASEC Nr. PB_2016-00816) was partially heparinized (0.43 IU ml⁻¹). Samples (supplied from Institut Straumann AG) were incubated with blood in a custom device made out of PTFE for 12 min at RT. After washing with PBS, samples were either analysed via microscopy or HBCs were seeded on top. After 28d of culture, cell numbers were determined and the osteogenic differentiation analysed via quantification of Ca²⁺.

RESULTS:

Lowest levels of protein adsorption (Fig.1A) were obtained for hydrophobic surfaces (SLA) but NS on top of SLA (SLAnano) were found to increase protein adsorption. Highest protein concentrations were obtained for all hydrophilic surfaces. In contrast to the hydrophobic surfaces, functio-

nalisation of hydrophilic surfaces (SLApmod) with NS (SLActive) did not affect protein adsorption. Analysis of the blood coagulation on top of the surfaces revealed a dense fibrin network on top of SLActive, spots of fibrin on top of SLA or SLAnano, and almost no fibrin on top of SLApmod. Investigation of HBC mineralisation after 28d of culture (Fig.1B) revealed lowest levels of Ca²⁺ for surfaces w/o NS, irrespective of the surface hydrophilicity. While NS always increased HBC mineralisation, highest levels of Ca²⁺ were obtained combining hydrophilic surfaces and NS.

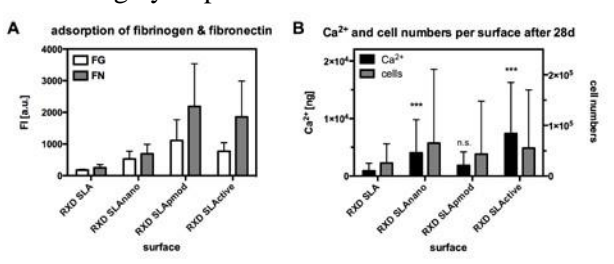


Fig.1: A) Protein adsorption as a function of the surface modification. B) HBC numbers and Ca^{2+} concentrations after cultivation on top of whole blood incubated surfaces. Asterisk denotes statistical significance compared to SLA *** p<0.001.

DISCUSSION & CONCLUSIONS:

Both NS and especially hydrophilicity were found to increase protein adsorption. On the contrary, the blood coagulation was only significantly increased for hydrophilic surfaces with NS. Furthermore the osseointegrative potential was always improved for NS surfaces, but not for hydrophilic surfaces w/o NS, when compared to SLA. The combination of hydrophilicity and NS drastically increased HBC mineralisation, but did not affect the concentration of adsorbed proteins. Protein orientation is key for successful cell receptor binding and guides cell fate decisions. Based on the findings of this study, NS might foster adhesion ligand presentation whereas hydrophilicity promotes the overall protein adsorption but not orientation. Thus, combination of NS and hydrophilic surfaces might result in highest densities of accessible adhesion motifs thereby triggering HBC differentiation.

Towards an injectable, growth factor-loaded hydrogel for cartilage repair

¹C Levinson, ¹E Cavalli, ¹N Broguiere, ²LA Applegate, ¹M Zenobi-Wong

¹Cartilage Engineering + Regeneration Laboratory, ETH, Zürich

²Regenerative Therapy Unit, University Hospital of Lausanne

INTRODUCTION: Articular cartilage focal lesions represent a therapeutic challenge due to the poor intrinsic healing capacity of the tissue. Surgical procedures, the current standard of care, have debatable long-term benefits and tissue engineering comes as a possible alternative. An enzymatically crosslinked hyaluronan hydrogel (HA-TG) was developed (1),which displays chondrogenic properties (2). It however does not retain active molecules such as growth factors (GFs), which is needed for a one-step, injectable treatment of cartilage lesions. We hypothesized that the addition of covalently bound heparin to the HA-TG network would support a sustained release of TGF-β1 (3), a potent chondrogenic factor, and therefore promote matrix deposition.

METHODS: HA-TG gels were obtained by grafting lysine- and glutamine-donor peptides, which can be crosslinked by activated factor XIII, (1). Glutamine-donor peptides were covalently bound to heparin to crosslink it to the HA-TG (Hep-HA-TG: 1 mg/ml of heparin in 20 mg/ml HA). The release of TGF-β1 was monitored using ELISA. Human chondroprogenitor cells (hCCs) were encapsulated in Hep-HA-TG and TGF-β1 (2 µg/ml to 5 ng/ml) was loaded before gelation. The constructs were cultured in serum free media for 21 days, without supplementation of TGF-β1. For exvivo experiments, 1 mm thick cartilage rings were obtained from calves knees. Immunostainings of collagen I and II was performed on 5 µm thick slices of the paraffin-embedded scaffolds.

RESULTS: The release assay showed that covalently Hep-HA-TG allowed a sustained release of TGF- β1 compared to HA-TG alone (Fig. 1A). Histological stainings further illustrated that the burst release of TGF-β1 from HA-TG did not allow the deposition of matrix components. When heparin was covalently crosslinked, a high deposition of collagen II and glycosaminoglycans was observed. Collagen I, normally absent from healthy hyaline cartilage, was also present but in low amounts. Unbound heparin, however, only led to collagen I production and very low amounts of collagen II and glycosaminoglycanes (Fig. 1B).

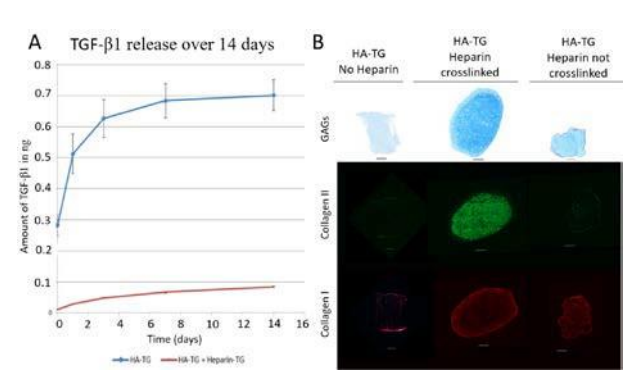


Fig. 1: Release of TGF- β 1 (A) and histological assessment of matrix proteins after 3 weeks (B). Scale bar: 500 μ m.

The ex-vivo experiments in cartilage rings indicated that TGF- β 1 concentration should be above 10 ng/ml when loaded in the gel, and 2 μ g/ml yielded the best result. The presence of the cartilage ring enhanced matrix production by hCCs at the interface (white arrows), which might be very beneficial for adhesion.

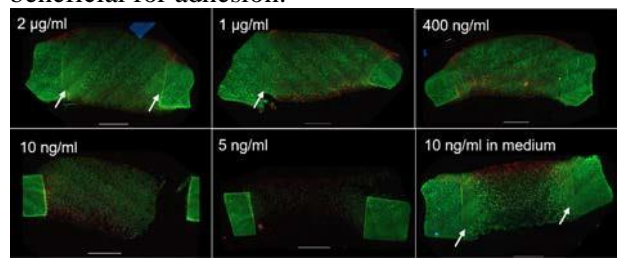


Fig. 2: Collagen I (red) and II (green) staining of scaffolds loaded with a range of TGF- β1 concentrations. Scale bar: 500 μm

DISCUSSION & CONCLUSIONS: We present a system for an efficient sustained release of TGF- β 1, which supports both the chondrogenic properties of the cells and ultimately the possibility to inject the hydrogel without preculture. Further work will aim at quantifying the effect of the growth factor concentration as well as characterizing the impact of environmental cues, such as glucose and oxygen levels. The role of the surrounding cartilage in the deposition of matrix will also be investigated.

Treatment of chronic implant-related infection in sheep in a single stage revision by local gentamicin delivery with a thermoresponsive hyaluronan hydrogel.

M. D'Este¹, W. Boot¹, F. Moriarty¹, T. Schmid¹, S. Zeiter¹, RG. Richards¹, D. Eglin¹

AO Research Institute Davos, AO Foundation, Davos, CH.

INTRODUCTION: Infection is a challenging complication in trauma surgery, joint replacements, medical device implantation and management, with detrimental consequences for the patients and exponential increase of social costs. Often, systemic antibiotics are not sufficient because of the dose limitations imposed by the systemic toxicity and failure to reach the infected tissues because of vascularization impairment. Hydrogels are ideal delivery systems in complex surgical sites as they can cover surfaces of every shape and reach small spaces. In this study we evaluated a gentamicin sulphate (GS) loaded thermoresponsive hyaluronan hydrogel (THH) which is a fluid at room temperature and a gel at body temperature in the treatment of a chronic intramedullary (IM) nail-related infection in a large animal model.

METHODS: THH was synthesized grafting poly N-isopropylacrylamide to hyaluronan amidation [1] and reconstituted at 13% w/w with 1% GS under sterile conditions. The THH distribution within the IM tibia cavity was evaluated in cadaveric limbs by imaging via microCT a gel made radiopaque by adding KI + BaSO₄. Twelve Swiss alpine sheep received an IM tibia nail and their IM cavity was inoculated with 10⁶ colony forming units (CFU) of Staphylococcus Aureus originally isolated from a human patient. A chronic infection was let to develop for 8 weeks. Revision surgery: radiographs were taken, the infected nails were removed and tissue biopsies harvested; the IM canal was debrided and filled with 25ml of THH containing GS for half of the animals (treatment group) and left empty for the control. Extracellular fluid from the IM cavity was collected with an ultrafiltration probe to determine the local GS levels for 10 days. All sheep were given systemic amoxicillin and clavulanic acid for 2 weeks, followed by 2 weeks of washout before the animals were euthanized. IM nail, bone marrow, bone and tissue samples were harvested for quantitative bacteriology.

RESULTS: The cadaver trial showed a uniform gel distribution in the IM cavity. Eight weeks after bacterial inoculation all sheep displayed radiographic signs of infection and the biopsies

taken were culture positive with *S. aureus*. At euthanasia for the group receiving THH/GS *S. aureus* was detected in 0/6 IM nails, 1/6 bone marrow, and 1/30 tissue samples. For the control group treated with only systemic antibiotics one sheep was excluded for superinfection; in the 5 remaining bacteria were detected in 5/5 IM nails, 5/5 bone marrows, and 8/25 tissue samples (Fig. 1).

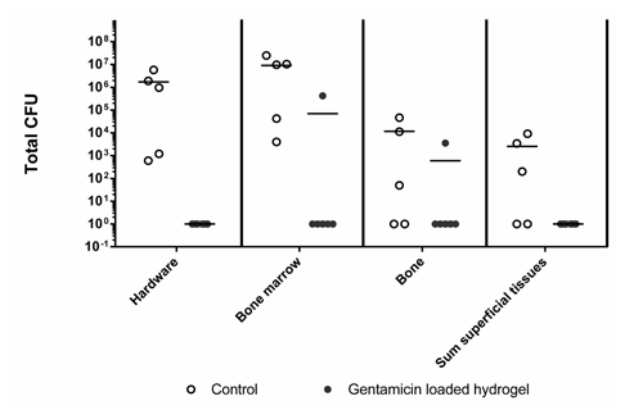


Fig. 1: Quantitative bacteriology of hardware and tissues at euthanasia.

DISCUSSION & CONCLUSIONS: We have tested THH with GS in a chronic device-related infection resistant to systemic antibiotics. The model is on human scale and recapitulates the challenges of treating chronic bone infections. Local GS administration using THH as delivery vehicle brought infection clearance in most of the specimens. In contrast, the infection was still present in the group not receiving THH/GS. In conclusion, a human-sized model of device-related infection was successfully established. Local GS delivery by a THH in combination with systemic antibiotics significantly reduced the infection rates whereas systemic therapy alone did not eradicate the infection.

Identifying cells with Raman spectroscopy to develop a quality control for tissue engineered cartilage

L. Power¹, M. A. Asnaghi², D. Wendt², and I. Martin^{1,2}

¹Tissue Engineering Technologies, Department of Biomedical Engineering, University of Basel, CH, ²Tissue Engineering Group, Department of Biomedicine, University Hospital Basel, CH.

INTRODUCTION: We are developing tissue engineered cartilage grafts to treat articular cartilage defects using autologous nasal chondrocytes¹ in an ongoing phase II clinical trial. To ensure high quality engineered grafts and to rigorously characterize the starting cell material for fulfilling regulatory requirements, it is essential to develop an assay to determine the identity of the cells isolated from the nasal cartilage biopsy. spectroscopy measures characteristic chemical bond vibrations and its application to biological samples is increasing. Measuring the characteristic Raman spectra is a potential method for identifying cell types.

METHODS: Nasal septal chondrocytes and septal perichondrial cells were expanded for one week and then fixed with 4% formalin. Raman spectra were acquired for one second per cell with a custom Raman spectrometer². The spectra were processed and plotted with the R hyperSpec package³.

RESULTS: Nasal septal chondrocytes and perichondrial cells were isolated from their respective tissues (*Fig. I*) and cultured for one week.

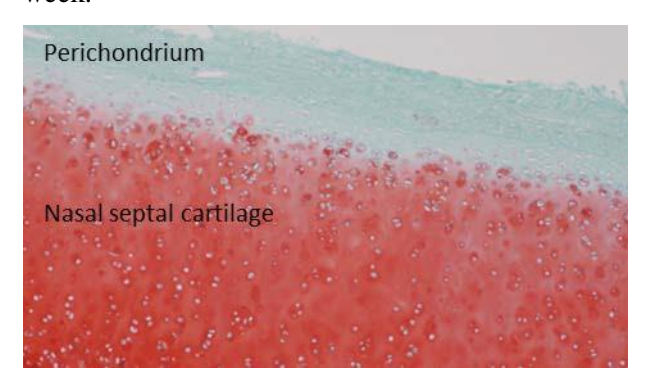


Fig. 1: Native nasal septal cartilage and the adjacent perichondrium. The glycosaminoglycans are stained with safranin O.

The means of the Raman spectra of the nasal chondrocytes and the perichondrial cells are plotted in *Fig.* 2. The spectra of the two cell types were not statistically different.

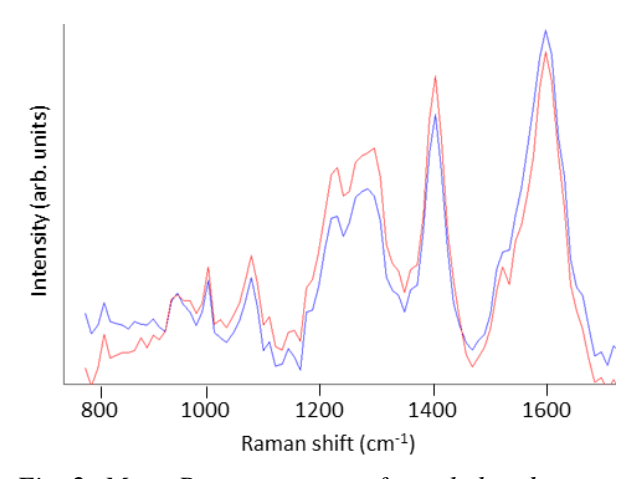


Fig. 2: Mean Raman spectra of nasal chondrocytes (blue) and perichondrial cells (red).

DISCUSSION & CONCLUSIONS: Raman spectroscopy has the potential to measure differences between cells due to their protein, DNA and RNA, and lipid contents, and might thus be able to identify the starting materials of cartilage tissue engineered grafts, ensuring product quality and meeting regulatory requirements. Although the Raman spectra after one week of expansion of nasal chondrocytes and perichondrial cells were not distinguishable, it is possible that the Raman spectra of cells immediately after isolation differ, since it has been shown in our lab that the cell phenotype and expressed genes change during culture in monolayer. The technical challenges of finding the proper instrument setup and methods to prepare samples, acquire measurements, and process the spectra have been overcome, therefore our next step is to measure the Raman spectra of freshly isolated

ACKNOWLEDGEMENTS: This work has received funding from the EU grant agreement No. 681103 (BIO-CHIP, www.biochip-h2020.eu).

Increasing porosity correlates with decreasing T-scores in the distal tibia of postmenopausal women

CM Sprecher¹, F Schmidutz^{1,2}, S Milz^{1,3}, D Schiuma¹, M Windolf¹, RG Richards¹, AW Popp^{1,4}

¹ <u>AO Research Institute</u>, AO Foundation, Davos, CH. ² Department of Orthopaedic Surgery,
University of Munich (LMU), Germany ³ Department of Anatomy II, University of Munich (LMU),
Germany. ⁴ Department of Osteoporosis, Bern University Hospital, University of Bern, CH

INTRODUCTION: Osteoporotic fractures are frequently observed in clinical practise. In a recent manuscript an increased cortical porosity was described¹. The aim of the current study was to assess the regional changes of porosity in the left distal tibia of postmenopausal women using histomorphometry (Histo) and high resolution computed tomography (CT).

METHODS: Each tibia was scanned 130 mm proximal to the talocrural joint using highresolution peripheral quantitative CT (HR-pQCT voxel size 82 µm) and µCT (voxel size 36 µm). Histological processing of specimens resulted in acrylate embedding, sectioning and staining with Giemsa-Eosin. DXA derived T-scores of the samples were described². Histomorphometry was performed using a custom made KS400 macro (Zeiss). Cortical thickness (CtTh), cortical porosity (CtPo) and pore sizes were measured semiautomatic. Pore size was used to calculate osteonal remodeling ratio, as the ratio between the number of osteons at rest (pore \emptyset 30 – 50 µm) and the number of still modeling osteons (Ø 100 – 200 um). Pearson's correlation coefficients r and the two tailed p-values were calculated. Comparisons between analysis on depending samples were tested on significances using General Linear Model for

RESULTS: The tibiae of 11 postmenopausal females with a T-score between 0.6 and -5.6 and a donor age range between 60 to 93 years were included. A significant correlation between CtTh or CtPo and the T-score was observed. The method with the lowest resolution (HR-pQCT) exhibited a lower r-value (Table 1). Absolute values for CtTh and CtPo were significantly higher (p<0.001) when using histomorphometry. Cortical porosity in the endosteal third was significantly higher (p<0.009) than in the periosteal third. All three cortical regions showed a high correlation to overall porosity with a $r \ge 0.78$ ($p \le 0.005$). Osteonal remodeling ratio decreased extensively with increasing cortical porosity (Fig. 1).

repeated measurements in SPSS.

DISCUSSION & CONCLUSIONS: Distal tibia porosity and cortical thickness correlated strongly

with T-scores of postmenopausal women. However, the measured values for cortical thickness and cortical porosity were significantly higher when obtained from histological sections. Osteonal remodelling ratio could not be detected using non-destructive CT-based methods and is still requiring histology.

Table 1. Comparison and Pearson's correlation between CtTh and CtPo by method and T-scores (SD=standard deviation).

	Cortical Thickness (CtTh)		
	Histo	μCT	HR-pQCT
mean \pm SD	$4.13 \pm$	2.49 ±	2.63 ±
[mm]	0.87	0.66	0.67
r to T-scores	0.91	0.78	0.98
p-value	< 0.001	0.001	< 0.001

	Cortical Porosity (CtPo)		
	Histo	μCT	HR-pQCT
mean \pm SD	$17.09 \pm$	6.56 ±	0.49 ±
[%]	10.31	6.51	0.49
r to T-scores	-0.80	-0.76	-0.57
p-value	0.003	0.001	0.007

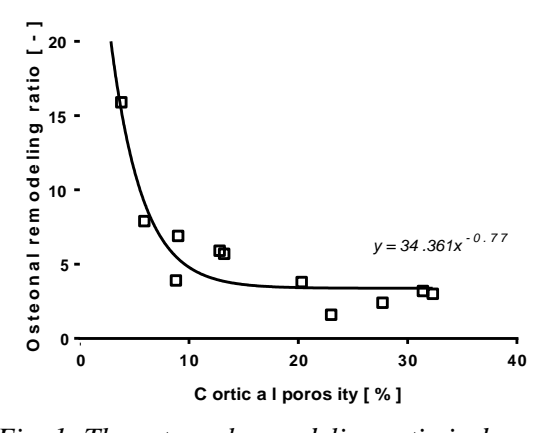


Fig. 1: The osteonal remodeling ratio is decreasing with increasing cortical porosity.

Bony integration of porous tantalum despite ongoing infection: histologic workup of an explanted shoulder prosthesis

P Wahl^{1,2}, CM Sprecher³, C Brüning², C Meier¹, E Gautier⁴, TF Moriarty³

¹ Cantonal Hospital Winterthur, Switzerland ² BG Trauma Centre Frankfurt, Germany ³ AO Research Institute Davos, Switzerland ⁴ HFR Fribourg - Cantonal Hospital, Switzerland

INTRODUCTION: Infection is a complication feared in implant surgery, not only because implants are very susceptible to infection, but also because infection admittedly prevents tissue integration or leads to loosening and dysfunction. This report documents an unexpected situation of good bony integration of a porous tantalum shoulder prosthesis despite ongoing infection since the implantation and lasting for years.

CASE REPORT: A 69 year old woman suffered a low-energy fracture of her proximal humerus, for osteoporosis. Following osteosynthesis, necrosis of the humeral head led to the implantation of an inverse shoulder prosthesis with a glenosphere with a porous tantalum base plate and a cemented stem. Shortly after surgery a fistula developed, proving infection¹ although Staphylococcus spp were first cultured at revision only 2 years later. After failed revision surgery, the patient was finally referred for further treatment 3 years after the implantation. The implant was removed and under adequate antibiotic therapy, the infection healed. While the stem was loose and could be removed relatively easily, the glenoidal component had to be chiselled out, leading to bone loss jeopardizing reconstruction. Despite poor function and persistent pain in her shoulder, the patient refused further treatment.

METHODS: The retrieved implant was fixed in buffered formaldehyde. After dehydration through ascending concentrations of ethanol, the sample was embedded in methyl-methacrylate. Then sections were cut and ground to a thickness of 150 μm. One section was stained with Giemsa-Eosin for light microscopy. Bone ongrowth was quantified through determination of the bone implant contact (BIC) index, and bone ingrowth into the porous tantalum through determination of the relative bone area. ^{2,3} The second section was analysed by scanning electron microscopy (SEM). Elemental analysis was performed through energy dispersive x-ray analysis (EDX).

RESULTS: Histologically normal bone had formed at the implants interface, respectively within the open cell structure of the porous

tantalum. The BIC index was 32%. After subtraction of the porous metal structure, the relative bone area for the full thickness was 8.2%, increasing to 11.9% in the outer 50% of the thickness. Due to the sections thickness, bone ongrowth on the porous tantalum could better be illustrated in SEM back scattered electron (BSE) images than in light microscopy. Elemental composition of the metallic components confirmed a titanium alloy in the base plate, and tantalum in the open cell structure.

DISCUSSION & CONCLUSIONS: Despite long-lasting and ongoing infection, the glenoidal base plate of the prosthesis showed good bony integration upon removal, while the cemented stem had obviously loosened. The bone ingrowth into the porous tantalum was comparable to, and the BIC index was even higher than, the values previously reported for the undersurface of retrieved proximal humerus resurfacing implants.³ The relative bone area within the porous tantalum structure appeared higher than values previously reported in native osteoporotic proximal humeri, even reaching values of normal trabecular bone, despite the presence of osteoporosis in this case, as indicated by the type of fracture the patient suffered.³⁻⁵ Despite good integration of the implant in bone, this did not solve the problem of infection, and of the related morbidity. While a case report is no sufficient proof in isolation, further evidence is provided that porous tantalum might have a favourable biological behaviour, compared to other implant materials, which might provide significant advantages in critical bone stock or in case of contamination at implantation.

Antibacterially active parylene coatings

D Hegemann¹, M Amberg¹, M Vandenbossche¹, Q Ren², H Damsir³, F Bourgeois³

¹ Empa, Advanced Fibers, Plasma & Coating, St. Gallen, CH. ² Empa, Biointerfaces, Bacteria at Surfaces, St. Gallen, CH. ³ Comelec SA, La Chaux-de-Fonds, CH

INTRODUCTION: Parylene (para-xylylene) is a high-tech polymer coating with outstanding properties: chemical inertness, biocompatibility and biostability, electrical insulation, high barrier properties, and transparency. The parylene coating is achieved with a vacuum process comparable to Chemical Vapour Deposition (CVD). Coatings thicker than ~150 nm are completely uniform, without pinholes, and suitable for devices with very complex shapes. Thanks to both exceptional material properties and process advantages, the parylene coating is widely used in technological fields such as electronics and microelectronics, micromechanics, sensors and MEMS, medical devices, and pharmacology. These properties, however, are related to the "bulk" properties of the coatings. Hence, it is highly demanded to modify the near-surface properties of parylene coatings to achieve further functionalities such as drug release and antimicrobial efficacy.

Therefore, the embedding of silver (Ag) using a cosputtering process is investigated to obtain Ag/parylene nanocomposite coatings. Different Ag components were incorporated close to the surface of the coatings to control the Ag release kinetics.² Antibacterial activity was determined with *S. aureus* using the ASTM standard test method.

METHODS: Parylene coatings were deposited from chlorine-containing dimers (Parylene C) at room temperature and a pressure of ~2 Pa after a pyrolysis step at around 650°C. Silver was sputtered from 2" targets with varying plasma power ranging from 50-200 W.3 Thus different amounts of Ag was incorporated: 6, 10, and 15 µg cm⁻². The nanocomposites were produced by first depositing a 2-5 µm thick parylene film on glass slides (2x2 cm²) before starting the silver sputtering process. Silver content and cumulative release were measured by ICP-OES (Perkin Elmer Optima 3000) by immersion of the samples into water for 6 hrs, 1, 4 and 7/8 days. ASTM E2180 standard test method was used to evaluate the antimicrobial efficacy of the coatings in a direct contact form with the grampositive bacteria S. aureus.

RESULTS: Different Ag-containing parylene nanocomposite coatings were prepared by incorporation of 6, 10, and 15 µg cm⁻² of Ag

forming embedded nanoparticles. The release kinetics (Fig. 1) showed a rather steady release of Ag ions – with higher Ag delivery for samples comprising higher Ag contents. Most of all, a low amount of incorporated Ag was found to enable a highly uniform release rate over at least one week. All samples revealed excellent antibacterial efficacy even after prolonged immersion times (up to 8 days) by reducing bacterial colonization by more than 6 log, in agreement with the observed Ag ion release rates.

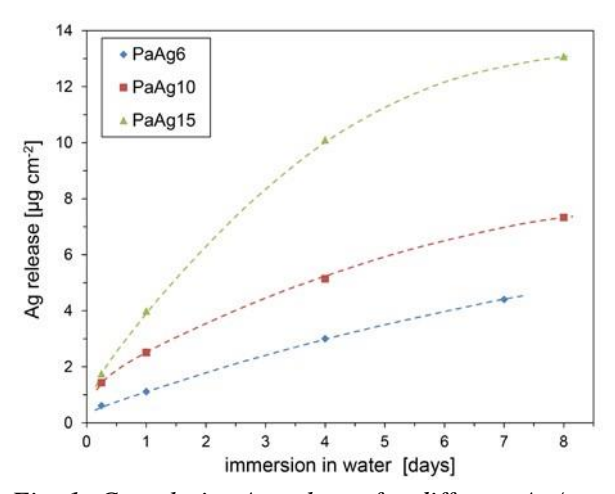


Fig. 1: Cumulative Ag release for different Ag/parylene nanocomposites denoted as PaAgx with x the Ag content in $[\mu g \text{ cm}^{-2}]$.

DISCUSSION & CONCLUSIONS: Ag/parylene nanocomposite coatings were found to deliver a well-defined amount of silver adding antibacterial properties to the beneficial characteristics of parylene.

ACKNOWLEDGEMENTS: Funding by CTI, Bern, CH, is acknowledged (18443.1 PFIW-IW).

Porous, ultralight 3D tubular scaffolds from short electrospun nanofibers

Markus Merk ¹, Christian Adlhart ¹

¹ Institute of Chemistry and Biotechnology, Zurich University of Applied Sciences ZHAW, Einsiedlerstrasse 31, 8820 Wädenswil, Switzerland, christian.adlhart@zhaw.ch

INTRODUCTION: Tubular organs ubiquitously found within the human body and include blood vessel, trachea gastrointestinal tract and urinary tract. These complex tubular tissues are composed of different types of cells, extracellular matrix and proteins but share the functional purpose of transporting nutrients in liquid or solid form. Using active contractions of muscles placed around the organ and specific cells within the lumen, transportation requires the underlining scaffold to be adaptable to various conditions. Repair and regeneration of these tubular organs is of great interest due to the high amount of surgeries performed annually. However, the design and fabrication of synthetic scaffolds that mimic the mechanical and structural characteristics of their natural counterparts remains challenging.[1] Here, we show the construction and comparison of different tubular structures fabricated via the two-dimensional combination of electrospinning and the freeze-casting method. [2] Together these techniques allow us to create 3D tubular scaffolds with high open porosity and adaptable mechanical properties depending upon the polymer used.

METHODS: All nanofibers were received from the University of Liberec except of pullulan/polyvinyl alcohol (PUL/PVA) which was produced using the Elmarco NanoSpider as reported previously. [2] Tubular structures were formed by freezing homogenized nanofiber- slurries using a self-constructed cryo-rotator. Subsequent freeze-drying and crosslinking formed the porous, ultralight 3D scaffolds.

Results:



Fig. 1: Image of 3D tubular scaffolds produced from short electrospun nanofibers and shaped via freeze-casting method. From left to right polyamide (PA), pullulan/polyvinyl alcohol (PUL/PVA), polyacrylonitrile (PAN) mixed with PUL/PVA and PAN.

ACKNOWLEDGEMENTS: The authors thank the University of Liberec for providing the electrospun nanofibers.

www.ecmconferences.org

Beneficial oral biofilms as an effective tool to maintain a balanced oral microbial community

B Gutt¹, Q Ren¹, I Hauser-Gerspach², P Kardas², S Stübinger³, M Astasov-Frauenhoffer², T Waltimo²

¹ Laboratory for Biointerfaces, Empa, Swiss Federal Laboratories for Materials Science and Technology, St. Gallen, CH. ² Department of Preventive Dentistry and Oral Microbiology, University Center for Dental Medicine, University of Basel, Basel, CH. ³ Image Guided Therapy, Medical Image Analysis Center (MIAC), University of Basel, Allschwil, CH

INTRODUCTION: Periodontitis is a prominent burden to overall public health. The disease is caused by pathogenic bacterial biofilms leading to reversible gingivitis and irreversible periodontal soft and hard tissue destruction finally tooth loss when left untreated. Commensal species found in the oral cavity possess multifunction. On the one side, they prevent pathogens from attachment, multiplications and invasion to epithelium. On the other hand, they can become host-adapted playing a role in regulation of epithelial development, and contribute to the maturation and maintenance of the immune system. However, when the commensal bacterial communities are invaded by pathogenic organisms leading to dysbiosis within the system, disease is triggered. The aim of this study was to investigate whether using a beneficial commensal biofilm can prevent or reduce the invasion of pathogenic microorganisms.

METHODS: *Streptococcus sanguinis* was used as a model strain to form the beneficial biofilm. The cell lysates of the known periodontal pathogens *Fusobacterium nucleatum* or *Porphyromonas gingivalis* were prepared and applied to block the beneficial biofilm. The blocked biofilm was then challenged with *F. nucleatum* or *P. gingivalis* to test the efficiency of the desired colonization resistance. Biofilm was quantified by crystal violet staining and characterized by fluorescence in situ hybridization (FISH) and confocal laser scanning microscopy (CLSM).

RESULTS: The beneficial *S. sanguinis* biofilm was first blocked by *F. nucleatum* or *P. gingivalis* lysate, and then challenged with secondary adhesion by *S. sanguinis*, *F. nucleatum* and *P. gingivalis*, respectively. It was found that both lysates of the pathogenic species led to a significant reduction of biofilms formed by pathogens compared to the control without any cell lysate (Fig. 1), suggesting that they are able to hinder the adhesion of pathogens onto the biofilm. In particular, the lysate of *P. gingivalis* resulted in around 50% reduction when either *F. nucleatum* or

P. gingivalis was used for secondary adhesion. Additionally, the distribution of single species within the biofilms was analysed by FISH and the results confirmed the blocking effect of the lysates on the secondary adhesion. These data demonstrate that beneficial biofilms can be an effective tool to prevent pathogen attack.

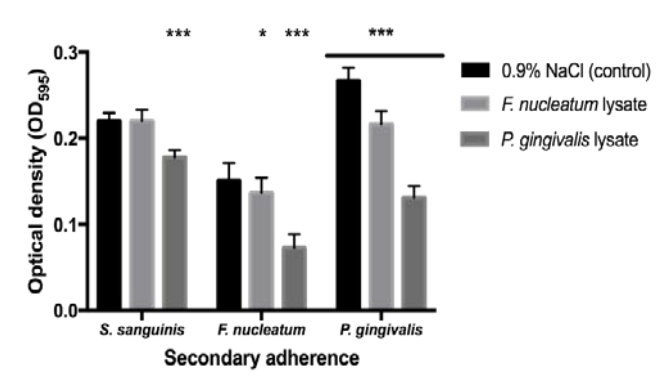


Fig. 1: Biofilm quantified by crystal violet staining. The 24-h-old S. sanguinis biofilms blocked with lysate or 0.9% NaCl before secondary adherence of S. sanguinis, F. nucleatum or P. gingivalis for another 24 h (N=16). Asterisks denote statistical significance as follows: *P<0.05, **P<0.01, ***P<0.001 (N=18).

biscussion & conclusions: This study showed that colonization resistance can reached when beneficial biofilm formation is controlled and influenced; creating a smart bioactive interface that acts as a bouncer for pathogenic species. However, it is important to note that oral microflora expresses multiple types of adhesins that are invoked when major receptors are blocked; therefore more complex beneficial biofilms and lysate mixtures must be evaluated.

ACKNOWLEDGEMENTS: The authors would like to thank Jürg Meyer and Clemens Walter for scientific input, Flavia Zuber for the technical support.

Stable drinking water until the point of use – towards a probiotic approach for polymeric materials in building plumbing installations

L Neu^{1,2}, F Hammes¹

¹ Eawag, Department of Environmental Microbiology, Dübendorf, CH. ² ETH Zürich, Department of Environmental Systems Science, CH.

INTRODUCTION: Treated drinking water in Switzerland is known to be of a very good quality, containing low concentrations of nutrients and therefore not supporting microbial growth. However, as soon as the water enters building plumbing systems, conditions change. Here, one substantial factor is the currently increasing use of various synthetic polymeric materials. When in contact with water, these materials leach high amounts of assimilable organic carbon (AOC) and consequently promote microbial growth^{1,2}. Any variations in microbial water quality can lead to undesirable changes in aesthetic and hygienic water quality. Therefore, we are interested in the characterization of building plumbing biofilms and in understanding determinants for their structure and community composition. Ultimately the aim is to manage and control biofilm formation in building plumbing installations.

METHODS: We studied biofilms on flexible plastic materials in contact with drinking water, which where either grown in real households under natural conditions or in the laboratory under controlled conditions. Biofilms were analysed with optical coherence tomography, scanning electron microscopy, flow cytometry after detachment, as well as Illumina sequencing.

RESULTS: We observed notable diversity in both structure and composition of biofilms grown on flexible plastic materials. For example, in shower hoses used for 12 months with daily shower events, biofilm thickness was measured up to $300 \, \mu m$ (Figure 1), while the bacterial coverage ranged between $1x10^8 - 8x10^8$ cells/cm² along the entire length of the hose, with considerable microheterogeneity observed.

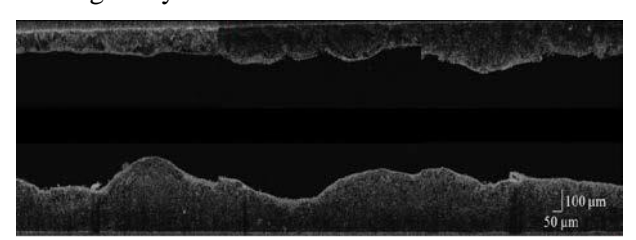


Fig. 1 OCT image of the biofilm inside a shower hose (3.2 cm), grown under controlled conditions (image not to scale).

In another example, the total number of bacteria covering the inner surface of plastic bath toys from real households ranged from $1x10^6$ to $2x10^7$ cells/cm². Also, community compositions varied between different toys (Figure 2), while overall dominated by representatives of the phyla *Proteobacteria*, *Bacteriodetes*, *Planctomycetes*, and *Actinobacteria*.



Fig. 2 SEM image of a biofilm inside a flexible plastic bath toy.

OUTLOOK: All polymeric materials leach AOC which bacteria use for growth. Future research will aim at a paradigm shift where this material liability is turned into an asset, i.e. focusing on materials, conditions and organisms that will enable the establishment of controlled, *probiotic* biofilms in pipes and hoses of building plumbing installations.

ACKNOWLEDGEMENTS: This work is funded by the Swiss National Science Foundation.

Characterization of an engineered collagen scaffold for bladder augmentation

RM Martell¹, K Bircher², E Vardar¹, HM Larsson¹, EM Balet¹, G Vythilingam^{1,3}, E Mazza², P Frey¹

¹Intitute of Bioengineering, EPFL, CH. ² Institute of Mechanical Systems, ETH, CH. ³ Department of Surgery, University of Malaya, ML

INTRODUCTION: Bladder diseases malformations affect 400 million people worldwide [1]. Surgical bladder augmentation is mostly needed as a common treatment modality. Presently, the common material used for bladder most augmentation are gastrointestinal segments. Unfortunately, this is accompanied with several complications: metabolic disturbencies, mucus production, stone formation, and carcinogenesis [2]. In this study, we propose the use of an engineered bovine collagen based scaffold as an alternative material. Mechanical properties of these scaffolds were evaluated and compared with porcine bladder wall tissue.

METHODS: In order to mechanically characterize the bovine collagen scaffold and porcine bladder wall tissue in similar physiological conditions a custom-built inflation device was used for monotonic and cyclic equibiaxial testing [3]. Tension-strain curves and pressure-apex displacement curves were evaluated. Cyclic uniaxial tension tests were performed using a planar biaxial testing machine [4]. Suture retention tests were performed with the bovine collagen scaffold in order to understand its suturability to the bladder wall. The suture was done 3-4mm from the edge in 10mm x 20mm samples using a 5-0 monofilament and the axis was pulled at 1mm/s.

RESULTS: Peak pressures of both the collagen scaffold and the bladder tissue decreased per cycle (Fig1A and Fig1B). The burst pressure of the bovine collagen scaffold before and after the inflation cycles ranged 75 to 120 mbar. The suture retention strength for the bovine collagen scaffold was 0.018±0.002N.

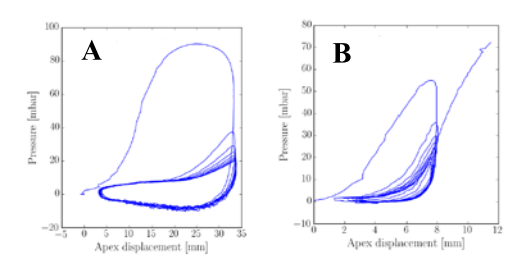


Fig 1: Representative pressure vs. apex displacement curves in cyclic inflation (equibiaxial) tests of porcine bladder wall tissue (A) and bovine collagen scaffolds (B). Note that

after 10 cycles, the bovine collagen scaffold was loaded until rupture.

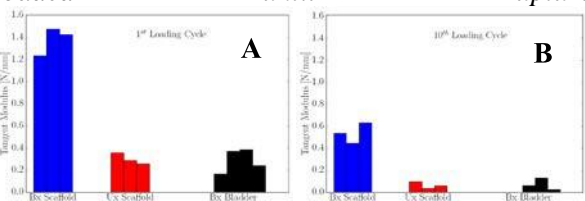


Fig 2: Tangent modulus (extracted around a strain of 10%) for the first (A) and the tenth (B) loading cycle in inflation (Bx) and uniaxial tension (Ux) tests for the bovine collagen scaffold and the porcine bladder wall tissue.

The tangent modulus (Fig2A and Fig2B) of both specimens showed a significant decrease from the first loading cycle to the tenth loading cycle.

DISCUSSION & CONCLUSIONS: The bovine collagen scaffolds showed to be much stiffer under biaxial loading as compared to uniaxial tensile tests. However, the porcine bladder tissue displayed three times less stiffness, under biaxial loading compared to the collagen scaffolds. The tension-strain and pressure-displacement curves suggested that the engineered specimens became softer after each cycle, due to structural modification. The pig bladder tissue showed to be more compliant than the scaffold. The suture retention strength of the scaffolds was very low, which suggest the need of modification of the material to increase its suturability. However, the measured maximal pressure applied to the intact scaffold was well within the range of maximum human bladder pressure. Currently, a biological characterization of the bovine collagen scaffold is being performed.

ACKNOWLEDGEMENTS: This project was supported by the Seydel Fellowship and a CTI-project (25281.2 PFLS).

The interplay of extracellular matrix glycation and inflammation in diabetic tendinopathy

Amro A. Hussien^{1,2}, Claude N. Holenstein^{1,2}, Jess G. Snedeker^{1,2}
¹Institute for Biomechanics, ETH Zurich ²Balgrist University Hospital, University of Zurich 8008 Zurich,
Switzerland

INTRODUCTION: Adults with diabetes have three times more risk of developing tendinopathy; a degenerative disorder of tendons characterized by pain and a reduce tolerance to exercise. Chronic hyperglycaemia contributes to tendinopathy onset and/or progression by accelerating the formation of Advanced Glycation End Products (AGEs). The molecular mechanisms of how AGEs predispose tendons to damage are yet to be uncovered. We hypothesize that (1) AGEs trigger a proinflammatory response in tenocytes; and that (2) ECM glycation may interfere with tenocytes contractility.

METHODS: <u>Isolation of human tenocytes</u>: Primary human tenocytes were isolated from hamstring tendons of two patients underwent anterior cruciate ligament reconstruction. Tissues were collected according to ethical procedures approved by the state of Zurich. Formation of AGEs: Rat tail collagen I was glycated with methylglyoxal (final conc. 250mM), and incubated at 37°C for 24h. PA gel substrates: PA gel composition was varied to have elastic moduli of 40kPa and 120kPa. Glycated and control collagen I were covalently tethered to PA gels. RT-PCR was used to assess gene expression. Cell traction stresses: Cellular traction and the corresponding substrate deformations were measured using a highresolution optical flow tracker and Fourier Transform Traction Cytometry (FTTC). (1)

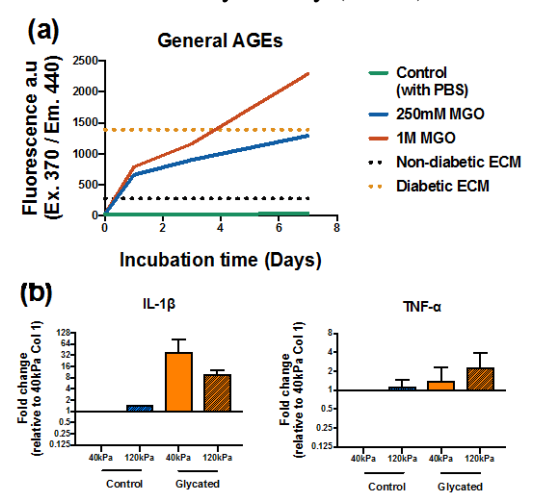


Fig. 1. (a) Autofluorescence levels of collagen AGEs. (b) Fold increase in mRNA levels of IL-1 β and TNF- α .

RESULTS: Fluorometric assay confirmed the formation of AGEs [Fig. 1 (a)]. As early as 24 hours, there was a tendency towards upregulation of the pro-inflammatory cytokines, IL- β 1 and TNF- α [Fig. 1(b)], and downregulation of matrix production of collagen type I and III (data not shown). Tenocytes seeded on glycated matrices exhibited a significant reduction in contractility as measured by TFM (Fig. 2).

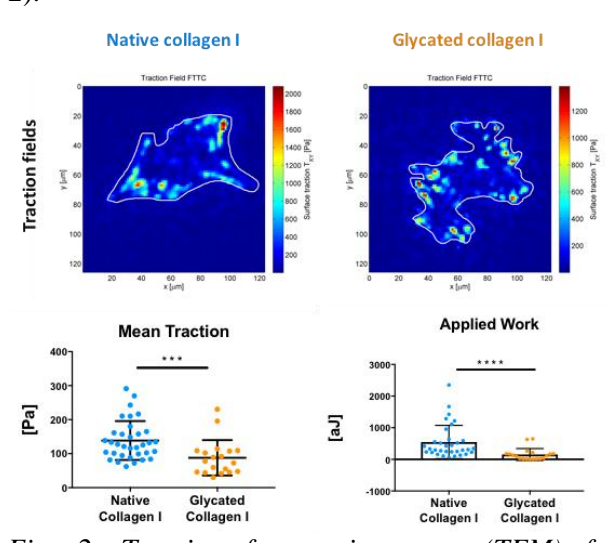


Fig. 2. Traction force microscopy (TFM) of tenocytes on glycated vs. control substrates.

DISCUSSION & **CONCLUSIONS:** Our experiments are consistent with the hypothesis that AGEs may induce an inflammatory response in tendon cells. This could be attributed to the AGE-RAGE signalling axis or an oxidative/dicarbonyl stress mediated by MGO-glycated matrices. (2) AGEs have been shown to interfere with cellular contractility (3) and adhesion (4) in other cells of mesenchymal origin. Further work is underway to confirm these preliminary findings within the context of diabetic tendinopathy.

ACKNOWLEDGEMENTS: This work was funded by Vontobel Stiftung.

Silver ion doped TiN coatings with antibacterial and cytocompatible properties

S. Guimond-Lischer¹, C. Acikgoz², M.H. Lindic², F. Zuber¹, B. Gutt¹, K. Grieder¹, Q. Ren¹, M. Rottmar¹, K. Maniura-Weber¹

¹Laboratory for Biointerfaces, Empa, CH-St. Gallen

²Oerlikon Balzers, Surface Solutions AG, Li-Balzers

INTRODUCTION: Bacterial infections, especially biofilm triggered infections, cause tremendous health problems in humans. More than 45% of nosocomial infections can be traced back to microbial biofilm contaminated medical devices¹. Therefore, it is imperative to develop materials with antimicrobial properties to prevent possible bacterial infections. Particularly, during the critical period after surgery, a high initial release of antimicrobial agents, followed by a continuous, but slow release for a sustained antibacterial effect is desired^{2,3}. Silver (Ag) releasing medical devices are of great interest because of their ability to kill bacteria including antibiotic-resistant strains. Biomaterials should not only inhibit bacterial colonization but also enable cell growth to ensure fast implant stabilization. In this study, Ag doped TiN coatings were developed and evaluated for their Ag release kinetics, cytocompatibility as well as antibacterial activity.

METHODS: Ag doped titanium nitride (TiN) coatings were applied to stainless steel (SS) substrates using the physical vapour deposition (PVD) technique (Oerlikon Balzers INNOVA coating system). These coatings were evaluated for silver release profile by ICP-OES measurements, their antibacterial effect against *Staphylococcus aureus* (MRSA) and *Pseudomonas aeruginosa* species according to ASTM E2180-07 (2012) standard technique as well as their potential cytotoxic properties against normal human dermal fibroblasts (NHDF) using the extract/direct contact tests according to ISO 10993-5, respectively.

RESULTS: TiN-Ag coatings in two configurations (V2/V4) were successfully developed. Both coatings showed an initial burst release followed by a continuous Ag release for up to 28 days (Fig. 1). After 5 days of Ag release from the V2 and V4 TiN-Ag coatings, the samples still displayed good antibacterial activity against *P. aeruginosa* and MRSA. Importantly, no cytotoxic effect could be detected for TiN-Ag coatings in comparison to both SS or TiN reference samples. Moreover, NHDFs cultivated on top of the coated as well as the reference samples showed good cell attachment and viability (Fig. 2).

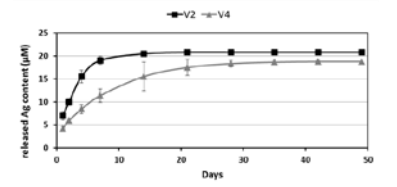


Fig. 1: Long term Ag release kinetics of TiN-Ag V2/V4 in DMEM with 10% fetal bovine serum FCS, measured by ICP-OES.

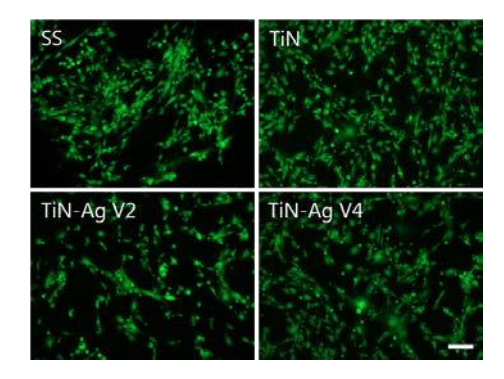


Fig. 2: Normal human dermal fibroblasts (NHDF) cultivated on SS, TiN, TiN-Ag V2 and V4 and stained for live (green) and dead (red) cells. Scale bar = 100 µm.

DISCUSSION & CONCLUSIONS: In this study, TiN-Ag coatings were developed that showed a continuous Ag release up to 28 days, an excellent antimicrobial effect even after 5 days of Ag release and good cytocompatibility. Ion release kinetics can be tuned by modifying coating architecture. Coatings thus represent an interesting tool to render medical devices antimicrobial.

ACKNOWLEDGEMENTS: This study was supported by the Commission for Technology and Innovation CTI (No. 16302.2 PFNM-NM).

Boc(βala)₂N₂H₃ and its interaction with silver

A. Holzheu¹, A. Crochet¹, K. M. Fromm¹

¹ Chemistry Department, University of Fribourg, Fribourg, CH.

INTRODUCTION: For centuries it is known that silver possesses antimicrobial properties. It was regularly used for the treatment of burns, wounds and several bacterial infections, but with the emergence of antibiotics it was nearly forgotten for almost 50 years^{1,2}. Nowadays, due to the rising concern regarding infectious diseases induced by multidrug-resistant bacteria, silver has made a remarkable comeback as a potential antimicrobial agent². Therefore, we study the antimicrobial effects of a dipeptide, Boc(βala)₂N₂H₃, that has four potential silver coordination sites and the capability, due to the hydrazine end group, to reduce silver ions to silver nanoparticles (AgNPs). **METHODS:** To obtain the Boc(βala)₂N₂H₃ dipeptide, a standard liquid phase synthesis was used³. The dipeptide was characterized by ¹H- and ¹³C-NMR, MS-ESI, thermal analysis (TGA, DSC), FT-IR and XRD measurements.

For crystal growth a saturated solution in DMSO was heated and slowly cooled down to RT.

A ¹H-NMR titration was performed with 10 mM Boc(βala)₂N₂H₃ and AgNO₃ (ratios 1:0.5, 1:1, 1:2, 1:3, 1:4 and 1:5) in DMSO.

AgNP formation of 1.25 mM Boc(β ala)₂N₂H₃ and 1.25 mM AgNO₃ in ddH₂O was recorded overnight by UV-Vis spectroscopy and analysed with TEM, MS-ESI and FT-IR. Different pH and temperature conditions where hereby investigated.

As hydrazine itself is known to be toxic, antimicrobial tests were performed with 10^6 CFU/ml E.coli (ATCC 25922) and with 1 and 2 mg/ml Boc(β ala)₂N₂H₃ in Müller Hinton Broth. The colonies were counted after 4 h of incubation at 37 °C and 250 rpm.

RESULTS:

Figure 1a represents the time-resolved formation of AgNP at pH 7 at 60 °C, while 1b depicts the obtained AgNPs. Figure 1c shows the crystal structure of $Boc(\beta ala)_2N_2H_3$.

A first trial of silver complexation with $Boc(\beta ala)_2N_2H_3$ by NMR titration gave a high-field shift for the hydrazine end group of 1.026 (NH₂) and 0.591 ppm (NH).

Antimicrobial tests revealed a growth of around $4*10^8$ CFU/ml for just E.coli, around $5*10^8$ CFU/ml for E.coli with 1mg/ml Boc(β ala)₂N₂H₃, and around $2*10^8$ CFU/ml for E.coli with 2 mg/ml Boc(β ala)₂N₂H₃.

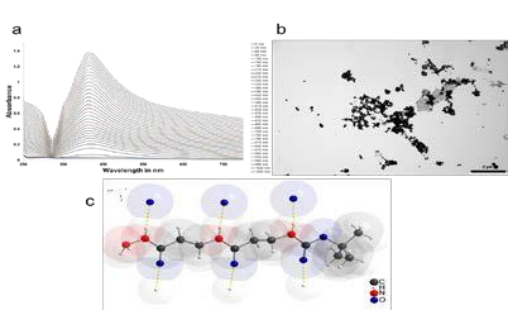


Figure 1: a) UV-VIS of AgNP formation with 1.25 mM Boc(β ala)₂N₂H₃ and 1.25 mM AgNO₃ at pH 7 and 60 °C; b) TEM of 30-90 nm big AgNP formed, scale 2 μ m; c) Crystal structure of Boc(β ala)₂N₂H₃, R = 3.61 %

DISCUSSION & CONCLUSIONS: The peptide crystallizes in the orthorhombic space group $P2_12_12_1$. The packing reveals three H-bonds of 2.03–2.13 Å, which connect the peptide molecules into 1D-ribbons, which are themselves connected in an anti-parallel fashion via H-bonds between the hydrazine groups to form dimers of ribbons. These dimers of ribbons are arranged in zigzag into layers, which are themselves assembled through short interactions into a 3D structure with a mean distance of ~ 2.3 Å.

First tests showed that $Boc(\beta ala)_2N_2H_3$ is capable to form AgNPs at different pH values and temperatures. This process could best be observed at pH 7 and 60 °C where AgNP formation occurred over several hours, reaching sizes of 30 to 90 nm. Other conditions showed faster AgNP formation with broader size distributions and precipitation. The NMR titration showed that the interaction with silver takes place mainly at the hydrazine end group. The antimicrobial tests indicated a slight decrease in bacterial growth for 2 mg/ml of $Boc(\beta ala)_2N_2H_3$.

ACKNOWLEDGEMENTS: The authors thank the Swiss National Science Foundation for generous support, as well as Dr. Jamshid Rajabi and Anne Schuwey for help with the synthesis and analysis.

Advances in lifetime predictions of DLC coated articulating implants

A Pardo, E Ilic, P Schmutz, T Suter, K Thorwarth, R Hauert

Empa, Swiss Federal Laboratories for Materials Science and Technology, 8600-Dübendorf, CH

INTRODUCTION: The in-vitro lifetime predictions of diamond-like carbon (DLC) coated articulating implants may not accurately represent their in-vivo performance, leading to undesirable revision surgeries. The aim of our studies is to develop an experimental methodology to improve the prediction of the implant lifetime by simulating its performance in the human body. The strategy deals with the study and characterization of time dependent corrosion and fatigue processes at the interface, accelerated by reciprocating sliding tests performed in simulated body working conditions. Considering that carbon coating wear overcomes the requested lifetime, this research focuses on the study of the few atomic rows of reactively formed material between the adhesion promoting interlayer and the substrate, which plays a crucial role in corrosion-enhanced delayed delamination processes [1].

METHODS: We tested a set of controlled oxygen contaminanted concentrations in the silicon containing DLC adhesion promoting interlayer, Si-DLC. The interlayer and the 4 µm DLC top coating were deposited from Tetramethylsilane (TMS), and acetylene (C₂H₂), respectively, by Radio Frequency Plasma Assisted Chemical Vapor Deposition (RF-PACVD) onto medical grade Ti₆Al₇Nb substrates. The interlayer was characterized by X-Ray Photon spectroscopy (XPS) as well as by an innovative technique which expands the a few nanometers thicknesses to a few microns by low angle crosspolishing. This enables both Auger Spectroscopy) compositional (by electrochemical characterization (by microcapillary technique) of the interlayer.

RESULTS:

There is a correlation between small amounts of contaminants at the interface growing stage, an increased delamination after the tribological test in corrosive media, Figure 1, and the electrochemical behaviour of the interlayer.

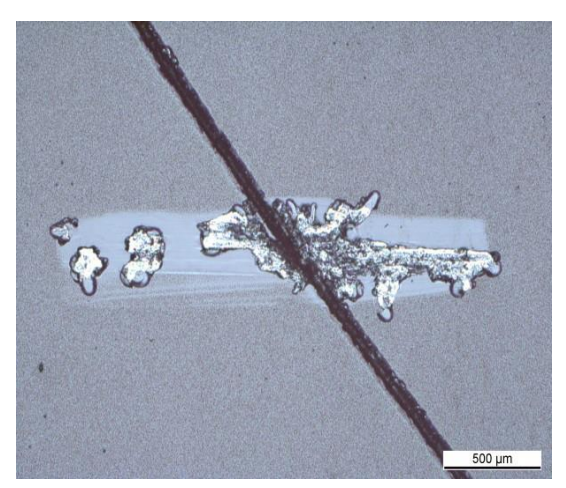


Fig. 1: Weartrack over a damaged DLC surface, with 50% oxygen content at the interface, after 30 minutes at 38°C under 2N load reciprocating sliding test in PBS with a 6mm Saphire counterball.

DISCUSSION & CONCLUSIONS: These fatigue and corrosion stability studies significantly contribute to a more reliable experimental method of estimating the lifetime of carbon coated implants.

Wound bandages and gels functionalized with peptide-displaying nanocomplexes for healing promotion

V Patrulea¹, LA Applegate², G Borchard¹, O Jordan¹

¹School of Pharmaceutical Sciences, University of Geneva, University of Lausanne, Geneva, Switzerland, ²University Hospital of Lausanne (CHUV-UNIL), Department of Musculoskeletal Medicine, 1066 Epalinges, Switzerland

INTRODUCTION: Dermal wound healing is a complex process, which includes four overlapping stages: inflammation, migration, proliferation and maturation [1]. Tissue repair refers to healing in which new growth restores damaged tissue to the normal state. The ability of skin to repair itself after a minor injury is remarkable, but this is not the case for difficult-to-healing, chronic wounds, ulcer and burns. There is thus an increasing need for biomaterials promoting wound healing. Wound regeneration needs to be guided by biological cues, such as Arg-Gly-Asp (RGD), a peptide known to adhesion and induce cell migration Nanocomplexes based on polyelectrolyte selfassembly are suitable carriers for these cues in order to accelerate the healing process and improve the completeness of the final repair

The aim of the study is to develop different formulations of polyelectrolyte nanocomplexes for topical wound application: a sprayable suspension of nanocomplexes, nano-structured hydrogels and freeze-dried foams, which would hydrate upon exudate absorption. Formulations are based on the chitosan derivative O-carboxymethyl-N,N,N-trimethyl-chitosan (CMTMC) grafted with RGDC peptide

METHODS: CMTMC was functionalized with through a 6-carbon spacer diaminohexane, DAH), leading to RGDC-DAH-CMTC. Nano-sized polyelectrolyte particles were prepared by complexation of the cationic chitosan derivative with anionic chondroitin sulfate. Hydrogels were obtained by mixing RGDCfunctionalized chitosan with hyaluronic acid (HA) at a 1:1 (v/v). Foams were produced by lyophilization of the previously prepared hydrogels. Both nanocomplexes suspensions and hydrogels were formulated and tested for their potential to induce human dermal fibroblast (HDF) adhesion, migration and subsequent wound healing.

RESULTS: The synthesis process allowed for controlled covalent binding of RGDC at a high peptide substitution degree (15.3 µg of peptide per mg of chitosan). Nano-sized polyelectrolyte particles were obtained with a size of about 200 nm as confirmed by differential light scattering (DLS) and scanning electron microscopy (SEM). Hyaluronic acid gels embedding RGDC-DAH-CMTMC nano-gels were fabricated, with viscosities adapted for topical patient application. Upon lyophilization, freeze-dried foam bandages were also obtained.

The new extra-cellular matrix based on chitosan derivatives was shown to be useful both as a carrier of RGDC peptide and for complete closure of wounds after 24 h. *In vitro* bio-adhesion assay showed that HDF treated with formulations based on RGDC-derivatized chitosan showed a phenotype typical of spreading and migrating cells, and an increased motility compared to CMTMC treated control cells. These results were only obtained in presence of the adhesion peptide.

DISCUSSION & CONCLUSIONS: Overall, adhesion peptide-bearing nano-formulations promoted HDF survival, motility and migration. They have the potential to accelerate cell migration *in vivo* and promote healing of chronic wounds.

The anabolic and anti-inflammatory effects of biological small molecules for treatment of osteoarthritis

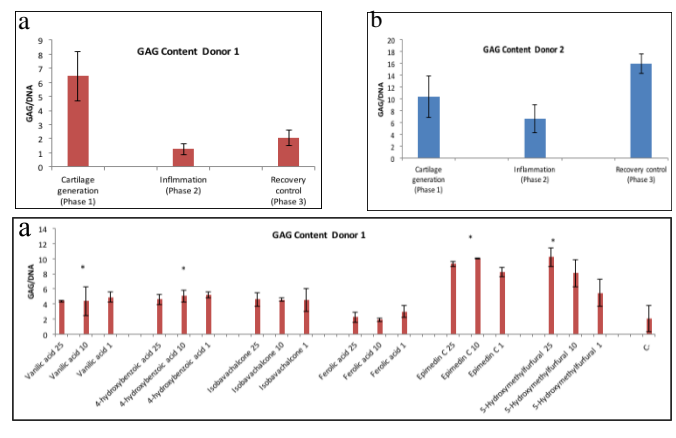
R Ziadlou^{1,2}, S Grad¹, M Stoddart¹, Wang Xinluan³, Qin Ling³, A Barbero², I Martin², M Alini¹

¹ AO Research Institute, AO Foundation, Davos, CH.

INTRODUCTION: Osteoarthritis (OA) is the most prevalent degenerative joint disorder that affects millions of patients worldwide. Due to the poor self-healing capacity of articular cartilage, there is currently no effective and standardised treatment available, neither for repair nor for prevention of onset or progression of this disease. The pharmacologic therapy for OA shows efficacy in pain relief but is frequently associated with adverse side effects, which has led to the transition from pharmacological to biological therapy.

METHODS: In this study, we tested 40 small molecules with biological structure which are derived from herbal extracts. Using a highthroughput screening method, the chondrogenic effects of a selection of 40 TCM (Traditional Chinese Medicine) compounds were assessed on human osteoarthritic chondrocytes in pellet cultures. Specifically, the DNA content and glycosaminoglycan (GAG) synthesis of the cells in response to different doses of TCM compounds were evaluated by using Hoechst dye and DMMB assay. In the next step, the anti-inflammatory effects of the compounds were investigated using an inflammatory model. For this respect, chondrocytes from osteoarthritic (OA) donors were chondrodifferentiated in pellets for 2 weeks. OA pellets were exposed for 72 hours to IL-1 β /TNF- α and then cultured up to 14 days in serum free medium with different concentrations (25, 10, 1 µM) of the compounds.

RESULTS: Our results showed that some specific compounds significantly increased the matrix production of chondrocytes. For instance, after 14 days of treatment of the pellets with different concentrations (50, 25, 10, 1 μ M) of the compounds, 4-Hydroxybenzoic Acid showed significantly higher GAG/DNA ratio compared to the negative control group. Interestingly, 4- Hydroxybenzoic Acid also restored matrix production in the inflammatory system.



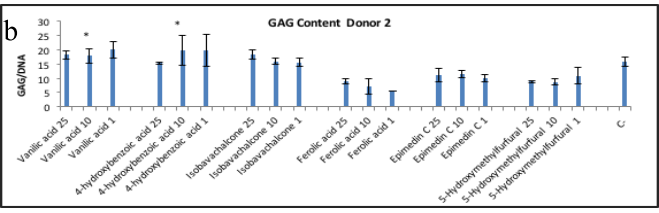


Fig. 1: Proof of concept for creating the inflammatory model (a) Donor1 (b) Donor2

Fig. 2: Anti-inflammatory effects of the compounds (a) Donor1 (b) Donor2

DISCUSSION & **CONCLUSIONS:** In conclusion, 4-hydroxybrnzoicacid not only increased cartilage matrix production of human OA chondrocytes towards a healthy phenotype but also had anti-inflammatory effects in our inflammatory model.

For the further experiments, a hyaluronan based release system for the delivery of the bioactive compound will be optimised and the bioactivity of released compound in terms of cartilage repair will be tested.

Successful completion of the project will provide a new minimally invasive therapy for early OA with the potential to be applied in pre-clinical studies.

ACKNOWLEDGEMENTS: Funded by Swiss National Science Foundation (SNF) under the SSSTC program with grant number 156362.

²Department of Biomedicine, University Hospital Basel, University of Basel, Basel, CH.

³Translational Medicine R&D Center, Shenzhen Institutes of Advanced Technology.

Easy-to-clean coating based on vapour-deposited trialkoxyfluorosilane

A Wäckerlin¹, E Külah¹, M Amberg², T Niessen², P Rupper², D Hegemann², Y Romanyuk¹, A Tiwari¹

¹ Empa, Laboratory for Thin Films and Photovoltaics, Dübendorf, CH. ² Empa, Laboratory for Advanced Fiber, Plasma & Coating, St. Gallen, CH

INTRODUCTION: Hydrophobic and oleophobic surfaces are of paramount importance for a broad range of applications including antimicrobial coatings, medical devices, and displays. 1,2 Intrinsic hydrophobic properties can be achieved by different classes of non-polar organic layers, e.g. parylene, cyclic olefins, silicones. Simultaneous hydrophobic and oleophobic properties can be induced by fluoropolymers when sufficient stability can be provided.³ Moreover, long-chain, terminated fluorocarbon coatings were shown to reduce protein adsorption.4 Here we report on the fast and solventfree preparation of fluoropolymer coatings, based tridecafluoro-1,1,2,2tetrahydrooctyltriethoxysilane (TTS) (see Fig. 1a) and grafting to the surface via condensation reactions. Lastly, we demonstrate their hydrophobic properties and stability in polar/non- polar solutions.

METHODS: plasma etching, chemical vapour deposition (CVD), X-ray photoelectron spectroscopy (XPS), water contact angle measurement (WCA).

RESULTS: The functional coating was prepared in-situ at a base pressure of 10⁻⁶ mbar following a two-step protocol: cleaning/activation of the surface and evaporation of the precursor. The activation of the SiO₂ substrate surface was performed by RF capacitively coupled Ar and O₂ plasma, in order to etch the surface physically and chemically, correspondingly. This treatment ensured activated surface sites and maximized the amount of hydroxyl groups. Grafting of the molecules TTS was performed by heating the source to ~120°C to obtain a defined vapour pressure, whereas the provided dose was controlled by duration of evaporation. The substrate surface was heated during and after evaporation to avoid any physisorption of water and hydrogen-bonding between OH groups, as well as to increase the reaction rate between the ethoxy group of the molecule and Si-OH groups of the surface. The relation between evaporation time, substrate temperature during evaporation and heating after evaporation (temperature, time) was investigated.

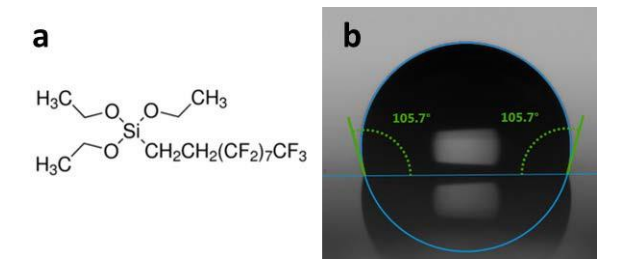


Fig. 1: (a) Molecular precursor, tridecafluoro-1,1,2,2-tetrahydrooctyl-triethoxysilane. (b) Measured WCA of the fluoropolymer coating as prepared by solvent-free CVD method.

DISCUSSION & CONCLUSIONS: In our study we have successfully grafted TTS molecules to the SiO₂ surface under varying conditions. We find that with increasing substrate temperature the heating time after evaporation can be reduced. Moreover with an increase of the heating temperature the evaporation time/dose of the precursor molecule should be increased in order to ensure a densely packed monolayer at the surface. Utilization of surface condensation reactions with the formation of covalent Si-O-Si bonds at the surface ensured good mechanical adhesion of the coating as well as chemical resistance. Well- performing coatings revealed a WCA of 105°C (see Fig. 1b) and stability in deionized water, ethanol and tetrahydrofuran. Our results demonstrate that suitable surface reactions and vacuum deposition methods, as CVD, are a promising approach to realize environmentally friendly solvent-free fluorocarbon coating processes yielding easy-to-clean surfaces.

FISH-based detection of bacteria in orthopedic implant-related infections

Willemijn Boot¹, Debby Gawlitta^{1,2}, Emiel van Genderen¹, Johannes G. Kusters³, Miquel B. Ekkelenkamp³, Ad C. Fluit³, Judith P.M. Vlooswijk³, Wouter J.A. Dhert^{1,4}, H. Charles Vogely¹

¹Department of Orthopaedics, University Medical Center Utrecht, Utrecht, the Netherlands ²Department of Oral and Maxillofacial Surgery & Special Dental Care, University Medical Center Utrecht, Utrecht, The Netherland ³Department of Medical Microbiology, University Medical Center Utrecht, Utrecht, the Netherland ⁴Utrecht University, Faculty of Veterinary Medicine, Utrecht, Netherlands

INTRODUCTION:

Correct diagnosis of infection is crucial for an adequate treatment of orthopaedic implant-related infections. In the orthopaedic field, infections can be difficult to diagnose (1). As a consequence, patients may suffer from an undiagnosed and untreated implant-related infection.

To solve this problem, we are searching for a diagnostic method to detect these so-called low-grade infections. The technique fluorescence in situ hybridization (FISH) can detect slow-growing and even dead bacteria. Further, as FISH results are available within an hour after tissue collection it is an ideal candidate for diagnostic purposes.

AIM: to evaluate the FISH technique for its potential to detect and identify orthopedic infections.

METHODS:

Sonication fluid (SF) was collected by sonicating retrieved implants (2) from 62 patients. All samples were subjected to bacterial culture for clinical diagnostics. In addition, a commercially available FISH kit (miacom diagnostics, specifically designed for blood analysis (hemoFISH Masterpanel), was used. The kit contained 16S rRNA probes (positive control), non-sense probes (negative control), probes for Staphylococcus spp., Staphylococcus aureus, Streptococcus spp., Streptococcus pneumoniae, Streptococcus agalactiae, Enterococcus faecium, Enterococcus faecalis, Enterobacteriaceae, Escherichia coli, Klebsiella pneumoniae. Proteus Pseudomonas aeruginosa, Acetinobacter spp., and Stenotrophomonas maltophilia. All FISH analyses were performed according to the protocol provided with the kit.

RESULTS:

Culture and FISH results were compared, considering culture as the gold standard. Culture resulted in 27 positive and 35 negative samples.

Comparing FISH (16S rRNA probe) with culture, 24 samples tested true-positive and 32 samples true-negative. Furthermore, 3 samples tested false-negative and 3 samples false-positive.

The species cultured with the highest incidence were *Propionibacterium acnes* and *Staphylococcus epidermidis*, both from 8 SF samples. As the kit did not contain a probe for *Propionibacterium acnes*, these strains were only detected by the 16S rRNA probe. In addition, the latter samples tested positive with the *Staphylococcus* spp. probe.

DISCUSSION & CONCLUSIONS:

Interestingly, 3 samples tested positive with FISH that were culture negative. This result could indicate a higher sensitivity for detection of bacteria with FISH than with culture.

Before FISH can be used for diagnostic purposes, the technique needs to be optimized to prevent false-negative results, for use on other patient materials and for detection of bacterial strains relevant for the orthopaedic field like Propionibacterium acnes.

In conclusion, FISH holds promise to be used as a diagnostic tool for identifying orthopaedic infections.

A microfluidics-based approach to investigate the factors influencing the initial phase of bacterial adhesion on surfaces

<u>H Straub</u>¹, HJ Zhang², K Maniura-Weber¹, RM Rossi², Q Ren¹

¹Laboratory for Biointerfaces, Empa St. Gallen Switzerland, ²Laboratory for Biomimetic Membranes and Textiles, Empa, St. Gallen Switzerland

INTRODUCTION: To develop antimicrobial materials to fight against increased occurrence of antimicrobial resistance, relevant in vitro biofilm models that allow assessment of the in vivo anti-biofilm performance of the materials are needed [1]. Microfluidics technologies can be applied in such assessment since they permit dynamic real time analysis and more precise control of relevant parameters compared to traditional static and flow chamber assays [2]. In this project we quantified the initial adhesion rate of Escherichia coli cells on glass in a microchannel under different medium compositions and fluid flow rates with optical microscopy.

METHODS: An *E. coli* suspension was injected inside a microchannel (PMDS bonded on glass with rectangular cross-section: height: $50\mu m$, width: $100\mu m$) (fig. 1). Bacteria suspended either in minimum medium (M9) or tryptic soy broth medium (TSB)) were injected at different flow rates (0.5, 1, $2\mu l/min$) and the bacteria adhering on the glass surface were imaged. The surface coverage (i.e. the ratio between the surface covered by bacteria and the surface of the channel) was computed from pictures taken at several time points during the perfusion of bacterial solution.

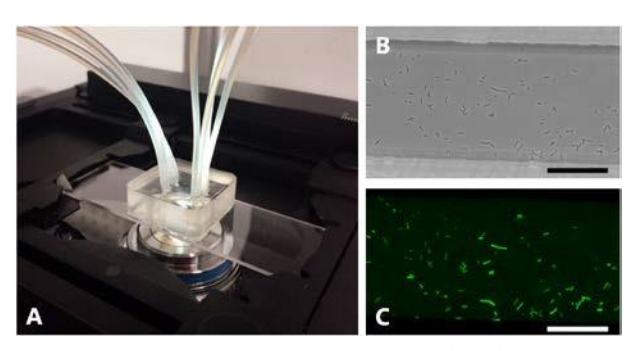


Fig. 1: (A) A PDMS-glass microfluidic chip mounted on an inverted microscope was used to study bacterial adhesion. Both phase contrast (B) and fluorescence (C) micrographs of the adhered bacteria could be automatically processed with an ImageJ routine to extract the surface coverage. Scale bar: 50 um.

RESULTS: As can be seen in fig. 2, bacteria suspended in nutrient-poor medium M9 showed a

greater adhesion compared to those suspended in nutrient-rich medium TSB. Higher flow rate decreased bacterial adhesion for both medium tested.

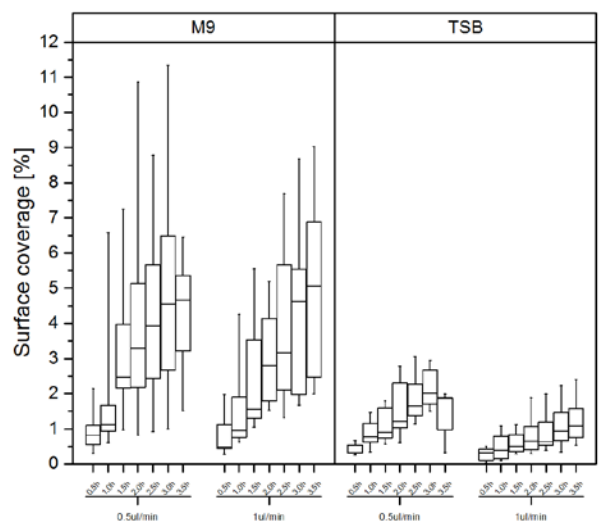


Fig. 2: Influence of medium composition on bacterial surface coverage. Bacteria suspended either in M9 or TSB medium were flown at 0.5 and 1 μ l/min in microchannels: boxplot range from the 25th to 75th percentile and are intersected by the median line. The whiskers extend to the minimum and maximum values for each data set.

DISCUSSION & CONCLUSIONS: The platform established here is useful in examining the effect of different physiological conditions and material surfaces on bacterial adhesion and biofilm formation. Further improvement of the microfluidic platform to allow direct comparison of various settings will be implemented.

PMMA-oleic acid composites as Candida biofilm repellent

M Petrović^{1,2}, H Hofmann¹, M Mionić Ebersold^{1,3,4}

¹ <u>Powder Technology Laboratory</u>, Institute of Materials, Ecole Polytechnique Fédérale de Lausanne, Switzerland. ² Department of Stomatology, Faculty of Medicine, University of Niš, Serbia. ³ <u>Department of Radiology</u>, University Hospital (CHUV) and University of Lausanne (UNIL), Lausanne, Switzerland. ⁴ <u>Center of Biomedical Imaging (CIBM)</u>, Lausanne, Switzerland.

INTRODUCTION: *Candida albicans* (*C.a.*) is fungus which is often found in oral cavity and which can adhere to the surface of denture typically made from PMMA polymer. In this way

C.a. is becoming pathogen and a formed biofilm lead to *Candida* associated denture stomatitis. Therefore, there is a need to modify PMMA in order to make it repellent for *C.a.* biofilm formation, *i.e.* to make it fungistatic. For this modification could be used only molecules which are known as nontoxic and which are ideally naturally abundant. Thus, for PMMA modification we chose oleic acid (OA) which in nontoxic and

which naturally occurs in numerous plants and animals. In this study, we incorporated different amounts of OA into standard dental PMMA polymer, characterised the obtained PMMA-OA composites and studied their antifungal properties.

METHODS: PMMA-OA composites were made by physical incorporation of suitable amounts of OA into a mixture of cold polymerized acrylic resin PMMA and MMA (Ivoclar Vivadent, Liechtenstein). Samples of composites containing 0, 3, 6, 9 and 12wt% of OA were made as solid discs (Ø 20mm) in Teflon moulds. Chemical analysis of the surface of composites and native materials was done by ATR-FTIR. Contact angles of water on composites obtained by sessile drop method were measured in ImageJ. For XTT reduction assay, composites were incubated for 24h with C.a. suspension (density 10⁶ cell/ml). For disk diffusion test (DDT) composite disks were placed on agar plates inoculated with C.a. and the zone of inhibition was measured after 48h incubation at 37°C. Both XTT and DDT were performed in two time points: upon preparation of composites (T₀) and six days after that (T₆). For embedded filamentation test (EFT) 50 ul of C.a. (10⁶ cells/ml) were incubated in 5ml of YPD agar with 0.0125wt% and 0.4wt% of OA at 37°C for 24h and imaged by optical microscope.

RESULTS: ATR-FTIR showed characteristic peaks of OA and their intensity corresponded to the amount of OA in composites (from 0 to 12wt%). Contact angle was 76.7 ± 2.5 , 75.3 ± 2.2 ,

73.6 \pm 1.4, 74.9 \pm 1.7, 74.5 \pm 1.3, on composites with 0, 3, 6, 9 and 12wt% of OA, respectively. The relative percentage of *C.a.* cells both *in* the medium above composites and *on* the surface of composites with different concentration of OA (3, 6, 9 and 12wt% OA) with respect to the native PMMA as a control were obtained in 2 different time points (T_0 and T_6) by XTT test (see Table 1 for the results "*on* the surface"). DDT showed that there is no inhibition zone around composite discs regardless the OA concentration.

Table 1. Viability of C.a. cells on the surface of composites in 2 time points: To and To.

Sample name	T_0	T_6
0wt% OA	$100.0\pm23.8\%$	$100.0\pm7.4\%$
3wt% OA	25.7±7.3%	46.6±9.7%
6wt% OA	$6.4\pm0.5\%$	$17.5\pm2.4\%$
9wt% OA	$4.7\pm1.9\%$	$15.3\pm9.5\%$
12wt% OA	6.1±1.2%	17.7±2.8%

DISCUSSION & CONCLUSIONS: From the contact angle measurement we can see that incorporation of OA into PMMA does not change wetting properties of PMMA. This could question the presence of OA on the surface of composites; that was, however, confirmed by FTIR. Due to this OA at the composites' surface, XTT test on the surface of composites showed for both studied time points a strong reduction of *C.a.* biofilm formation, especially for ≥6wt% of OA. However, OA does not have fungicidal effect, and this, as expected, DDT did not show any inhibition zone. In all, OA showed fungistatic and not fungicidal effect. Until now, this effect of OA was explained by prevention of hyphal formation by OA.[1] To verify this, we did EFT which showed presence of hyphal form for both concentration of OA. Hence, an understanding of effects of OA on biofilm formation needs to be revised. In summary, we showed that our novel PMMA-OA composites are *C.a.* biofilm repellent.

.a. bioiiiii repenent.

Application of Lab-based X-ray Micro-CT for Visualizing Bacterial Biofilms with Non-Destructive Contrast Enhancing Agents

R Kaufmann¹, M Carrel², MA. Beltran¹, VL Morales^{2,3}, M Holzner²

¹Empa, Center for X-ray Analytics, Dübendorf, Switzerland, ²ETHZ, Institute of Environmental Engineering, Zurich, Switzerland, ³UC Davis, Dept. of Civil and Environmental Engineering, Davis CA. USA

In porous media biofilm growth has been shown to affect the hydrodynamics in a complex fashion at the pore-scale by either inducing preferential flow pathways and anomalous transport [2] or clogging of individual pores [1]. The dynamics of local bacterial attachment and biofilm development, the effect of biofilms on pore networks and how bioclogging influences flow and mass transport processes is not completely understood. One of the limitations being the lack of three dimensionally spatially resolved flow and structural experimental information. X-ray and synchrotron micro-CT have been used lately [3,4] to image biofilms in porous media with contrast agents but still present some major drawbacks. They are toxic and interact with the biofilm. We are here presenting the first results on the development of a non-destructive, non-toxic method that should enable the imaging of biofilms in porous samples. The method is based on iron sulfite as a contrast agent that maintains the integrity of the biofilm. Furthermore, an optimised postprocessing Lorentz-filter applied on the projection images before CT reconstruction enhances the contrast of similarly absorbing materials. With this combination it is possible to distinguish biofilm and water and hence visualise the behaviour of biofilm over time.

An *in vitro* model for evaluating novel skin wound healing therapies

C Griffoni, B Sentürk, M Rottmar, K Maniura

<u>Laboratory for Biointerfaces</u>, Empa Swiss Federal Laboratories for Materials Science and Technology, St Gallen, CH

INTRODUCTION: The increasing occurrence of chronic skin wounds in patients highlights the need for novel wound healing therapies. However, one of the major challenges at a pre-clinical stage is to evaluate and predict the clinical success of novel therapies designed to improve healing. Currently used in vitro models lack an important aspect of human skin, namely the immune component, and are hence of limited value for testing novel wound healing treatments. But also in vivo data obtained from animals cannot be reliably correlated with data from humans due to the different skin morphology and physiology of the wound healing process¹. Our aim was to establish an in vitro model for assessing the effect of drugs or materials developed for improving healing and to implement an immune component to increase the physiological relevance.

METHODS: Primary human fibroblasts and keratinocytes were used for all experiments. Skin equivalents were established encompassing a dermal compartment consisting of fibroblasts in collagen I, and an epidermal compartment consisting of keratinocytes differentiated with airlift culture. Excisional wounds were created with a biopsy puncher of 2mm diameter and wound closure was evaluated by means of confocal microscopy and histological analyses. Preliminary studies were performed to identify a suitable coculture medium for fibroblastic and epithelial primary cells with THP-1 derived macrophages. Cell viability, proliferation and morphology were evaluated.

RESULTS: H&E staining confirmed that the *in vitro* skin had a structure similar to the human native skin, showing the presence of a stratified epithelium after 7 days of air-lift culture (Fig. 1). Co-culture preliminary results showed that all cell types remained viable and maintained a normal morphology over 7 days of culture in the selected medium (Fig. 2). Fibroblasts and keratinocytes additionally showed increasing proliferation rates.

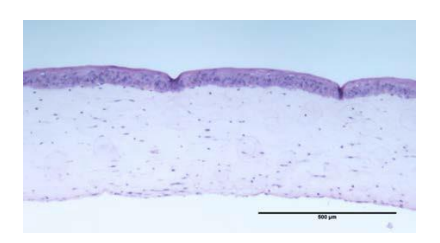


Fig. 1: H&E stain of a representative in vitro skin equivalent after 7 days of air-lift culture. Scalebar: 500 µm.

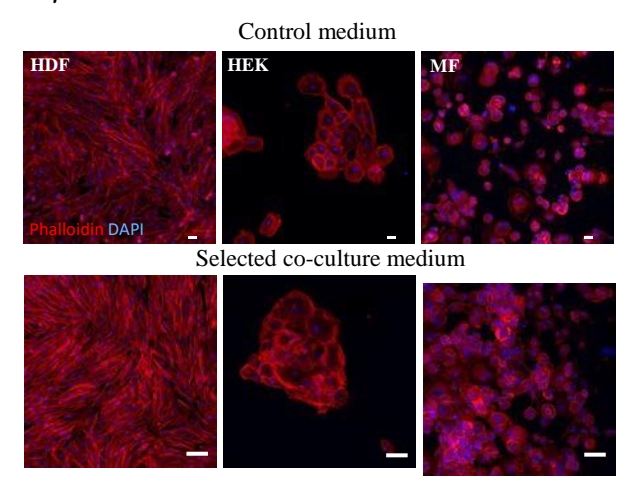


Fig. 2: Phalloidin/actin and DAPI staining of human primary fibroblasts (HDF) and keratinocytes (HEK) and THP-1 derived macrophages (MF) cultivated in their respective proliferation media and in the selected co-culture medium for 7 days. Scalebar: 100 µm.

DISCUSSION & CONCLUSIONS: A full-thickness skin model including human primary cells with an excisional wounding method was established, and preliminary experiments indicated that calcium pantothenate is a suitable positive reference for improving the healing process. The medium composition for integrating THP-1 derived macrophages into the *in vitro* 3D skin to obtain an immunocompetent skin model was established. For future applications, the described platform will be used for evaluating novel wound healing treatments at a pre-clinical stage and also to understand the molecular mechanisms of skin disease.

Engineering biomolecules for advanced nanocellulose based antimicrobial coatings

R Weishaupt¹, L Heuberger¹, G Faccio¹, G Siqueira², T Zimmermann², K Maniura-Weber¹

¹Laboratory for Biointerfaces, Empa, St. Gallen, CH., ²Laboratory for Applied Wood Materials, Empa, Dübendorf, CH.

INTRODUCTION: Nosocomial infections are today by far the most common complication affecting hospitalized patients. In this regard, the development of coatings that prevent pathogen associated surface colonization at an early stage is of utmost interest. Nanocelluloses (NC) from both, plant- and microbial origin are highly durable materials, which cause low inflammatory response and can, promote tissue regeneration if deployed as wound dressing or body implant.² Their high specific surface area and hydrophilic concurrent properties allocate nanocelluloses as excellent carrier material for various biomolecules.³

The development of nanocellulose-based implant coatings that preclude inflammation and elicit broadspectrum antimicrobial activity would be highly advantageous. Cationic antimicrobial peptides (AMPs) are among the most prominent candidates for such applications. The therapeutic potential of AMP's are currently explored extensively in research and development. However, the majority of these studies have focused on free peptides and only few addressed the development of molecular tools for efficient surface immobilization or cytotoxicity aspects.

METHODS: A synthetic AMP sequence was either recombined with a peptide (CBP) or protein based carbohydrate-binding motif (CBM). Solid phase synthesis or recombinant expression in *E. coli* BL21 in combination with affinity column chromatography was applied to produce and purify the engineered ligands (Fig. 1).

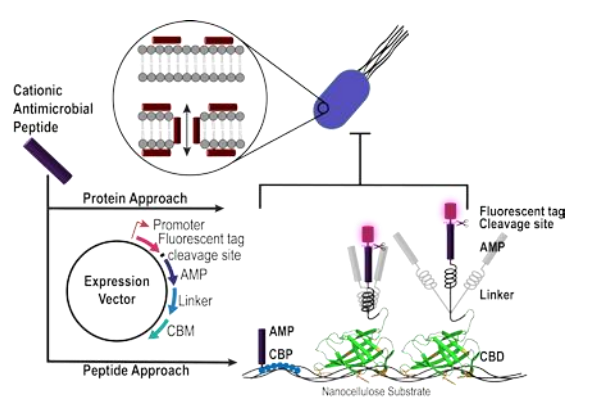


Fig. 1. Design and expression of protein/peptide molecules for bio-affinity driven immobilization of AMP's on nanocellulose substrates.

The spontaneous interaction of the elaborated ligands with nanocellulose substrates was investigated as previously described³. The antimicrobial potential against clinical isolates of *P. aeruginosa sp. and S. aureus sp* was measured using a modified killing assay⁴. The minimal inhibitory concentration (MIC) was taken as the concentration at which no growth was observed.

RESULTS: The peptide-based ligands were found to be highly antimicrobial in solution with MIC values (eg. *P. aeruginosa*) as low as 1.6 μ g/mL for the unmodified AMP and 8 μ g/mL for the CBP tagged AMP. (Figure 2A).

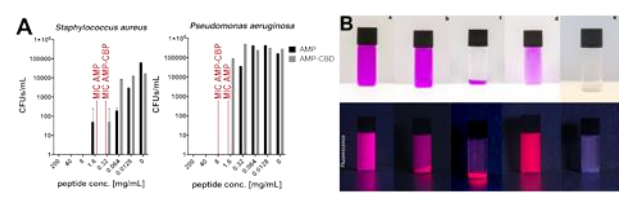


Fig. 2:Antimicrobial activity of unmodified peptide based antimicrobial ligands (A). Specific interaction of protein based antimicrobial ligands with nanocellulose substrates and subsequent protease-catalyzed activation (B).

Co-incubation of cell free extract revealed selective and stable binding of the protein-based ligands to the nanocellulose substrate via their concomitant CBM (Figure 2B). The addition of a site-specific protease successfully exposed the antimicrobial moiety to the solvent by cleaving off the fluorescent protection tag.

DISCUSSION & CONCLUSIONS: Current results confirm the potential of the developed strategy for efficient functionalization of NC substrates with active biomolecules. Currently the antimicrobial potential of the protein-based constructs in solution and immobilized to NC substrates are being addressed.

ACKNOWLEDGMENTS: The authors thank Matthias Buhmann, Beatrice Gutt & Qun Ren-Zulian for their contribution

An inorganic antimicrobial surface modification for orthopaedic implants

P Gruner¹, W Moser², M Wittwer³, J Rüegg³, H Holeczek⁴, O Braissant⁵, K Maniura⁶, M de Wild³

¹ MEDICOAT AG, Mägenwil, CH. ² Atesos AG, Aarau, CH.

³ University of Applied Sciences Northwestern Switzerland, School of Life Sciences, Muttenz, CH.

⁴ Fraunhofer-Institut, Institut für Produktionstechnik und Automatisierung, Stuttgart, D.

⁵ University of Basel, Center of Biomechanics & Biocalorimetry, Allschwil, CH.

⁶ Biointerfaces, Laboratory for Materials-Biology Interactions, Empa, St. Gallen, CH.

INTRODUCTION: The rising number of periprosthetic infections has led to the development of various strategies for bactericidal implant coatings. [1] We investigated the aproach of an inorganic calcium hydroxide Ca(OH)₂ coating that expresses an initial antibacterial effect before it transforms into hydroxyapatite. [2] While safety of this electrochemically deposited antimicrobial coating was previously shown preclinically [3], we here verified the bactericidal effect in-vitro.

METHODS: Ø15mm titanium disks were coated by titanium plasma spray (TPS) before a 20 μm thick Ca(OH)₂ coating was electrochemically deposited. The surface was inspected by SEM (Zeiss Supra). Ca(OH)₂ pellets (Fluka) with a calcium hydrogen phosphate dihydrate filler (Emcompress Premium JRS Pharma) were manufactured (Ca(OH)₂/CaHPO₄ · 2 H₂O

=50%:50%) and served as standardized positive control.

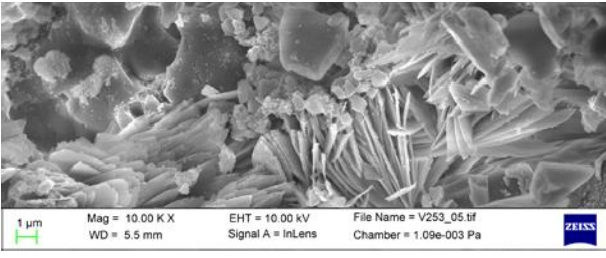


Fig. 1: SEM image of TPS surface electrochemically coated with a lamellar Ca(OH)2-layer.

S.aureus ATCC® 35556TM was prepared in 10 ml Luria Broth (LB) media (Invitrogen) and cultivated over night at 37°C. OD600 measurements (Jenway 6320D spectrophotometer) and dilutions were performed to provide 10⁴ cfu in 20 μl LB media. The bacteria suspension was plated on LB-agar (Invitrogen) after mixing with additional 480 μl of LB media. After 10 minutes of soaking time, the Tidisks or pellets were placed an incubated at 37°C overnight. The inhibition and diffusion zones around the disk/pellets were then determined along three orientations.

RESULTS: The morphology of the coating consists of fine lamellae on top of the TPS coating, see Fig. 1. Bacterial growth is inhibited in a region around the Ca(OH)₂ pellet due to increased pH, see Fig. 2 left. Whereas unaffected colonies are found around the uncoated Ti-disks, an inhibition zone and a diffusion zone is observed around the Ca(OH)₂-coated disks, see Fig. 2 right and Table 1.

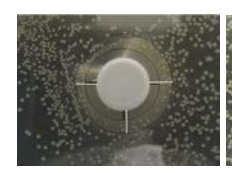






Fig. 2: Growth of S.aureus. a) Standardized Ca(OH)₂-loaded tablets are used as positive control: growth is repressed in the inner ring. A diffusion ring extends to the outer ring, b) uncoated Ti as a negative control: No impact to bacteria growth. c) Ca(OH)₂-coated Ti: Complete inhibition in the close proximity, reduced bacteria growth in the diffusion zone.

Table 1. Inhibition (I) and diffusion (D) zones.

	<i>I</i> [mm]	D [mm]
Ca(OH) ₂ pellet	3.0 ± 0.2	4.9 ± 0.2
Ti control	0 ± 0	0 ± 0
disk 1	0.7 ± 0.3	2.1 ± 0.5
disk 2	0.5 ± 0.4	1.8 ± 0.5
disk 3	0.6 ± 0.3	2.6 ± 0.6
disk 4	0.4 ± 0.2	1.0 ± 0.2

DISCUSSION & CONCLUSIONS: The antibacterial effect of the electrochemically deposited Ca(OH)₂-coating in LB agar without additional buffer is confirmed.

ACKNOWLEDGEMENTS: This project with project number 120331-06 was supported by the Forschungsfonds Aargau.

Non-congruent dissolution of copper-doped β-tricalcium phosphate

B Le Gars Santoni¹, C Stähli¹, N Döbelin¹, M Bohner¹

¹ Bioceramics and biocompatibility group, RMS Foundation, Bettlach, CH

INTRODUCTION: Calcium phosphates and particularly β-tricalcium phosphate (Ca₃(PO₄)₂; β-TCP) are widely used to improve the self-healing potential of bone¹. Nevertheless, during the surgical treatment of bone defects, a risk of bacterial infection exists. As copper ions have antibacterial and angiogenic properties², doping β- TCP with those ions could reduce bacterial infection and help the formation of new bone. However, doping the β-TCP with copper can lead to copper ions segregations, especially at the grain boundaries. Thus, copper release might vary during resorption. Moreover, since resorption starts generally at grain boundaries, Cu-doping might modify β-TCP resorption behavior. Therefore, it is of importance to study Cu location in Cu-doped β- TCP and assess its effect on β -TCP in vitro dissolution behavior. The aim of this preliminary study was to synthesize and characterize a Cu- doped β-TCP and study its dissolution behavior.

METHODS: Cu-doped β-TCP was produced by precipitation of amorphous calcium phosphate (ACP) in aqueous media³ followed by calcination, milling, and sintering (1100 °C, 3 h). For the precipitation, (NH₄)₂PO₄, Ca(NO₃)₂.4H₂O and Cu(NO₃)₂.xH₂O were used in precise quantities in order to obtain a [Ca + Cu]/[P] molar ratio of 1.5. Flat cylinders (Ø = 13 mm; H = 1.2 mm) were made by slip casting³ using Darvan C-N as a dispersant during ball milling. Dissolution tests (0.01 M HCl) were carried out in triplicate. The evolution of the dissolution products was determined by Inductively Coupled Plasma Mass Spectroscopy (ICP-MS).

RESULTS: Cu-doping changed β-TCP colour from cream to light blue (Fig. 1a). The samples were phase pure, had a Ca/P ratio of 1.50 ± 0.01 , a relative density of 94-96 %, a grain size close to 2 μm (Fig. 1b). The specimens contained 6393 ± 12 ppm Cu, 297 ± 7 ppm Sr, 25 ± 5 ppm Mg, and 9 ± 1 ppm Na. Cu-doped β-TCP dissolved noncongruently because the composition of the dissolved species varied during dissolution. It also depended on the nature of the ions (Na, Mg, Sr, Cu). The Cu/Ca ratio was initially below the expected stoichiometric amount (p < 0.05) and after one hour was significantly higher (p < 0.0002). At increasing dilutions of the same solution, an increase of the Na/Ca, Mg/Ca, and

Sr/Ca ratio and a decrease of the Cu/Ca ratio were measured.

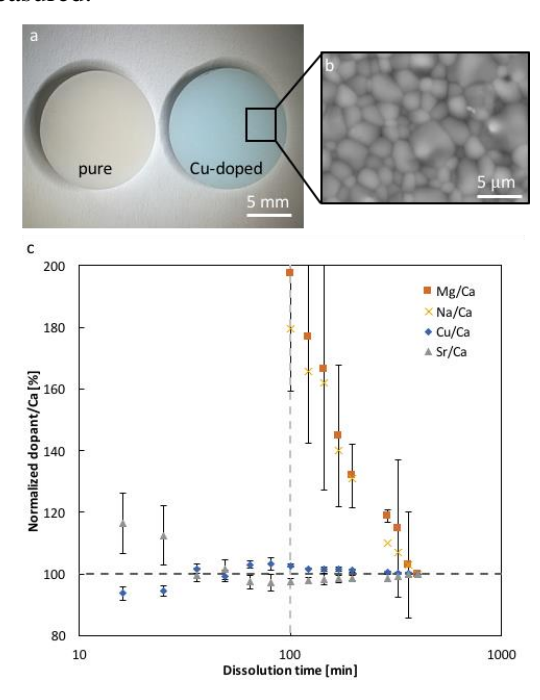


Fig. 1: (a) Image of dense β-TCP pellets. (b) SEM-BSE image of the surface of Cu-doped β-TCP. (c) Evolution of normalized Cu/Ca, Na/Ca, Sr/Ca and Mg/Ca ratios over the dissolution time.

DISCUSSION & CONCLUSIONS: Dissolution tests performed with Cu-doped β -TCP demonstrate that doping ions are not homogeneously distributed within β -TCP: significantly more copper and less Sr were found in the dissolution solution compared to the mean bulk concentration. Our tests also showed that erroneous concentrations were measured at high dilutions. This limits our ability to draw conclusions at short dissolution times and for low concentrations of doping ions (Na and Mg). This study shows that the dissolution behaviour is complex and is related to the nature of dopants and impurities. Future experiments will focus on the dissolution of Cu-doped β -TCP with various contents of dopants.

ACKNOWLEDGEMENTS: Pascal Michel for the SEM images and the Swiss National Science Foundation funding (grant n°200021_169027).